Bangor University

DOCTOR OF PHILOSOPHY

Polarisation properties of externally driven vertical cavity surface emitting lasers

Qader, Abdulqader

Award date:
2013

Awarding institution:
Bangor University

Polarisation Properties of Externally Driven Vertical Cavity Surface Emitting Lasers

Abdulqader Abdullah Qader
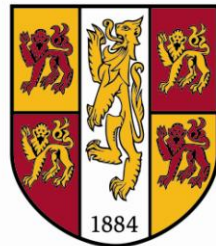
PRIFYSGOL

BANGOR

UNIVERSITY

A thesis submitted for the degree of

Doctor of Philosophy

School of Electronic Engineering

Bangor University

June 2013

Declaration and Consent

Details of the Work

I hereby agree to deposit the following item in the digital repository maintained by Bangor University and/or in any other repository authorized for use by Bangor University.

Author Name: Abdulqader Abdullah Qader

Title: Polarization Properties of Externally Driven Vertical Cavity Surface Emitting Lasers

Supervisor/Department: Prof. K. Alan Shore / School of Electronic Engineering

Funding body (if any): Ministry of Higher Education and Scientific Research (MOHESR), and the University of Sulaimani, Sulaimani/ Iraq

Qualification/Degree obtained: PhD

This item is a product of my own research endeavours and is covered by the agreement below in which the item is referred to as "the Work". It is identical in content to that deposited in the Library, subject to point 4 below.

Non-exclusive Rights

Rights granted to the digital repository through this agreement are entirely non-exclusive. I am free to publish the Work in its present version or future versions elsewhere.

I agree that Bangor University may electronically store, copy or translate the work to any approved medium or format for the purpose of future preservation and accessibility. Bangor University is not under any obligation to reproduce or display the Work in the same formats or resolutions in which it was originally deposited.

Bangor University Digital Repository

I understand that work deposited in the digital repository will be accessible to a wide variety of people and institutions, including automated agents and search engines via the World Wide Web.

I understand that once the Work is deposited, the item and its metadata may be incorporated into public access catalogues or services, national databases of electronic theses and dissertations such as the British Library's EThOS or any service provided by the National Library of Wales.

I understand that the Work may be made available via the National Library of Wales Online Electronic Theses Service under the declared terms and conditions of use (http://www.llgc.org.uk/index.php?id=4676). I agree that as part of this service the

National Library of Wales may electronically store, copy or convert the Work to any approved medium or format for the purpose of future preservation and accessibility. The National Library of Wales is not under any obligation to reproduce or display the Work in the same formats or resolutions in which it was originally deposited.

Statement 1:

This work has not previously been accepted in substance for any degree and is not being concurrently submitted in candidature for any degree unless as agreed by the University for approved dual awards.

Signed …………………………………………... (candidate)

Date …………………………………………...

Statement 2:

This thesis is the result of my own investigations, except where otherwise stated. Where correction services have been used, the extent and nature of the correction is clearly marked in a footnote(s).

All other sources are acknowledged by footnotes and/or a bibliography.

Signed …………………………………………. (candidate)

Date ………………………………………….

Statement 3 (bar):

I hereby give consent for my thesis, if accepted, to be available for photocopying, for inter-library loans and for electronic repositories after expiry of a bar on access.

Signed …………………………………………… (candidate)

Date ……………………………………………

Statement 4:

Choose **one** of the following options

a) I agree to deposit an electronic copy of my thesis (the Work) in the Bangor University (BU) Institutional Digital Repository, the British Library ETHOS system, and/or in any other repository authorized for use by Bangor University and where necessary have gained the required permissions for the use of third party material.	
b) I agree to deposit an electronic copy of my thesis (the Work) in the Bangor University (BU) Institutional Digital Repository, the British Library ETHOS system, and/or in any other repository authorized for use by Bangor University when the approved **bar on access** has been lifted.	X
c) I agree to submit my thesis (the Work) electronically via Bangor University's e-submission system, however I **opt-out** of the electronic deposit to the Bangor University (BU) Institutional Digital Repository, the British Library ETHOS system, and/or in any other repository authorized for use by Bangor University, due to lack of permissions for use of third party material.	

Options B should only be used if a bar on access has been approved by the University.

In addition to the above I also agree to the following:

1. That I am the author or have the authority of the author(s) to make this agreement and do hereby give Bangor University the right to make available the Work in the way described above.
2. That the electronic copy of the Work deposited in the digital repository and covered by this agreement, is identical in content to the paper copy of the Work deposited in the Bangor University Library, subject to point 4 below.
3. That I have exercised reasonable care to ensure that the Work is original and, to the best of my knowledge, does not breach any laws – including those relating to defamation, libel and copyright.
4. That I have, in instances where the intellectual property of other authors or copyright holders is included in the Work, and where appropriate, gained explicit permission for the inclusion of that material in the Work, and in the electronic form of the Work as accessed through the open access digital repository, *or* that I have identified and removed that material for which adequate and appropriate permission has not been obtained and which will be inaccessible via the digital repository.
5. That Bangor University does not hold any obligation to take legal action on behalf of the Depositor, or other rights holders, in the event of a breach of intellectual property rights, or any other right, in the material deposited.
6. That I will indemnify and keep indemnified Bangor University and the National Library of Wales from and against any loss, liability, claim or damage, including without limitation any related legal fees and court costs (on a full indemnity bases), related to any breach by myself of any term of this agreement.

Signature: …………………………………………………… Date : ……………………………………………

Abstract

Polarisation properties of externally driven vertical cavity surface emitting lasers

This thesis explores the polarisation properties and lasing characteristics of externally driven vertical cavity surface emitting lasers (VCSELs). Polarisation properties including polarisation state selection and polarisation switching of VCSELs were investigated experimentally using various schemes of optical injection and optical feedback. Optical injection and optical feedback are known to induce a diverse range of effects in VCSELs, which can be advantages to the operating characteristics of such devices.

New approaches namely circularly polarised optical injection and circularly polarised optical feedback have been used experimentally for the first time. Using circularly polarised externally optical injection, the output polarisation of electrically pumped VCSELs can be strongly influenced. The linear polarisation of VCSELs emission can become circularly polarised for bias currents below or near the threshold current of the stand-alone VCSELs. In addition, using a new circularly polarised optical feedback scheme, the VCSELs emission was made to exhibit a degree of circular polarisation. The degree of circular polarisation depends on the feedback power ratio and the VCSEL bias current.

The role of the suppressed mode in the polarisation switching characteristics of VCSELs was investigated using different forms of linearly polarised optical injection. The minimum injection power for polarisation switching to occurs has been found to be decreases dramatically with increasing VCSELs bias current. Polarisation switching in multimode VCSELs was investigated using optical injection. Irreversible polarisation switching in two-mode operation VCSELs was observed using parallel/orthogonal optical injection. Furthermore, polarisation bistability and ultra-wide hysteresis were obtained for two-mode operation regime with orthogonal optical injection.

In addition, lasing threshold characteristics of directly modulated VCSELs was demonstrated experimentally. Dynamical hysteresis, depending on thermal effects, in the lasing threshold turn-on and turn-off of were observed and compared to theoretical predictions.

PUBLICATIONS

Following is a list of refereed journal papers (that have been published/ accepted for publication) and conference papers (presented/ accepted) that have arisen from the experimental wok of the thesis:

1- Journal papers:

➢ **Abdulqader A. Qader**, Y. Hong and K. Alan Shore, "Ultra-wide hysteresis frequency bistability in vertical cavity surface emitting lasers subject to orthogonal optical injection," Appl. Phy. Lett., June 2013. (accepted for publication)

➢ **Abdulqader A. Qader**, Y. Hong and K. Alan Shore, "Robust irreversible polarisation switching in optically injected VCSELs," IEEE, Photo. Techn. Lett., vol. 25, no. 12, pp. 1173-1176, June 2013.

➢ **Abdulqader A. Qader**, Y. Hong and K. Alan Shore, "Role of suppressed mode in the polarisation switching characteristics for optically injected VCSELs," IEEE J. of Quantum Electron., vol. 49, no. 2, February 2013.

➢ **Abdulqader A. Qader**, Y. Hong and K. Alan Shore, "Circularly polarized optical feedback effect on the polarisation of VCSEL emission," IEEE, Photo. Techn. Lett., vol. 24, no. 14, pp 1200-1202, July 2012.

➢ **Abdulqader A. Qader**, Y. Hong and K. Alan Shore, "Lasing Characteristics of VCSELs subject to circularly polarized optical injection", IEEE, J. of Lightwav. Techn., vol. 29, no. 24, December 2011.

➢ Y. Hong, Cristina Masoller, Maria S. Torre, Sanjay Priyadarshi, **Abdulqader A. Qader**, Paul S. Spencer, and K. Alan Shore, "Thermal effects and dynamical hysteresis in the turn-on and turn-off of vertical-cavity surface-emitting lasers", Optic. Lett. ,vol. 35, no. 21, pp3688 - 3690 November 2010.

2- Conferences Papers:

➢ **Abdulqader A. Qader**, Y. Hong and K. Alan Shore "Ultra-wide frequency bi-stability in VCSELs" Sixth 'RIO DE LA PLATA' Workshop on laser dynamics and nonlinear photonics, Montevideo, Uruguay, December 9-12, 2013.

- **Abdulqader A. Qader**, Y. Hong and K. Alan Shore "Persistent polarisation switching in VCSELs " Optics, Lasers and Applications conference, RIO/ OPTILAS, Porto, Portugal, 22-26 July 2013.

- **Abdulqader A. Qader**, Y. Hong and K. Alan Shore "Low switching power polarisation bistability in optically injected VCSELs," The 10th Conference on Lasers and Electro-Optics Pacific Rim (CLEO-PR & OECC/PS), Japan 2013, Kyoto international conference centre, Kyoto- Japan; June, 2013.

- **Abdulqader A. Qader**, Y. Hong and K. Alan Shore "Polarisation switching characteristics in optically injected VCSELs," Institute of Physics (IOP) conference, poster session, 50th Anniversary of the Laser Diode, at University of Warwick, Coventry, UK. 20-21 September, 2012.

- **Abdulqader A. Qader**, Y Hong and K. Alan Shore "Polarisation characteristics of VCSELs with circularly polarized optical feedback " Conference in Semiconductor & Optoelectronics, SIOE'11, at Cardiff University, Cardiff, Wales, UK. 2nd-4th April 2012.

- **Abdulqader A. Qader**, Y. Hong and K. Alan Shore, "Effects of optical injection on the lasing characteristics of vertical cavity surface emitting lasers", Centre for Advanced Functional Materials and Devices (CAFMaD), May 2011.

- **Abdulqader A. Qader**, Y Hong and K. Alan Shore "Laser threshold characteristics in optically injected VCSELs" Conference in Semiconductor & Optoelectronics, SIOE'11, at Cardiff University, Cardiff, Wales, UK. 18th-20th April 2011.

- Y. Hong, C. Masoller, M. S. Torre, S. Priyadarshi, **Abdulqader A. Qader**, P. S. Spencer and K. A. Shore, "Experimental and theoretical study of thermal effects on the dynamical hysteresis in VCSEL turn-on and turn –off" Optoelectronic and Microelectronic Materials and device (COMMAD) Conference, IEEE Conference Publications, Canberra, Australia; December 2010.

- Y. Hong, S. Priyadarshi, **Abdulqader A. Qader**, P. S. Spencer and K. A. Shore, " Experimental study of dynamical hysteresis of turn-on and turn -off in vertical-cavity surface-emitting lasers", Conference in Semiconductor & Optoelectronics, SIOE'10, at Cardiff University, Cardiff, Wales, UK, 29-31 March 2010.

Acknowledgements

To:

Professor K. Alan Shore

For continuous support, dedication, and encouragement throughout this research project. For providing a great opportunity to pursue this interesting research and obtaining variety of experiences and knowledge, I am eternally grateful.

Dr. Yanhua Hong

For sharing the profound lab experience, guidance and continues support.

School of Electronic Engineering staff- Bangor University

For providing support, help, exciting, and sociable work environment. Also I would like to thank the international student support and academic development unit for support and giving many opportunities for skills development.

Iraqi Cultural attaché – London

For their encouragement and continues financial support. Also thanks for Ministry of Higher Education and Scientific Research (MOHESR), and the University of Sulaimani, Sulaimani/ Iraq for the research scholarship.

Finally I would like to thanks my family for their endless support and understanding. Special thanks for my wife for her help and patience during the course of this research.

Contents

CHAPTER ONE

INTRODUCTION

◆━━━◆

In the last two decades, semiconductor diode lasers have become ubiquitous at the forefront of the modern laser technology. They have established a greater variety of applications than any other type of laser. Such applications range from laser pointers, optical memory, optical computer components to modern communication systems, optical sensors, medical diagnostics, and even in atomic physics. Compared to solid state lasers and gas lasers, semiconductor lasers (SLs) combine relatively high efficiency, extremely small size, low cost and ease of use.

After the first experimental observation of the light amplifications by stimulated emission of radiation (LASER) in 1960 [1], efforts were made to broaden the available sources of this very special form of light. These efforts lead to the demonstration in 1962 of coherent light emission from semiconductors using a GaAs p-n junction [2-4]. That followed work in 1960 and 1961 which reported radiative recombination in semiconductors [5, 6]. These initial steps in the laser diode field were followed by extensive research and development of their design to enable devices which are amenable to widespread applications.

Although the history of SLs essentially coincides with the history of the laser, the progress in SLs has been rather distinct from that of other laser systems. This is due to the fact that SLs are more closely aligned to semiconductor physics and electronics than to solid state physics, atomic and optics that underpin many other laser systems.

The year 2012 was the 50th anniversary of laser diode invention. SLs have become part of 'the way of life' as stated at the end summary of the 50th anniversary international conference held in University of Warwick, UK, 20-21 September 2012.

A conventional SL consists of an active layer sandwiched between two cladding layers. The injection of a current via a metal-strip contact through a p-n junction is used to create population inversion in the valence and conduction bands. The laser light is emitted from cleaved facets of the device leading to the term edge-emitting to describe such conventional lasers. The active layer is formed using heterostructure or double heterostructure (DH). In heterostructure SLs the active layer material is different from the cladding materials and the thickness of the layer can be chosen to produce either a bulk (~

100 nm) or more advanced quantum well (5-10 nm). Use of DH materials enabled room temperature operation of the device in the 1970 [7].

Depending on the direction of the emitted light with respect to the plane of the active layer two common types of the SLs may be identified as edge emitting laser (EELs) and vertical cavity surface emitting lasers (VCSELs). In VCSELs the laser emission is perpendicular to the plane of the active layer. The cavity length of VCSELs is usually much shorter (few µm) than that of conventional EELs (~ 300 µm). It is widely expected that the VCSEL, aspects of which are the topic of this thesis, will replace conventional diode laser for most advanced applications. This chapter contains a brief introduction to VCSELs in section 1.1 where the physical principle of VCSELs including their structure and types are provided. Section 1.2 describes the most common VCSELs configurations. Section 1.3 includes the most important advantages of VCSELs as well as some drawbacks from an applications point of view. Finally in section 1.4 the main thesis contributions together with an overview of the thesis are presented.

1.1 Vertical-cavity surface-emitting lasers: *Historic overview*

The first surface emitting laser was demonstrated in 1979 [8]. That led to the development of present-day vertical cavity surface emitting lasers (VCSELs- pronounced "vixels") which are perceived as having several advantages associated with its so-called vertical-cavity geometry. Bulk double-heterostructure (DH) design with GaInAsP wafer active region and metallic mirror were used for the first VCSEL [8]. In 1984 the first room temperature (RT) electrically pumped pulsed VCSELs was reported [9], which was followed by achievement of the first room temperature, continuous-wave (CW) operation, 895 nm VCSEL in 1989 [10]. In 1993 the first CW room temperature electrically pumped 1300 nm VCSEL was demonstrated [11] and the first 1550 nm VCSELs were operated at room temperature in 1996 [12].

The rapid development of GaAs-based VCSELs led to the commercialization of short wavelength devices (850–980 nm) in the 1996, and voluminous research has been reported on their optical, electrical and thermal properties. The progress in the development of GaAs based VCSELs was due to promising properties of optical materials and epitaxial growth of distributed Bragg reflector (DBR). The DBR is formed of multiple periods of high and low refractive index layers, each period being of half wavelength thickness.

The structure of VCSEL lasers consists of an active layer sandwiched between two DBRs mirrors which provide feedback [13]. Figure 1.1 illustrates schematically the structure of a

typical VCSEL. In VCSELs the active medium is made from several quarter wavelength thick layers of semiconductor materials of alternating low and high refractive index. The short cavity length of the device results in making the gain region shorter and longitudinal mode spacing larger (which is advantageous for making single longitudinal mode lasers). To compensate for the short gain region the mirror reflectivity of the VCSEL has to be very high of order 99.9%.

Further development in the VCSEL structure were made to achieve smaller active regions, which led to significant threshold reduction as well as better control of transverse mode. In addition, the operating wavelengths of the device have been extended from visible range (0.41 µm) to mid infrared (3-5 µm) VCSELs.
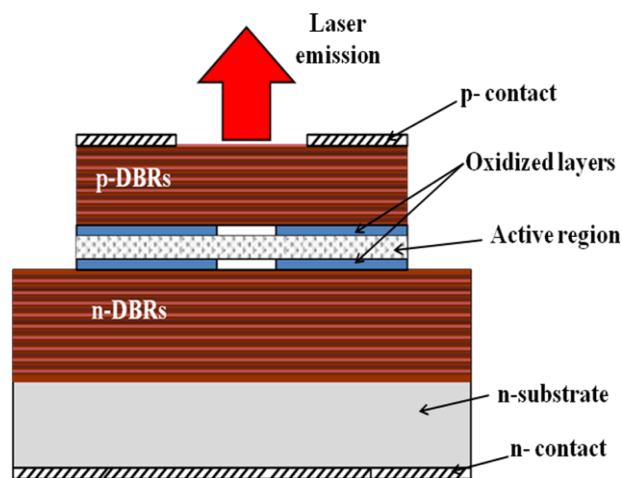
Figure 1.1 schematic layers structure of double oxide-confined VCSELs.

1.2 VCSEL configurations:

VCSELs can be divided into several categories depending on the optical and electrical confinement mechanism, emitted wavelengths, and active layer. Optical confinement is considered as the most important issue in VCSELs fabrication, due to the fact that good optical confinement will enhance the electrical-to-optical conversion efficiency.

Refractive index guiding, gain guiding, and antiguiding mechanisms are the most common confinement mechanisms found in the literature, which confine the optical field inside the laser cavity (transverse mode confinement). Using gain guided VCSEL the lateral extent of the laser field is controlled with injection current distribution. In index guided VCSEL the refractive index profile which form an optical waveguide used to control lateral extend of the laser field. The most popular and commercially widespread are VCSELs with refractive index guiding.

- **Oxide confined VCSELs**

  Index guiding mechanism provides strong transverse mode confinement of the optical field due to large difference in refractive index between semiconductor and oxide layer. Several types of the index guiding VCSELs can be found in the literature including: oxide-confined [14], air-post [15], and buried heterostructure VCSELs [16]. However only VCSELs with oxide aperture active layer have been mass-produced.

  With oxide confinement the current is confined by oxidizing the material around the aperture of the VCSEL using a high content aluminium layer that is grown within the VCSEL structure, the oxidized layer in figure 1.1. Oxide-confined structures provide both electrical and optical confinement simultaneously and are a preferred VCSEL configuration. Using oxide-confined VCSELs the threshold current reduced significantly, this is due the fact that the oxide apertures are insulating layers forcing the injection current through the aperture which increases wallplug efficiency [17]. The lasing threshold current is an important merit for device applications as it governs the minimum power consumption for lasing operation. The Wallplug efficiency is the total electrical to optical power conversion efficiency of the device.

  Oxide aperture VCSELs are now most promising device for use in Local Area Networks (LAN) and Metropolitan Area Networks (MAN), due to their high modulation speed, low power consumption, and low production cost.

- **850 nm VCSELs**

  A wide range of VCSEL emission wavelengths have been reported including "short wavelength" (830 nm, 850 nm, 980 nm) [14, 15] and "long wavelength" (1320 nm, 1550 nm) [17, 18]. Although, most SLs operate in the infrared or optical communication wavelengths region of the electromagnetic spectrum, new VCSELs are being developed that can produce output in the blue/violet region of the spectrum. Short wavelength VCSELs are attractive because of potential large scale applications such as laser printing, optical storage devices (DVD, blue ray) and displays.

  Different materials for the active layer emitting around 850 nm have been used, including GaAS, InGaAs, and InAlGaAs. Perhaps the most interesting and widely deployed VCSEL from the standardization point of view is that emitting at a wavelength of 850 nm, since it has been already standardized for LAN and storage area network (SAN) applications [19].

- **Quantum well VCSELs**

  The first VCSELs were built with active layers of bulk DH material [8], which was later replaced by quantum well (QW) active layer material. QWs are thin layered semiconductor structures, in which charge carriers (electrons and holes) free in two dimensions (2D) compared to the three dimensions (3D) for bulk semiconductor. The thinning of the active layer leads to profound difference in device performance, e.g. decrease in the threshold current that is nearly proportional to the thinning.

  Quantum well VCSELs are the most commercially and widespread VCSELs nowadays. Use of QW in active layer of the VCSEL has led to superior performance and greater flexibility in the emission wavelength. The devices used in the experimental work reported in this thesis were all quantum well VCSELs.

  In addition, Quantum Dot (QD) and Quantum Wire (QWR) VCSELs have been reported [15, 20]. Compared with quantum well, QD active region offers 3D carrier confinement, while QWR active region offers 2D carrier confinement.

1.3 Advantages and drawback of VCSELs

In the previous section the basic principles of VCSELs have been presented and the importance of oxide-confined, 850 nm, quantum well VCSELs as used in this work have been highlighted. In this section, the intrinsic advantages of VCSELs as well as their main drawbacks will be presented.

VCSELs structure provide a number of advantages, these including : ultra low threshold currents operation; wavelength and thresholds are relatively insensitive to temperature variation; they have device lifetimes of order 15 million hours at 40°C [21] ; easy coupling to optical fibres, and wafer level testing capability for low-cost manufacturing [21, 23]. The small volume of the active layer and extremely high reflectivity of the output coupler contribute to the ultra low threshold current obtained in VCSELs, which leads to low power consumption and reduced heating effects in the device.

Another important advantage of VCSELs (and SLs in general) is their amenability to direct current modulation. Using directly modulated VCSEL optical pulses as short as a few picoseconds have been obtained [24]. These optical pulses can be used for carrying information at high bit rates in optical communications system as well as for time resolved dynamical studies of the device.

Drawbacks:

VCSELs possess a number of challenging properties including a propensity to exhibit multiple-transverse mode operation [25]. Current spreading and carrier diffusion in the confinement region in conjunction with spatial hole burning and thermal effects, results in multiple transverse modes operation especially at high injection currents [26, 27]. This leads to multiple wavelengths in the emission spectra and limits the maximum achievable distance due to dispersion effects.

A second potential disadvantage of VCSELs is their complex polarisation characteristics. The polarisation characteristic of VCSEL emission (the subject of this thesis) is found to vary from one device to another. The fundamental transverse mode is generally linearly polarised; however the polarisation direction often varies with increase injection current [28]. Details of the polarisation characteristics in VCSELs will be discussed in chapter two, which also provides the background for the thesis experimental work.

Another drawback of the device is the limited or low output power (few mW) compared to EEL, which comes from the high reflectance of the output mirror. This high reflectivity of the DBR mirror led to low quantum efficiency and low output power.

1.4 Thesis contribution and outline

This thesis is mainly devoted to the experimental exploration study of the polarisation properties of externally driven VCSEL. This includes polarised optical injection, optical feedback and direct current modulation of VCSELs. Despite the fact that a large amount of experimental work has been conducted on the characteristics of commercially electrically pumped VCSELs, their polarisation properties are still not completely understood. Therefore, the main goal of the present thesis is to provide some new aspects on the study of polarisation characteristics of VCSELs including circularly polarised optical injection and optical feedback. Means available to change or control the polarisation state of the VCSELs emission are also discussed and this is providing the main motivation for this work.

The present thesis consists of nine chapters. In chapter 2 the background for the thesis experimental work is provided. Polarisation selection mechanisms, polarisation switching and polarisation bistability are discussed. Externally optical injection and optical feedback are described as external means to control aspects of the VCSEL optical properties. Also a simple method for the measurement of the polarisation state is described.

Chapter 3 presents experimental results on the effects of circularly polarised optical injection on the polarisation state of VCSEL emission and is compared to the effects of linear polarised optical injection. In addition, the influence of the optical injection on the light–current (L-I) curve and polarisation resolved output power have been studied.

Chapter 4 concerns circularly polarised optical feedback effects on the emission polarisation of VCSELs. Also the effect of linear polarisation feedback (including polarisation selective and orthogonal polarisation feedback) have been investigated and compared to the circularly polarised optical feedback.

In chapter 5 the role of the suppressed mode in polarisation switching of optically injected VCSELs is investigated and the characteristics of the device are explored over a wide range of frequency detuning and optical injection power. The switching power required for polarisation switching is studied at various bias current and polarisation angles of the injected light.

In chapter 6 irreversible polarisation switching characteristics in optically injected two-mode VCSELs are addressed. In this operated regime robust and irreversible polarisation switching were observed with scanning frequency detuning and optical injection power. In addition, intensity induced polarisation switching bistability have studied. Furthermore, polarisation resolved output power for VCSEL using optical injection has been presented

Chapter 7 reports ultra-wide hysteresis frequency bistability of VCSELs subject to orthogonal optical injection. Bistability and hysteresis were investigated at high bias currents (higher-order transverse mode regime) for a wide range of frequency detuning.

Dynamical hysteresis and thermal effects in directly modulated VCSELs were investigated experimentally in chapter 8. The observations were compared to numerical results.

Finally chapter 9 gives the overall conclusions of the entire experimental work carried out in this thesis. Proposals for future work are also presented in chapter 9.

References:

[1] **T. H. Maiman,** "Stimulated radiation in ruby," Nature, vol. **187**, pp. 493-494, Aug. **1960.**

[2] **M. I. Nathan,** W. P. Dumke, G. Burns, F. H. Dill, and G. Lasher, "Stimulated emission of radiation from GaAS p-n junctions," Appl. Phys. Lett., vol. 1, pp. 62-63, Nov. **1962.**

[3] **N. Holonyak**, and S. F. Bevacqua, "Coherent (visible) light emission from Ga(As1-xpx) junctions," Appl. Phys. Lett., vol. 1, pp. 82-83, Dec. **1962.**

[4] **R. N. Hall,** G. E. Fenner, J. D. Kingsley and R. O. Carlson, "Coherent Light Emission From GaAs Junctions," Phys. Rev. Lett., vol.9, pp. 366–368, Nov. **1962.**

[5] **M. G. A.** Bernard and G. Duraffoug, "Laser condition in semiconductors," Phys. Status Solidi, vol.1, pp. 699-673, **1961.**

[6] **J. I. Pankove,** "Influence of degeneracy on recombination radiation in germanium," Phys. Rev. Lett., vol.4, pp.20–21 Jan. **1960.**

[7] **I. Hayashi,** M. B. Panish, P. W. Foy, and S. Sumski, "Junction lasers which operate continuously at room temperature," Appl. Phys. Lett., vol.17, pp. 109-111, **1970.**

[8] **H. Soda,** K. Iga, C. Kitahara and Y. Suematsu, "GaInAsP/InP surface emitting semiconductor lasers," JPN. J. Appl. Phys., vol. 18, pp. 2329- 2330, **1979.**

[9] **K. Iga,** S. Ishikawa, S. Ohkouchi, and T. Nishimura, "Room temperature pulsed oscillation of GaAlAs/GaAs surface emitting injection laser," Appl. Phys. Lett., vol. 45, pp. 348–350, **1984.**

[10] **F. Koyama,** S. Kinoshita, and K. Iga, "Room temperature continuous wave vertical cavity surface emitting laser and high-power 2D laser arrays," in Tech. Digest, Conf. Lasers and Electro-Optics, paper FC1, pp. 380–381, **1989.**

[11] **T. Baba,** Y. Yogo, K. Suzuki, F. Koyama, and K. Iga, "Near room temperature continuous wave lasing characteristics of GaInAsP/InP surface emitting laser," Electron. Lett., vol. 29, pp. 913–914, May **1993.**

[12] **J. J. Dudley,** D. I. Babic, R. Mirin, L. Yang, B. I. Miller, R. J. Ram, T. Reynolds, E. L. Hu, and J. E. Bowers, "Low threshold, wafer fused long wavelength vertical cavity lasers", Appl. Phys. Lett., vol. 64, pp.1463-5, **1994.**

[13] **G. M. Yang,** M. MacDougal, and P. D. Dupkus, "Ultralow threshold current vertical cavity surface emitting laser obtained with selective oxidation," Electron. Lett., vol. 31, pp. 886–888, **1995.**

[14] **Y. Hayashi,** T. Mukaihara, N. Hatori, N. Ohnoki, A. Matsutani, F. Koyama, and K. Iga, "Lasing characteristics of low-threshold oxide confinement InGaAs-GaAlAs vertical-cavity surface-emitting lasers," IEEE Photon. Technol. Lett., vol. 7, pp. 1234–1236, Nov. **1995**.

[15] **A. H. Saito,** K. Nishi, I. Ogura, S. Sugou, and Y. Sugimoto, "Room temperature lasing operation of a quantum dot vertical cavity surface emitting lasers," Appl. Phys. Lett., vol. 69, pp. 3140–3142, **1996.**

[16] **C. Carlsson,** C. A. Barrios, E. R. Messmer, A. Lövqvist, J. Halonen, J. Vukusic, M. Ghisoni, S. Lourdudoss, and A. Larsson, "Performance characteristics of buried heterostructure VCSELs Using semi-Insulating GaInP:Fe regrowth," IEEE J. Quantum Electron., vol.**37**, pp. 945-950, Jul. **2001.**

[17] **G. M. Yang,** M. MacDougal, and P. D. Dupkus, "Ultralow threshold current vertical cavity surface emitting laser obtained with selective oxidation," Electron. Lett., vol. 31, pp. 886–888, 1995.

[18] **M. Muller**, W. Hofmann, T. Grundl, M. Horn, P. Wolf, R. D. Nagel, E. Ronneberg, G. Bohm, D. Bimberg, and M.-C. Amann, "1550-nm high-speed short-cavity VCSELs," IEEE J. Select. Top. Quantum Electron., vol. **17**, pp. 1158-1166, Sep.–Oct. **2011.**

[19] D. Bimberg, "Ultrafast VCSELs for datacom," IEEE Photo. Journal, vol. 2, pp. 273-275, Apr. **2010.**

[20] **Y. Ohno,** S. Shimomura, S. Hiyamizu, Y. Takasuka, M. Ogura, and K. Komori, " Polarization control of vertical cavity surface emitting laser structure by using self-organized quantum wires grown on (775)B-oriented GaAs substrate by molecular beam epitaxy," J. Vac. Sci. Technol. B, vol. 22**,** pp. 1526 -1528, **2004.**

[21] **M. V. R. Murty,** Leo M. F. Chirovsky, Syn-Yem Hu, D. Venables, M. Cheng, and C. M. Ciesla, "Performance and reliability of 12.5-Gb/s oxide-free 850-nm mesa VCSELs," IEEE J. Quantum Electron., vol. 44, pp. 226-231, Mar. **2008.**

[22] **K. Iga,** "Surface-emitting laser-its birth and generation of new optoelectronics field," IEEE J. Select. Top. Quantum Electron., vol. 6, pp.1201-1215, Nov.–Dec. **2000.**

[23] **F. Koyama**, "Recent advances of VCSEL photonics," IEEE, J. of Lightwav. Tech., vol. 24, pp. 4502-4513, Dec. **2006.**

[24] **C. Lin,** Y. Chi, H. Kuo, P. Peng, C. J. Chang-Hasnain, and G. Lin, " Beyond-bandwidth electrical pulse modulation of a TO-Can packaged VCSEL for 10 Gbit/s injection-locked NRZ-to-RZ transmission," IEEE, J. of Lightwav. Tech., vol. 29, pp. 830-841, Mar. **2011.**

[25] **J.M. Catchmark,** L.E. Rogers, R.A. Morgan, M.T. Asom, G.D. Guth, and D.N. Christodoulides, "Optical characteristics of multitransverse-mode vertical-cavity top surface-emitting laser arrays," IEEE J. Quantum Electron., vol. 32, 986-995, **1996.**

[26] **C. Degen,** I. Fischer and W. Elsaber, "Transverse modes in oxide confined VCSELs: Influence of pump profile, spatial hole burning, and thermal effects," Optic. Exp., vol. 5, pp. 38-47, August **1999.**

[27] **G. C. Wilson,** D. M. Kuchta, J.D.Walker, and J.S. Smith, "Spatial hole-burning and self-focusing in vertical-cavity surface-emitting laser diodes," Appl. Phys. Lett., vol. 64, 542-544, **1994.**

[28] **C.J. Chang-Hasnain,** J.P. Harbison, G. Hasnain, A.C. Von Lehmen, L.T. Florez and N.G. Stoffel, "Dynamic, polarization and transverse mode characteristics of vertical-cavity surface-emitting lasers," IEEE J. Quantum Electron., vol. 27, 1402-1408, Jun.**1991.**

CHAPTER TWO

VCSEL POLARISATION CHARACTERISTICS

◆━━━━━━━━━━━━━━━━━━━━━━━━━━━━━━◆

In chapter 1, a brief introduction to VCSELs including, their advantages and main challenges was given. In particular, attention was drawn to their complicated polarisation properties which are one of the main challenges to their deployment in polarisation-sensitive applications. In this chapter an overview of the polarisation properties of VCSELs is presented. The physical principles underlying polarisation selection, polarisation switching and polarisation control in VCSELs are outlined here. The treatment includes a discussion of means for obtaining circularly polarised emission from VCSELs and an indication of the utility of such circularly polarised emission.

The contents of this chapter are organised as follows:

In section 2.1 VCSEL emission characteristics including, polarisation-resolved light-current characteristics and linear polarisation properties are presented. Section 2.2 describes the physical principles underpinning linear polarisation state selection, polarisation switching and polarisation bistability in stand-alone VCSELs. In section 2.3 circularly polarised VCSELs and their advantages are addressed. Section 2.4 provides a brief introduction to approaches, including optical injection and optical feedback, to control the polarisation of VCSELs. In section 2.5 a simple method for measuring the polarisation state of light is presented. Finally section 2.6 summarizes the physical background for the experimental work described in the thesis.

2.1   Introduction

The performance of a laser is characterised by a number of properties including lasing threshold, optical spectra, emission wavelength, dynamical behaviour and polarisation characteristics (the polarisation here being the optical polarisation). The emission characteristics are, in particular, determined by a number of factors such as the laser cavity geometry, gain profile in the active region, optical, electrical and thermal processes inside of the laser.

The light-current (L-I) curve is an important indicator of optical properties for VCSELs giving: the output power of the device at a certain input current ; enabling the threshold current of the laser to be determined; the efficiency of VCSELs can also be derived from

the L-I curve characteristics. In the case of single transverse mode 850 nm VCSELs, high output power of several milliwatts (mW) and high differential efficiency (80%) have been obtained [1]. (Differential efficiency is the differential change of the output power with injected current.) Although VCSELs are widely used in low power applications, they have the inherent potential of producing very high output power (more than 4 kW) using two dimensional arrays [2].

Despite the fact that typical VCSEL designs result in single longitudinal mode operation there are possibilities that the laser output will contain a number of transverse modes. For VCSELs operating well above threshold multi-transverse mode operation is expected. The excitation of such higher order transverse modes may be accompanied by changes in the polarisation direction of the device output. The excitation of multi-transverse mode emission is usually a consequence of spatial hole burning (SHB) in the laser gain [3]. Considerable research effort was devoted in the early 1990s to understanding the fundamental properties of VCSELs including the selection of the polarisation state and the transverse mode dynamics [3-8].

In addition, measurements of optical properties include determining the optical polarisation characteristics of the device (e.g. polarisation switching, polarisation state selection and polarisation bistability). More general properties and design characteristics of VCSELs are covered in more detail e.g. in references [9, 10]. In the following sections the state of the art of determining the polarisation properties of the device are reviewed as a basis for the novel experimental aspects considered in this thesis.

2.2 Emission polarisation of VCSELs : *An overview*

The polarisation properties of VCSELs emission are rather complicated and at the same time a very exciting research field. The complication arises due to the fact that several physical mechanisms may contribute to polarisation selection. Due to the cylindrical geometry of typical VCSELs, the direction of polarisation of VCSEL emission is not, in general, pre-defined. Typically VCSELs emission may be aligned in one of two linearly polarised orthogonal modes, and denoted as the parallel mode ($P_{||}$) and the orthogonal mode ($P_{\perp}$).

Near threshold stand-alone VCSELs usually exhibit linearly polarised emission in a specific direction which is defined in this work as the x-direction and sometimes referred to as the parallel mode; light polarised orthogonal to x polarisation is termed y-direction or the orthogonal mode. These two modes are separated in frequency by birefringence whose

value is dependent on the bias current [11]. Birefringence has been found to be vary from device to device with values ranging from smaller than 1 GHz to tens of GHz [12].

In [13] two ingredients were suggested to explain the physical principles behind the polarisation state selection in SLs. The first ingredient is the angular momentum of the quantum states involved in the optical transitions. The second ingredient is associated with linear effects of the laser cavity, which include anisotropies (birefringence, dichroism), geometry and waveguiding effects. Dichroism means that the light absorption of material depends on the polarisation direction.

In VCSELs the cylindrical symmetry and the isotropy of the linear optical properties of the semiconductor compounds make the nonlinear gain dynamics (first ingredient) much more important in determining polarisation state of the emitted light. In addition, the linewidth enhancement factor and birefringence are also important mechanisms of polarisation selection in VCSELs [13].

Furthermore, the model described in [14] suggested that the geometry of the laser plays an important role in the selection of the preferred polarisation direction. It was predicted that the dominant polarisation depends upon the manner in which the current is injected into the active region, while the degree of polarisation depends on the transverse dimensions of the device.

Despite numerous studies conducted toward understanding mechanisms of polarisation selection in VCSELs, polarisation selection and polarisation control are not fully understood. Therefore, chapter 3 & 4 of this thesis are devoted to investigate experimentally the polarisation of the VCSELs emission using external optical injection and optical feedback.

Polarisation switching (PS) and polarisation bistability (PB) are considered as the most prominent effects observed in VCSELs. PS is defined as a sudden change of the output power from one initially polarised mode to the orthogonally polarised mode, while PB means both polarisation modes are stable. In the following both phenomena are discussed in more detail.

2.2.1 Polarisation switching: stand-alone VCSELs

Polarisation instabilities e.g. PS between fundamental modes are often observed in stand-alone VCSELs when operating parameters (bias current/device temperature) are changed. Two types of PS between the fundamental modes have been found; the first involves a switch from the high frequency mode to the low frequency mode named (PS type 1) ; the

second one occurs from the low frequency mode to the high frequency mode (PS type 2) [11]. Depending on the device structure, the device may exhibits PS type 1 or PS type 2 and in some cases both types of PS can be observed.

Uncontrollable PS in VCSELs can be a disadvantage in many applications. This polarisation instability in VCSELs is not attributed to a single effect but is dependent on several nonlinearities inside laser cavity [3-7]. Different physical models were used to describe PS in VCSELs. The most commonly used models to explain PS in VCSELs are the thermal model (thermal origin) and the spin flip model (SFM).

The early explanation for PS in VCSELs output was given by Choquette et al. [15], and based on the change of the modal gain with increasing bias current. Another explanation [4] for PS was offered in terms of the gain differential between the modes. When the gain differential is small there are two peaks in emission spectrum near threshold and PS observed when bias current increases. While for large gain differential there is single mode operation without PS between fundamental modes [4].

In addition, the four- level SFM model has been widely used to describe a number of polarisation properties including the observation of PS in VCSELs [5]. In the framework of the SFM model, the different polarisations directions/state of the VCSEL emission are associated with different spin sub-levels of the lasing transitions between conduction and valence bands. The main challenges for SFM model is that the fundamental parameter (spin flip parameter/ spin flip relaxation -γ_s) of the model has not been measured directly.

In brief, the commonly attributed mechanisms responsible for PS in VCSELs include linear effects such as thermal shift (i.e. thermal shift of the semiconductor band gap) [11] and nonlinear effects such as the so-called saturable dispersion effect associated with the carrier and frequency dependence of the refractive index [16].

2.2.2 Polarisation bistability in VCSELs

Polarisation bistability (PB) in VCSELs has attracted considerable attention over the last two decades. Extensive studies have been devoted to both experimental [17-20] and theoretical [21-22] investigations of PB in VCSELs. The physical principle of the PB may attributed to various factors, however, Agrawal et al. [23] explained that the bistability behaviour in semiconductor lasers is due to nonlinearities associated with above threshold gain saturation.

 In VCSELs for most operating conditions one state of linear polarisation is stable. These conditions include the combination of the influence of birefringence and weak dichroism.

On the other hand, VCSELs under certain conditions regions appear where both polarisations are stable thereby enabling bistability. A polarisation bistable VCSEL is characterised by two orthogonally polarised lasing modes. In [20] PB in the L-I curves of the VCSELs was observed for the first time. The PB behaviour of VCSELs is found to be dependent on device temperature. For VCSELs PB can be observed over a wide range of bias currents. Recently, oxide confined polarisation-bistable VCSELs (850 nm, 1550 nm) were suggested for use in future ultrafast all-optical communications network [24].

Furthermore, PB was commonly observed in VCSELs supporting a single transverse mode, however a multi-transverse mode VCSELs subject to orthogonal optical injection also exhibited PB [25]. In Quirce et al. [25], a square shape and very wide hysteresis cycle was obtained for output power of parallel-polarised higher-order modes using orthogonal optical injection. In Chapter 7 the polarisation bistability of VCSELs under external optical injection is investigated experimentally.

2.3 Circular polarisation VCSELs

Despite the fact that most commercial available VCSELs emit linearly polarised light, some aspects and device structures make circularly polarised (CP) VCSELs possible. Various design and techniques have been proposed to favour the emission of circularly polarised light by VCSELs. This includes electrically pumped spin-VCSELs which are still under development [26]. In [27] an external cavity laser proposed consisting a Bragg grating and quarter wave plate, which result in producing highly degree of circularly polarised externally cavity laser operated at~1550 nm.

On the basis of the SFM mentioned in section 2.2 the coexistence of two different electron-hole recombination transitions, gives rise to circularly polarised fields with opposite direction [5]. The high degree of transverse symmetry of the circular VCSEL cavity is a factor for potential of circular polarisation state emission even though practical devices almost always have a preference for linear polarisation. Recently, new approaches have been proposed to influence the polarisation state of VCSELs emission [28, 29]. These include circularly polarised optical injection and circularly polarised optical feedback. Using such means the polarisation state of VCSELs emission has been amended to include some degree of circular polarisation. More detail about these novel aspects will be presented in Chapter 3 and Chapter 4.

Furthermore, by introducing misalignment between birefringence and dichroism elliptically polarised VCSELs emission was predicted [30]. The elliptical polarisation state of

electrically pumped VCSELs was investigated experimentally and theoretically [31] where elliptical polarised emission and dynamical states accompanied polarisation switching. This was explained as a strong indication that the spin dynamics determine the state of polarisation in the VCSELs.

The increasing interest in CP laser emission is due to a number of applications for such sources of light. This includes ultra-fast optical switching and high speed optical communication system above 40 gigabit/sec (Gb/s). The next section provides a brief introduction of the approaches for controlling the polarisation properties of VCSEL emission.

2.4 Approaches to polarisation control of VCSELs

The lack of a pre-determined direction of polarisation of VCSELs was highlighted in Chapter 1 (section 1.3) as one of the main drawbacks of these devices, and has been extensively studied [3-8]. The polarisation properties of VCSELs were explored in the early stages of device development [32]. The identification of factors to enable control of the polarisation is quite difficult due to the complex structure of VCSELs. In fact, a precise meaning of complete polarisation control is not defined in the literature. The complete polarisation control reported in [33] applied, in fact, only for specific operating conditions. These conditions include specific bias currents or a range of device operating temperatures.

A variety of techniques and methods have been proposed to control the polarisation state of the VCSELs emission. These include techniques which control polarisation at the device fabrication level and using external controls. As stated in section 2.2 the unpredictability of the polarisation direction of the VCSELs arises mainly from the circular symmetry of typical VCSELs. Therefore pre-determination of the polarisation direction can be achieved by breaking that symmetry. A number of techniques for polarisation control at the fabrication level have been indicated and are mostly based on the introduction of anisotropic optical gain or loss. Such techniques include asymmetric cavities [33], asymmetric current injection [34], asymmetric oxide aperture [35], non-circular resonators (e.g. elliptical current apertures) [36], and high contrast grating [37].

Polarisation control by external methods mainly concerns the use of optical injection from an external laser or optical feedback. These two approaches have been used in the experimental work of this thesis. In the following two sub-sections these schemes are described in more detail.

2.4.1 External optical injection

VCSELs subject to external optical injection offer a number of methods for controlling laser characteristics and performance which have been researched actively over the past two decades. Both theoretical and experimental investigations of different type of VCSELs subject to various forms of external optical injection have been undertaken [38-40].

Figure 2.1 shows a simple diagram of external laser optical injection. The master laser was the injecting laser; the slave laser was the target VCSEL. The optical isolator is used to ensure uni-directional optical injection.

The operating characteristics of the target VCSELs are changed using available optical injection control parameters.

The influence of the optical injection depends on a number of parameters including:

1- The frequency detuning $\Delta \upsilon$ being the difference optical frequency of the injecting or master laser ($\upsilon_{ml)}$ and that of the target or slave laser (υ_{sl}).

$$\Delta \upsilon = \upsilon_{ml} - \upsilon_{sl} \dots\dots\dots\dots\dots\dots\dots\dots\dots\dots\dots\dots\dots\dots\dots \ (1)$$

2- The optical injection strength (the optical power injected into the target or slave laser).

3- The polarisation of the injected beam.

Figure 2.1 Schematic setup of the master-slave laser configuration
Optical isolator is used for unidirectional coupling.

Using external optical injection a rich variety of dynamical behaviours of VCSELs output has been reported [41, 42]. VCSELs subject to external optical injection can exhibit several forms of nonlinear dynamics which include limit cycle behaviour, periodic dynamics, wave mixing and deterministic chaos [43]. Other interesting phenomena arising in VCSELs subject to optical injection are polarisation switching and polarisation bistability [44-46]. Most experimental work concerning optical injection in VCSELs has made use of linearly polarised optical injection either orthogonal or parallel to the stand-alone VCSEL polarisation [38-43].

2.4.2 Optical feedback

The effect of external optical feedback (OF) on semiconductor lasers and particularly VCSELs is of great importance both for understanding device properties and for practical applications of the lasers. Generally, semiconductor lasers including VCSELs are characterised by a high optical gain [48]. Figure 2.1 shows the setup of the feedback scheme in semiconductor lasers.

Figure 2.2 Schematic setup of the SL subject to optical feedback

Although, VCSELs have major differences with conventional EELs in terms of their design structure and output beam characteristics, however, VCSELs are as sensitive to OF as EELs. In both types of semiconductor lasers the similar kinds of dynamical regimes - defined below - are observed when subject to optical feedback. This similarity of response to OF comes from the fact that high reflectivity of VCSELs compensated by extremely short laser cavity (i.e. round trip time inside laser cavity) resulting in both types of device having similar photon lifetimes [49].

Optical feedback techniques can lead to lasing threshold reduction, linewidth narrowing or broadening, stable laser output power; improve spatial and temporal coherence, low frequency fluctuations (LFF) and chaotic dynamics. Despite the fact that numerous number of researches carried out using OF to investigate SLs characteristics, the research field is still very active [50, 51].

Regimes of optical feedback in VCSELs

The feedback strength is quantified with the so called feedback power ratio. In [52] depending on the feedback ratio five regimes for VCSELs subject to optical feedback were found. These regimes determine how VCSELs behave when subject to increasing external feedback.

- In regime 1: single mode operation, spectral line narrowing and broadening were observed.

- Regime 2: multimode operation, mode hopping and spectral line splitting occurs.

- Regime 3: spectral line narrowing was observed, mode hopping suppressed.

- Regime 4: large spectral line broadening coherence collapse occurs.
- In regime 5: single mode operation, which cannot be observed in VCSELs due to their highly reflection of DBRs.

Understanding VCSELs characteristics under OF is of great importance in applications such as optical communication where coupling laser light into an optical fibre can induce small amount of unavoidable feedback light into the laser. This small amount of feedback can affect SL dynamics, spectral characteristics, or introduce new attractive properties in some cases.

2.5 Measurement of the polarisation state

Information about the polarisation characteristics of VCSELs including polarisation direction/state is important for device characterisation. One important means of obtaining this information makes use of the Stokes polarisation parameters (SPPs). These parameters provide information about the degree of linear and circular polarisation.

Several methods have been found to measure SPPs [53]. The SPPs have been widely used for the complete description of the polarisation state [27-29]. The method which has been used in the present work involves a linear polariser (LP) and quarter wave plate (QWP) and is illustrated in figure 2.3. The QWP is wavelength dependent; therefore, QWP for 850 nm was selected in the experiments to match the wavelength of the laser beam. The SPPs are useful because they are amenable to direct measurement.

The parameters $[S_0, S_1, S_2,$ and $S_3]$ express the polarisation state of the optical beam in an intensity formulation.

$$S_0 = I_0,$$
$$S_1 = I_x - I_y,$$
$$S_2 = I_{+45} - L_{45},$$
$$S_3 = I_r - I_l, \quad \dots\dots\dots\dots\dots\dots\dots\dots\dots\dots\dots (2)$$

Where:

I_0 is the total intensity of the optical beam.

I_x, I_y are intensities along the x and y axis of the linear polariser.

I_{45}, L_{45} represents the intensities at 45° and -45° degree angles to the x axis of the linear polariser.

I_r and I_l represent the light intensities of the right and left circularly polarised respectively.

The first Stokes parameter, S_0, simply measures the total intensity of the optical beam; S_1 describes the amount of linear horizontal (0° or x) or linear vertical (90° or y) polarisation, S_2 describes the amount of linear +45° or -45° polarisation and the fourth Stokes parameter S_3 describes the amount of right/left circular polarisation.
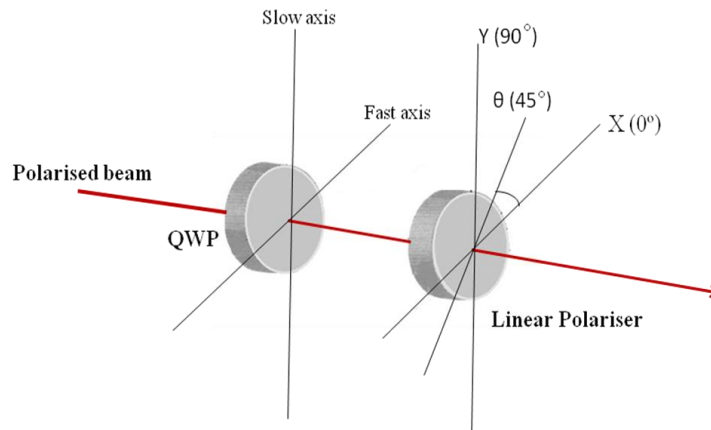

Figure 2.3 the basic setup of polarisation analyser to measure Stokes polarisation parameters. QWP- quarter wave plate.

The conditions for linear polarised light are $S_1 \neq 0$, $S_2 \neq 0$, $S_3 = 0$, while for circularly polarised light are $S_1 = 0$, $S_2 = 0$, $S_3 \neq 0$ indicating that the fourth parameter S_3 will indicate whether the polarisation state is linear or circular [53]. The degree of circular polarisation (DoCP) of the light is defined as the ratio of the absolute value fourth Stokes parameter (S_3) divided by the total intensity of the beam (S_0).

$$DoCP = \frac{|S_3|}{S_0} \quad \cdots\cdots\cdots\cdots\cdots\cdots\cdots\cdots\cdots\cdots (3)$$

2.6   Summary

This chapter has given an overview of the physical principles underlying polarisation selection in VCSELs. Section 2.2 described polarisation instabilities in VCSEL emission including polarisation switching and polarisation bistability, which are investigated experimentally in chapter 5, chapter 6 and chapter 7. Various approaches to the control of polarisation characteristics including external optical injection and optical feedback were discussed.

In section 2.3 interest in VCSELs having circularly polarised emission was indicated. This aspect will be explored in chapter 3 and chapter 4. Novel experimental investigations of

circularly polarised optical injection (chapter 3) and circularly polarised optical feedback (chapter 4) in VCSELs have been undertaken in the present work.

In chapter 3 the influence of circularly polarised optical injection on the polarisation state of VCSELs emission is addressed.

References:

[1] **J.-W. Shi,** C.-C. Chen, Y.-S. Wu, S.-H. Guol, C. Kuo, and Y.-J. Yang**, "**High-power and high-speed Zn-diffusion single fundamental-mode vertical-cavity surface-emitting lasers at 850-nm wavelength," IEEE Photon. Tech. Lett., vol. 20, pp. 1121-1123, Jul. **2008.**

[2] **J.-F. Seurin,** G. Xu, A. Miglo, Q. Wang, R. V. Leeuwen, Y. Xiong, W.-X. Zou, D. Li, J. D. Wynn, V. Khalfin, and C. Ghosh, "High-power vertical-cavity surface-emitting lasers for solid-state pumping," Proc. of SPIE, vol. 8276, pp. 827609-1, **2012.**

[3] **A. Valle,** L. Pesquera, and K. A. Shore, "Polarization behavior of birefringent multi-transverse mode VCSEL's," IEEE Photon. Tech. Lett., vol. 9, pp. 557–559, **1997**.

[4] **C. J. Chang-Hasnain,** J. P. Harbison, G. Hasnain, A. C **.** Von Lehmen, L. T. Florez, and N. G. Stoffel, " Dynamic, polarization, and transverse mode characteristics of vertical cavity surface emitting lasers," IEEE J. Quantum Electron. vol**.** 27, pp. 1402-1409, Jun. **1991**.

[5] **M. San Miguel,** Q. Feng, and V. Moloney, "Light –polarization dynamics   in surface-emitting semiconductor lasers," Phys. Rev. A. vol. 52, pp. 1728-1739, Aug. **1995**.

[6] **S. J. Schablitsky,** L. Zhuang, R. C. Shi, and S. Y. Chou, "Controlling polarization of vertical-cavity surface-emitting lasers using amorphous silicon subwavelength transmission gratings," Appl. Phys. Lett. vol. 69, pp. 7-9, Jul. **1996**.

[7] **J. Martin-Regalado,** F.Prati, M. S. Miguel, and N. B. Abraham, "Polarization properties of vertical-cavity surface-emitting lasers," IEEE J. Quantum Electron., vol. 33, pp. 765–783, May **1997.**

[8] **S. Bandyopadhyay,** Y. Hong, P. S. Spencer, and K. A. Shore, "VCSEL polarization control by optical injection," J. Lightwav. Technol., vol. 21, pp. 2395-2303, **2003.**

[9] **K. Iga,** "Surface-emitting laser—its birth and generation of new optoelectronics field," IEEE J. Select. Top. Quantum Electron. vol. 6, pp.1201-1215, Nov.–Dec. **2000.**

[10] **F. Koyama,** "Recent advances of VCSEL photonics," IEEE, J. of Lightwav. Tech., vol. 24, pp. 4502-4513, Dec. **2006.**

[11] **T. Ackemann** and M. Sondermann, "Characteristics of polarization switching from the low to the high frequency mode in vertical-cavity surface-emitting lasers," Appl. Phys. Lett., vol. 78, pp. 3574-3576, Jun. **2001.**

[12] **M. B. Willemsen,** M. P. van Exter and J. P. Woerdman, "Anatomy of a polarization switch of a vertical-cavity semiconductor laser," Phys. Rev. Lett. vol. 84, pp. 4337–4340, May **2000.**

[13] **M. San Miguel,** "Polarization properties of vertical-cavity surface-emitting lasers," Semiconductor Quantum Optoelectronics, Institute of Physics, Bristol, pp. 339-366, **1999.**

[14] **A. Valle,** K. A. Shore, and L. Pesquera, "Polarization selection in vertical-cavity surface emitting lasers," IEEE J. Lightwav. Technol., vol. 14**,** pp 2062-2068, Sep. **1996.**

[15] **K. D. Choquette,** D. A. Richie, and R. E. Leibenguth, "Temperature dependence of gainguided vertical cavity surface emitting laser polarization," Appl. Phys. Lett. vol. 64, pp. 2062-2064, Apr. **1994.**

[16] **S. Balle,** E. Tolkachova, M. San Miguel, J. R. Tredicce, J. Martin-Regalado, and A. Gahl, " Mechanisms of polarization switching in single-transverse-mode vertical-cavity surface-emitting lasers: thermal shift and nonlinear semiconductor dynamics," Optic. Lett., vol. 24, pp. 1121-1123, Aug. **1999.**

[17] **I. Gatare,** J . Buesa, H . Thienpont, K .Panajotov, and M. Sciamanna, "Polarization switching bistability and dynamics in vertical-cavity surface-emitting laser under orthogonal optical injection," Optical and Quantum Electron., vol. 38, pp. 429–443, **2006**.

[18] **M. Torre,** A. Hurtado, A. Quirce, A. Valle, L. Pesquera, and M. Adams, "Polarization switching in long-wavelength VCSELs subject to orthogonal optical injection," IEEE, J. of Quantum Electron. vol. 47, pp. 92-98, Jan. **2011.**

[19] **A. Quirce,** J. R. Cuesta, A. Valle, A. Hurtado, L. Pesquera, and M. Adams, "Polarization bistability induced by orthogonal optical injection in 1550-nm multimode VCSELs," IEEE J. of Selec. Top. in Quantum Electron., vol. 18, pp. 772-777, Mar./Apr. **2012**.

[20] **H. Kawaguchi,** I. S. Hidayat, Y. Takahashi, and Y. Yamayoshi, "Pitchfork bifurcation polarization bistability in vertical cavity surface emitting lasers," Electron. Lett., vol. 31, pp. 109–111, **Jan. 1995**.

[21] **S. F. Yu,** "Theoretical analysis of polarization bistability in vertical cavity surface emitting semiconductor lasers," IEEE, J. of Lightwav. Tech. vol. 15, pp. 1032-1041, Jun. **1997**.

[22] **M. F. Salvide,** M. S. Torre, A. Valle, and L. Pesquera, "Transverse mode selection and bistability in vertical-cavity surface-emitting lasers induced by parallel polarized optical injection," IEEE, J. of Quantum Electron. vol. 47, pp. 723-730, May **2011**.

[23] **G. P. Agrawal** and N. K. Dutta, " Optical bistability in coupled cavity semiconductor lasers," J. Appl. Phys., vol. 56, pp. 664-669, Aug. **1984**.

[24] **H. Kawaguchi,** "Recent progress in polarization bistable VCSELs," 14th International conference on transparent optical networks (ICTON), **2012**.

[25] **A. Quirce,** J. R. Cuesta, A. Valle, A. Hurtado, L. Pesquera, and M. Adams, "Polarization bistability induced by orthogonal optical injection in 1550-nm multimode VCSELs," IEEE J. of Selec. Top. in Quantum Electron., vol. 18, pp. 772-777, Mar./Apr. **2012.**

[26] **H. Kawaguchi,** S. Koh, "(110) Quantum well based spin VCSELs," CAOL *2010 International Conference on Advanced Optoelectronics & Lasers, pp. 58-60, Sept. **2010.**

[27] **R. K. Kim,** J. H. Song, Y. Oh, D.-Hoon Jang, J. R.Kim, and K. S. Lee, " Circularly Polarized External Cavity Laser Hybrid Integrated With a Polyimide Quarter-Wave Plate on Planar Lightwave Circuit," IEEE Photo. Techno. Lett., vol. 19, pp. 1048-1050, Jul. **2007.**

[28] **A. A. Qader,** Y. Hong and K. Alan Shore, "Lasing characteristics of VCSELs subject to circularly polarized optical injection," IEEE J. Lightw. Technol., vol. 29**,** pp 3804-3809, Dec. **2011.**

[29] **A. A. Qader,** Y. Hong and K. Alan Shore, "Circularly polarized optical feedback effects on the polarization of VCSEL Emission," IEEE Photo. Technol. Lett., vol. 24, pp. 1200-1202, Jul. **2012.**

[30] **M. Travagnin,** "Linear anisotropies and polarization properties of vertical cavity surface-emitting semiconductor lasers," Phys. Rev. A, vol. 56, pp. 4094-4105, Nov. **1997**.

[31] **M. Sondermann,** T. Ackemann, S. Balle, J. Mulet, K. Panajotov, "Experimental and theoretical investigations on elliptically polarized dynamical transition states in the polarization switching of vertical-cavity surface- emitting lasers," Optic. Commun., vol. 235, pp421–434, Feb. **2004.**

[32] **M. Shimizu, F. Koyama**, and K. Iga, "Polarization characteristics of MOCAD grown GaAs/ AlGaAs CBH surface emitting lasers," JPN. J. Appl. Phys., vol. 27, pp. 1774-1775, Sep.**1988.**

[33] **T. Yoshikawa,** H. Kosaka, K. Kurihara, M. Kajita, Y. Sugimoto, and K. Kasahara, "Complete polarization control of 8×8 vertical-cavity surface-emitting laser matrix arrays," Appl. Phys. Lett., vol. 66, pp. 908-910, Feb. **1995.**

[34] **G. Verschaffelt,** W. van der Vleuten, M. Creusen, E. Smalbrugge, T. G. van de Roer, F. Karouta, R. C. Strijbos, J. Danckaert, I. Veretennicof , "Polarization stabilization in vertical-cavity surface- emitting lasers through asymmetric current injection," IEEE Photonics Technology Letters, vol. 12, pp. 945-947, Jan. **2000.**

[35] **K.-H. Ha,** Y.-H. Lee, H.-K. Shin, K.-H. Lee and S .- M. Whang, "Polarization anisotropy in asymmetric oxide aperture VCSELs ," Electron. Lett., vol. 34 pp. 1401-1402, Jul. **1998**.

[36] **B. Weigl,** M. Grabherr, C. Jung, R. Jäger, G. Reiner, R. Michalzik, D. Sowada, and K. J. Ebeling, "High-performance oxide-confined GaAs VCSEL's," IEEE J. Sel. Topics Quantum Electron., vol. 3, pp. 409–415, Apr. **1997.**

[37] **C. J. Chang-Hasnain,** Y. Zhou, M. C. Y. Huang, and C. Chase, "High contrast grating VCSELs," IEEE Sel. Topics Quantum Electron., vol. 15, pp. 869–878, May/Jun. **2009.**

[38] **Z. G. Pan,** S. Jiang, and M. Dagenais, "Optical injection induced polarization bistability in vertical-cavity surface-emitting lasers," Appl. Phys. Lett. vol. 63, pp. 2999-3001, **1993**.

[39] **M. Sciamanna** and K. Panajotov, "Two-mode injection locking in vertical-cavity surface- emitting lasers," Optic. Lett., vol. 30, pp. 2903-2905, Nov. **2005.**

[40] **Y. Hong,** P. S. Spencer, S. Bandyopadhyay, P. Rees and K. A. Shore, "Polarization- resolved chaos and instabilities in a vertical cavity surface emitting laser subject to optical injection," Optic. Commun., vol. 216, pp. 185-189, **2003.**

[41] **T. B. Simpsony,** J M Liuz, K F Huangx and K Taix, "Nonlinear dynamics induced by external optical injection in semiconductor lasers," Quantum Semiclass. Opt., vol. 9, p**p.** 765–784, **1997**.

[42] **I. Gatare,** M. Sciamanna, J. Buesa, H. Thienpont, and K.Panajotov, "Nonlinear dynamics accompanying polarization switching in vertical-cavity surface-emitting lasers with orthogonal optical," Appl. Phys. Lett. vol. 88, pp. 101106, **2006**.

[43] **A. Hurtado,** A. Quirce, A. Valle, L. Pesquera, and M. J. Adams,"Nonlinear dynamics induced by parallel and orthogonal optical injection in 1550 nm vertical-cavity surface-emitting lasers (VCSELs)," Optic. Exp. vol. 18, pp. 9423- 9428, Apr. **2010**.

[44] **J. Martı´n-Regalado,** J. A. Chilla, and J. J.Rocca "Polarization switching in vertical-cavity surface emitting lasers observed at constant active region temperature,", Appl. Phys. Lett. vol. **70**, pp. 3350-3352, Jun. **1997**.

[45] **Y.Hong,** K. A. Shore, A.Larsson, M.Ghisoni and J.Halonen, "Polarization switching in a vertical cavity surface emitting semiconductor laser by frequency detuning," IEE Proc. Optoelectron., vol. 148, pp. 31-34, **2001**.

[46] **I. Gatare,** J . Buesa, H . Thienpont, K .Panajotov, and M. Sciamanna, "Switching bistability and dynamics in vertical-cavity surface-emitting laser under orthogonal optical injection," Optical and Quantum Electronics, vol. 38, pp. 429–443, **2006**.

[47] **Y. Hong,** Rui Ju, P. S. Spencer, and K. A .Shore, "Investigation of polarization bistability in vertical-cavity surface-emitting lasers subjected to optical feedback," IEEE J. of Quantum electron., vol. 41, pp. 619-624, May **2005**.

[48] **M. S. Demokan** and A. Nacaroglu, "An analysis of gain-switched semiconductor lasers generating pulse-code-modulated light with a high bit rate," IEEE J. Quantum Electron., vol. QE-20, Sep. **1984**.

[49] **Y. C. Chung** and Y. H. Lee, "Spectral characteristics of vertical-cavity surface emitting lasers with external optical feedback," IEEE Photo. Tech. Lett., vol. 3, pp. 597-599, Jul. **1991**.

[50] **A. Larsson,** "Advances in VCSELs for communication and sensing," IEEE J. of Selec. Top. Quantum Electron. , vol. 17, pp. 1552-1567, Nov. /Dec. **2011**.

[51] **A. Al-Samaneh,** M. B. Sanayeh, S. Renz, D. Wahl, and R. Michalzik, "Polarization control and dynamic properties of VCSELs for MEMS atomic clock applications," IEEE Photo. Techn. Lett., vol. 23, pp. 1049-1051, Aug. **2011.**

[52] **Y. C. Chung** and Y. H. Lee, "Spectral characteristics of vertical-cavity surface-emitting lasers with external optical feedback," IEEE Photo. Techn. Lett., vol. 3, pp. 597-599, Jul. **1991.**

[53] **D. H. Goldstein,** Polarized light, third edition, CRC press, USA, **2011.**

CHAPTER THREE

CIRCULARLY POLARISED OPTICAL INJECTION EFFECTS ON VCSEL CHARACTERISTICS

In chapter two the polarisation properties of VCSELs have been presented. In particular, the physical mechanisms which explain the selection of the polarisation state, and factors determining the linear polarisation of the VCSEL emission were discussed. In this chapter, experimental investigations of the effects of circularly polarised optical injection (CPOI) on the lasing characteristics of VCSELs are addressed.[1] The effects of CPOI will be compared to those arising with various linearly polarised optical injections. With CPOI the linear output polarisation of the stand-alone VCSEL can be amended to create some degree of circularly polarised emission. In addition, highly non-linear light-current characteristics are observed in the vicinity of threshold of optically injected VCSEL.

The content of this chapter are organised as follows:
In section 3.1 the principles of the CPOI configuration are presented. Section 3.2 includes the detail of the experimental setup used to demonstrate the influences of CPOI on the lasing characteristics of VCSELs. In section 3.3 the stand-alone VCSELs characteristics including L-I curve, polarisation resolved output properties and beam profile are provided. In section 3.4 the output polarisation characteristics of the VCSEL emission under CPOI are analysed. In section 3.5 the role of frequency detuning and injection strength on lasing threshold characteristics of VCSELs has been addressed. Section 3.6 provides polarisation resolved output power of VCSELs with CPOI and compared to linear polarised optical injection. In section 3.7 the spectral characteristics of VCSELs subject to CPOI are presented. Finally section 3.8 summarises the main conclusions derived from the experimental results.

3.1 Circularly polarised optical injection configuration:

Most previously experimental work concerning optical injection into VCSELs has made use of linearly polarised optical injection either orthogonal or parallel to the stand-alone

---

[1]*This chapter is based on the paper:*

A.A. Qader, Y. Hong and K. A. Shore, IEEE, J. Lightwav. Tech., vol. 29, pp. 3804-3809, Dec. 2011.

VCSEL polarisation [1-5]. Recently the first CPOI was reported in [6]. Followed that experimental work a theoretical and experimental work using elliptical and circular polarised optical injection were reported in [7]. The basic principles of the CPOI configuration are presented in the following.

As mentioned in chapter two the optical injection involves two semiconductor lasers, the first one which named a master laser (is a tuning single-frequency laser diode) and second one named a slave laser. Figure 3.1 shows a simplified schematic representation of the various external optical injection schemes. Figure 3.1 (a) which represent the common schematic diagram for linear polarisation optical injection, the polarisation of the injected beam normally controlled through half wave plate (HWP). Using this scheme; parallel, orthogonal and various angles of linear polarised optical injections have been performed.

Figure 3.1(b) shows the schematic diagram for circularly polarised optical injection, which simply can be achieved by replace the HWP with quarter wave plate (QWP). The right- and left-circularly polarised optical injection produced by passing the linearly polarised master laser beam through QWP. The fast axis of the QWP positioned at a 45° (-45°) degree angle to the x direction to produce left (right) CP light respectively.
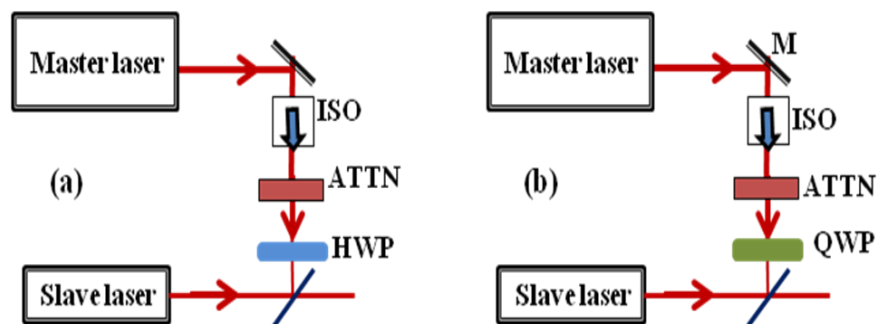

Figure 3.1: Optical injection schemes; a) linear polarised optical injection,
                   b) circularly polarised optical injection.

3.2 Experimental setup

The experimental setup shown in figure 3.2 is used to demonstrate the influence of circularly-polarised optical injection on the behaviour of the target or slave VCSEL. Two commercial oxide-confined VCSELs with operating wavelengths around 850 nm were used in this work. One, termed here VCSEL 1, was obtained from Laser Components (UK) Ltd, and the second, named here as VCSEL 2, was supplied by AVALON Photonics. No details of the VCSEL structure are available. The VCSELs were driven by a programmable DC source (7651 YOKOGAWA) and were temperature controlled with a thermoelectric

temperature controller (TED 200) to within 0.01^0C. A tunable single-frequency laser diode (model SDL-TC10), with a centre wavelength of 850 nm and wavelength tuning range of about 20 nm was used as the master laser. The tunable laser has mode-free-scan over an 800 GHz tuning range. The device also includes means for both coarse and fine tuning of the frequency. A zero order quarter waveplate (QWP) was employed to change the linear polarisation state of the injected field to circular polarisation state. A variable optical attenuator (ATTN) was used to change the strength of the optical injection into the VCSEL slave laser. The output of the SL was collimated using a laser diode objective lens (Newport model F-LA11, Aspheric, 6.24 FL, 0.40 NA, and 3.0 WD).

A beam splitter (believed to be non-polarised) with splitting ratio of 50/50 was used. An optical spectrum analyser (OSA) with resolution of 0.06 nm was used to record the laser spectra. A Fabry–Pérot interferometer (FPI) with a free spectral range of 30 GHz and a finesse of 150 was used to observe the spectral modes of master and slave lasers; two optical isolators were used with effective isolation > 40 dB to prevent feedback from the FPI into the slave laser.

A digital phosphor oscilloscope (Tektronix TDS 7404) with high bandwidth (4 GHz) was used to record the frequency detuning. An optical power meter (Anritsu) was used to record the output power at the position of removable beam block [6].
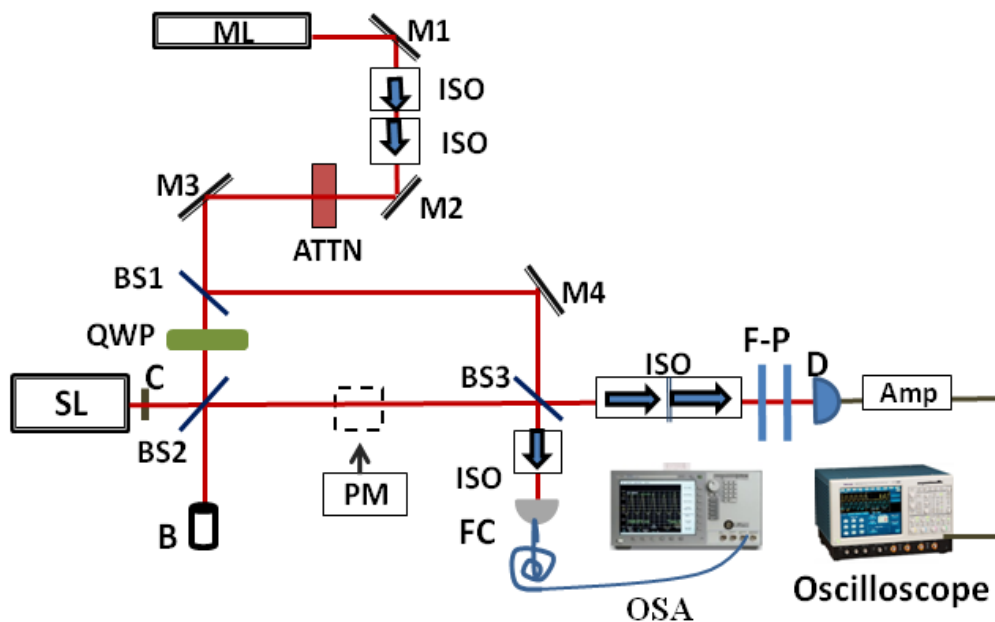

Figure 3.2: *Experimental setup*
ML– master laser; SL– slave laser; C– laser diode objective lens; ISO– optical isolator; BS– beam splitter; ATTN– variable optical attenuator; QWP– Quarter wave plate; M– mirror; D– detector; Amp– amplifier; PM power meter, F-P- Fabry –Pérot interferometer; B– Removable beam block; FC– fibre coupling; OSA–optical spectrum analyser.

3.3   Stand-alone VCSELs characteristics

In this section the optical properties of VCSELs under study are presented. This is including light-current characteristics, polarisation resolved output power and beam profile of the stand-alone VCSELs.

3.3.1 The light-current characteristics:

The L-I curve for VCSELs under study were measured. Figures 3.3(a) and 3.3(b) show the L-I curve of stand- alone VCSEL 1 and VCSEL 2 was obtained using Labview running on a personal computer. The kink in L-I curve of VCSEL 2 is considered to be related to polarisation switching between fundamental modes near 7 mA. The threshold currents of VCSEL 1, VCSEL 2 were 3.7 mA and 2.8 mA, respectively.
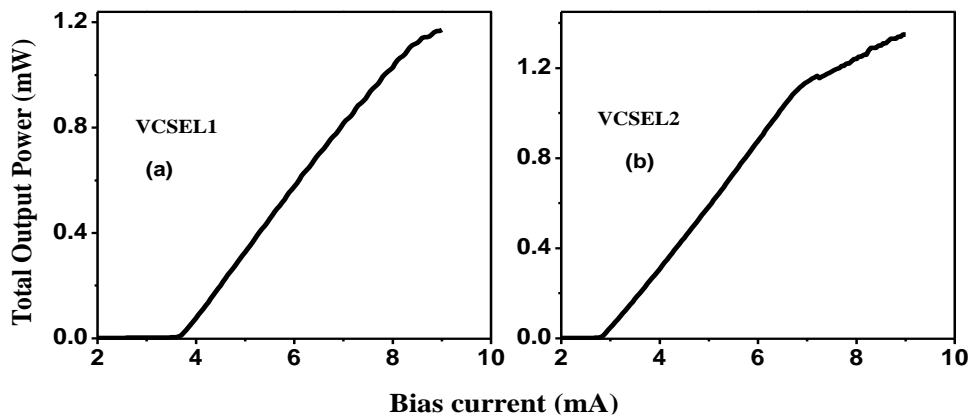
Figure 3.3: *Light-current characteristics of the stand-alone VCSELs under study (a) VCSEL1 and (b) VCSEL2.*

In order to investigate the laser output power includes for any bistability or hysteresis behaviour, the bias current is increased and decreased. The measurements show that for both VCSEL1 and VCSEL2 there is no bistability or hysteresis observed for totally power in L-I curve characteristics of stand-alone VCSELs.

3.3.2 Polarisation resolved output power:

Near threshold both VCSELs exhibit linearly polarised emission in a direction which we define as the x-direction (lasing mode) the black curve the orthogonal polarisation direction is defined here as the y-direction (suppressed mode) the red curve. The difference in power between the lasing mode and suppressed mode increases with increasing VCSEL bias current. The polarisation resolved output power of the stand-alone VCSEL 1, and VCSEL 2 were obtained in Figures 3.4(a) and 3.4(b), respectively.

In Figure 3.4 (a) it can be seen that that VCSEL 1 does not exhibit any polarisation switching (PS) at any value of the bias current, whilst two polarisation switches occurred for VCSEL 2 at bias currents 7.2 mA and 8.2 mA respectively. For VCSEL 1 the increase of power in the y polarisation is related to the excitation of orthogonal higher order modes. Higher order mode spectral characteristics will be discussed further in chapter 5, section 5.4.1.
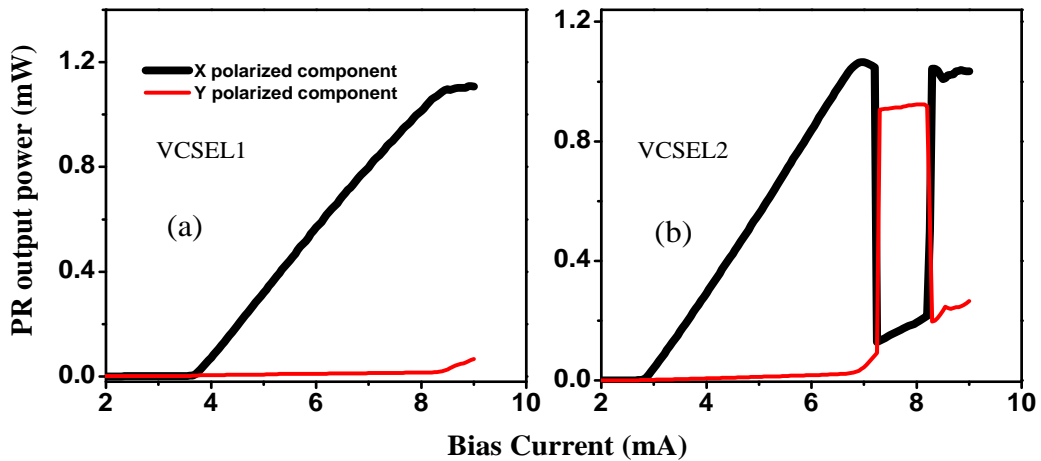

Figure 3.4: Polarisation resolved output power for stand-alone (a) VCSEL1and (b) VCSEL2.

The polarisation state of the VCSEL emission is analysed using Stokes polarisation parameters. The Stokes polarisation parameters for VCSEL 1 and VCSEL 2 were measured at different bias currents. The stand-alone VCSEL emission was found to be linearly polarised and neither VCSEL 1 nor VCSEL 2 exhibits any elliptical polarisation state at any bias current.

3.3.3 Beam profiles for VCSELs and master laser

Beam profile for both slave laser (stand-alone VCSEL 1) and master laser were recorded using charged coupled detector (BeamStar FX-50). Figures 3.5 a1 and a2 show the beam profile for stand-alone VCSEL1 at a bias current 5 mA, indicating circular beam profile. VCSEL2 possesses a similar beam profile as VCSEL1. Figure 3.5 b1 and b2 show the elliptical beam profile of the master laser. For optical injection experiments it is preferred using master laser with circular beam profile. This is due to the fact that the elliptical beam profile is less effective and may choose one polarization mode more than the other of the slave laser.
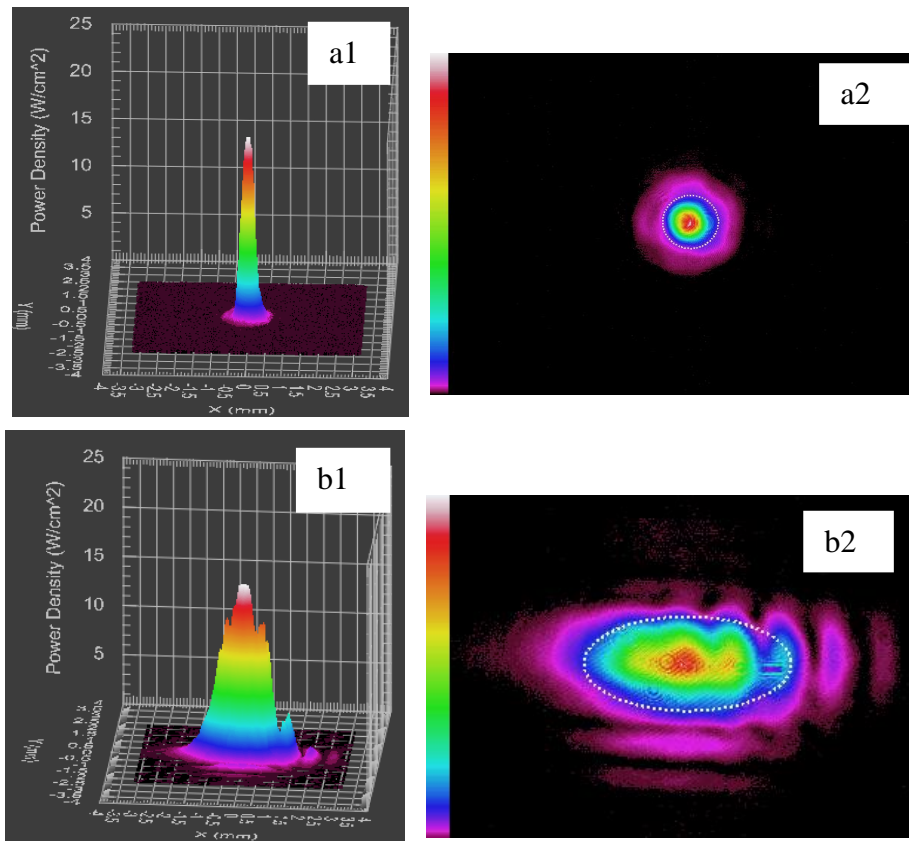
Figure 3.5: *shows 3 D and 2D display a1 and a2 for VCSEL 1*
at I= 5 mA, b1 and b2 for master laser beam profile.

3.3.4 Birefringence in stand-alone VCSELs

In order to measure the frequency spacing between the two orthogonal polarisation modes, a Fabry-Perot interferometer with free spectral range of 30 GHz was used. Figure 3.6 (a) show the optical spectra of VCSEL1 using the Fabry-Perot interferometer, indicating that the birefringence of this device is about -11 GHz when the VCSEL is biased at 6mA. In contrast to what has been observed in [8] the birefringence of the VCSELs used in the experiments here were independent of the VCSELs bias current. Figure 3.6 (b) shows the birefringence as a function of the VCSEL bias current and indicates that the birefringence remains essentially constant (about -11 GHz) over the operating range.

The VCSEL2 birefringence is -10.5 GHz and, again essentially constant over the bias current operating range figure 3.6 (d). For both VCSEL1 and VCSEL2 the lasing mode has higher frequency compared to the suppressed mode (low frequency mode).
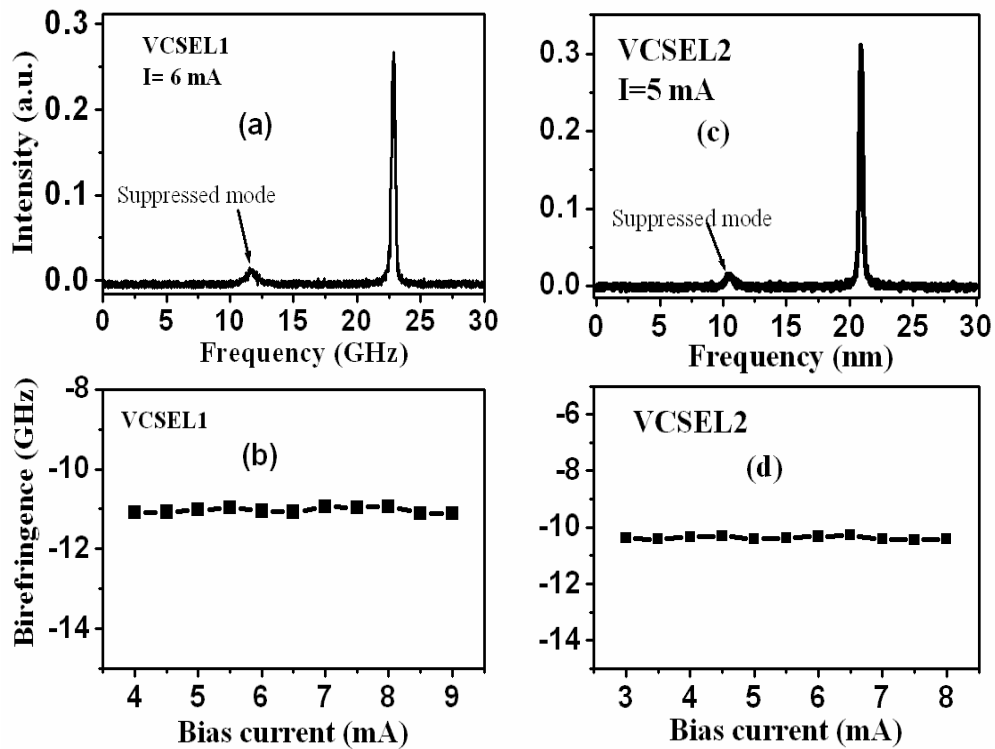
Figure 3.6: *The birefringence of the stand-alone a) VCSEL1, c) VCSEL2 and birefringence as a function of bias current b) VCSEL1, d) VCSEL2.*

3.4 VCSEL polarisation state with circularly polarised optical injection

The polarisation state of vertical cavity surface emitting lasers emission is often linearly polarised. However, the misalignment of birefringence and dichroism axes has potential to produce an elliptical polarised emission in VCSELs [9]. An elliptical polarisation state in the vicinity of polarisation switching in VCSELs has been observed [10] and also in the presence of circular phase anisotropy produced by a magnetic field [11].

In this section use has been made of CPOI using a master- slave laser configuration, to provide additional means for investigating physical processes at work in VCSELs. It is illustrated in the following that the emission below threshold shows interesting polarisation features. This potentially yields interesting insights into the mechanisms involved in the polarisation selection.

In chapter two (section 2.5) the polarisation state of a light beam was discussed in term of Stokes polarisation parameters. The polarisation properties can be characterised using four Stokes polarisation parameters **[S_0, S_1, S_2, S_3].** The Stokes polarisation parameters were obtained simply through measurements of optical intensities I_x, I_y, I_{45}, I_{-45}, I_R and I_L. Where I_x, I_y are intensities along the x and y axis of the linear polarizer; I_{45}, I_{-45} represent the intensities at 45° and -45° degree angles to the x axis of the linear polariser, while I_R and I_L

represent the light intensities of the right and left circularly polarised respectively. All intensities are measured just after BS2 in Figure 3.2.

The Stokes parameters near threshold for stand-alone VCSEL1 and VCSEL 2 were [1, 0.98, 0, 0] and [1, 0.96, 0, 0] respectively, thus indicating linearly horizontally polarised (x-direction) VCSEL light emission. Left/right circularly polarised optical injection into the target VCSEL was produced by passing linearly polarised laser light through the quarter-wave plate (QWP), with the fast axis positioned at 45°/-45° relative to the x axis.

Figure 3.7 shows the degree of circular polarisation of VCSEL 1, as a function of the slave laser bias current. Using left/right CPOI and linear orthogonal polarised optical injection, with optical injection power P_{inj}= 1 mW, at frequency detuning ($\Delta \upsilon$) = − 10 GHz.
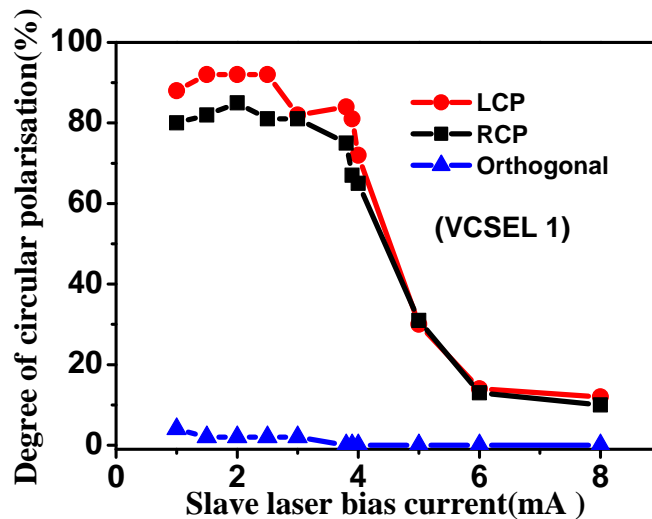

Figure 3.7: *Degree of circular output polarisation of VCSEL 1 under left circularly (red circle), right circularly (black square) and orthogonal (blue triangle) polarised injection. Optical injection strength $P_{inj} = 1$ mW, with $\Delta \upsilon = -10$ GHz.*

The degree of circular polarisation (CP) output of VCSEL 2 under left/right CPOI as a function of the slave laser bias current is shown in Figure 3.8 for an optical injection power P_{inj}= 1.5 mW and a frequency detuning ($\Delta \upsilon$) = − 10 GHz.

For both stand-alone VCSELs it was found that S_3=0 confirming that the VCSELs emission is linearly polarised at any bias current. However, for circularly polarised optical injection S_3 takes different values depending on the VCSEL bias current. Three regimes can be distinguished:

Regime I: Below threshold (i.e. the threshold of the stand-alone VCSEL), **S3** $\cong \pm 0.9$ which indicates a high degree of left/right circularly polarised of VCSEL 1 and VCSEL 2 with injected left/right circularly polarised in figures 3.7 and 3.8. In this region the polarisation

of VCSELs emission will be determined mainly by the optically injected field through injection locking.

Regime II: Near threshold, $S_3 \cong \pm 0.6$ (with non zero values for the other Stokes polarisation parameters) indicating circularly polarised output of VCSEL 1 and VCSEL 2. The competition between external optical injection and electrical excitation determines the circularly polarised state of the VCSELs emission.

Regime III: Far above threshold, $S_3 \cong \pm 0.1$ the DoCP decreases with increasing VCSELs bias current, and the output polarisation of VCSEL 1 emission exhibits a small amount of CP, while the output polarisation of VCSEL 2 switches back to linear polarisation. Here the polarisation of the VCSEL emission is determined mainly by the structure of laser. Recent theoretical work reported in [7] predicted similar relationships between the circular polarisation degree versus bias current.
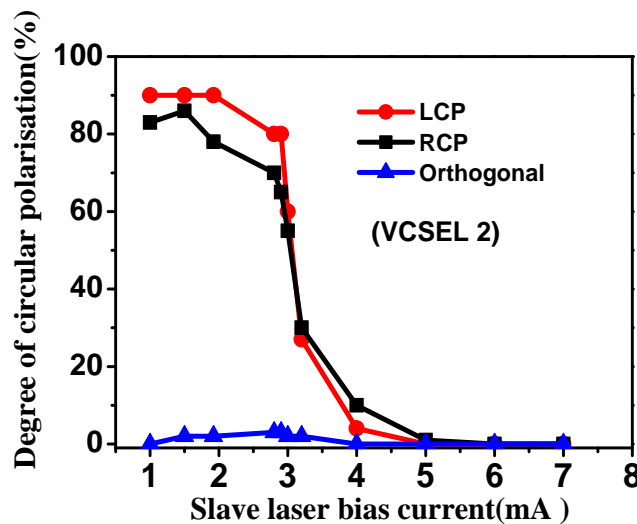

Figure 3.8: Degree of circular output polarisation of VCSEL 2 under left circularly (red circle), right circularly (black square) and orthogonal (blue triangle) polarised injection. Optical injection strength $P_{inj} = 1.5$ mW, with $\Delta \upsilon = - 10$ GHz.

The output polarisation of VCSEL 1 and VCSEL 2 was also analysed using linear orthogonal optical injection as a function of slave laser bias current (see blue triangles in figures 3.7, 3.8). It can be seen that linear orthogonal optical injection does not change the linear polarisation of the VCSEL emission.

For the results in figure 3.7 and 3.8 the injected beam of master laser was not perfect circular profile as show in figure 3.5 (see b1 and b2). The perfect circular profile may reduce the injection power level for obtain specific influence on the VCSELs emission and also avoid preferred linear polarisation along its long axis [12].

3.4 Lasing threshold in optically injected VCSEL

In this section, the influence of optical injection on the lasing threshold of VCSELs will be investigated experimentally. It is well known that the lasing threshold of VCSELs is considerably affected by external optical feedback e.g. reduction in lasing threshold current of VCSELs has been studied theoretically and experimentally [13]. However, the experimental measurement of the influence of optical injection on lasing threshold characteristics of VCSELs has not been investigated previously. It was predicted by Li [14], that the semiconductor laser gain can be enhanced by optical injection and hence the laser threshold current reduced. Experimental studies of the influence of optical injection on gain change and threshold current in edge emitting lasers was investigated in [15].

Figure 3.9 show the influence of the circularly polarised optical injection on the L-I curve characteristics of a) VCSEL1, b) VCSEL2 using three different values of optical injection input power; P_{inj} = 0.5 mW black curve, P_{inj} = 1 mW blue curve, and P_{inj} = 1.5 mW red curve when the frequency detuning $(\Delta \upsilon)$ = − 10 GHz, with respect to the VCSEL slave laser frequency at threshold. It can be seen that CPOI reduces the laser threshold current. Using stronger optical injection accentuates the change. In [15] the reduction in threshold current with optical injection was explained in term of injection locking. Figure 3.9 also shows that the influence of CPOI on the lasing characteristics of VCSELs is dependent on the VCSEL structure. It can be seen clearly that the VCSEL1 output characteristics more affected with optical injection than VCSEL2, in particular for bias current below and near threshold.

In general, for both optically injected VCSELs these regimes can be distinguished in the L-I curve characteristics.

❖ Below and near threshold (is the threshold of stand-alone VCSEL1): The optical injection acts to enhance the VCSEL emission thus effecting a reduction of the lasing threshold current. The nonlinearity below threshold was observed. The possible mechanism for this nonlinearity in term of the interplay below spontaneous emission and external optical injection. Although other mechanisms may be involved, however there is no specific evidence for any alternative explanation. In figure 3.9 the threshold of the injected VCSEL defined as the point at which the total output power suddenly reduces and then increase again is considered as the new threshold with optical injection.

❖ In the vicinity of the stand- alone VCSEL threshold the effect of optical injection is nonlinear. This nonlinearity has its origins in the interplay between spontaneous emission

and optical injection effects on the laser threshold current.

❖ **Far above threshold:** In general, optical injection will increase the output power of the VCSEL slave laser [14], when the optical injection power is sufficiently strong and within a defined frequency detuning range.
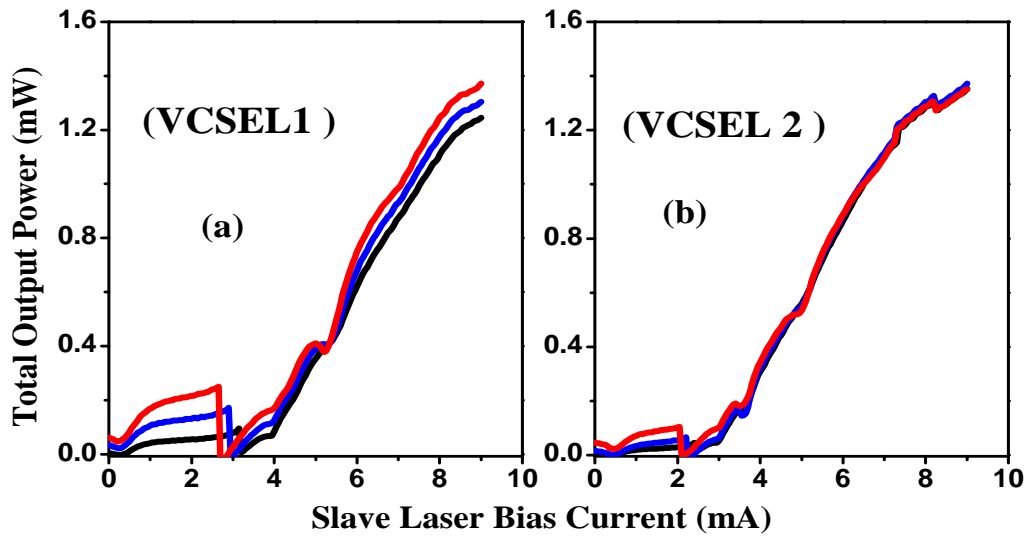

Figure 3.9: *Light-current curves of a) VCSEL 1 and b) VCSEL 2 using P_{inj} = 0.5 mW black curve, P_{inj}= 1mW blue curve, and P_{inj} = 1.5 mW red curve when the $\Delta \upsilon = -10$ GHz.*

In general the VCSELs lasing characteristics are shown to be more affected by optical injection than those of edge emitting lasers (EELs) compared to figure 2 in ref. [15]. This is due to the enhanced change of optical gain within the smaller active volume of VCSELs compared to that in EELs. The precise origin of the non-linearities in L-I curve is not clear, however, they are likely to be associated with changes in the transverse modes.

Figure 3.10 shows the influence of circularly polarised optical injection on the L-I curve characteristics of VCSEL 1, VCSEL 2 for a fixed optical input power (P_{inj}) of 1 mW, 1.5 mW respectively, using two different values of frequency detuning ($\Delta \upsilon$), with respect to the VCSEL slave laser frequency at threshold. In figure 3.10 (a) when $\Delta \upsilon$ =-10 GHz, it can be seen that the lasing threshold of VCSEL 1 red circle and VCSEL 2 black circle are shifted to a lower bias current of about 3 mA, 2.2 mA respectively, compared to the stand- alone threshold 3.7 mA, 2.8 mA. Increasing the frequency detuning to 0 GHz, as shown in figure 10(b), the lasing threshold for both VCSEL 1, VCSEL 2 become 2.8 mA and 2.1 mA respectively.
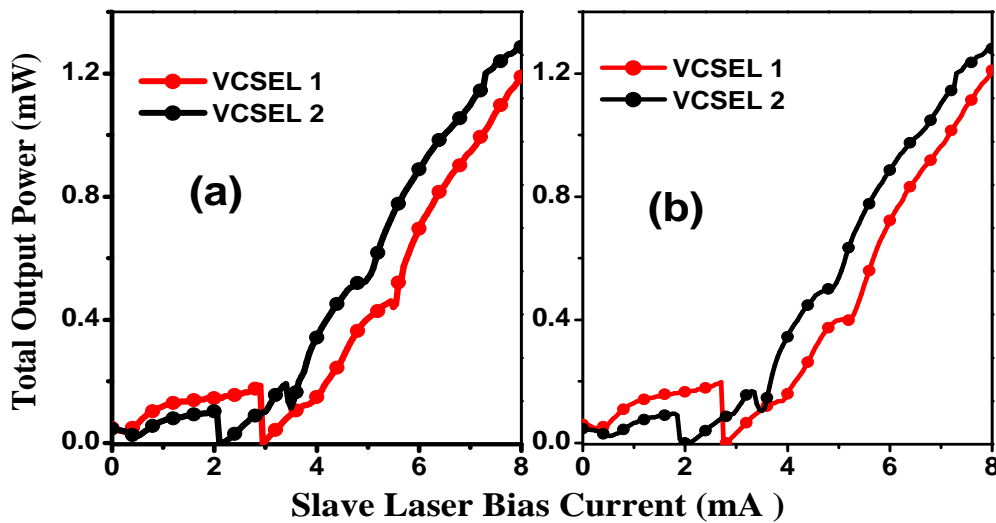
Figure 3.10: *Light- current curves of VCSEL 1 red circle, VCSEL 2*
black circle, a) at $\Delta v = -10$ GHz and b) at $\Delta v = 0$ GHz.

The dynamical behaviour of the total output power of both optically injected VCSEL 1 and VCSEL 2 were recorded at different slave laser bias currents using AC coupled photodector. Figure 3.11 shows the time traces of optically injected VCSEL1 and VCSEL2 at bias current 5 mA and 4 mA respectively. The optical injection power was 1 mW for VCSEL1 and 1.5 mW for VCSEL2, FD in both cases was -10 GHz. The figures show that both were dynamically stable.
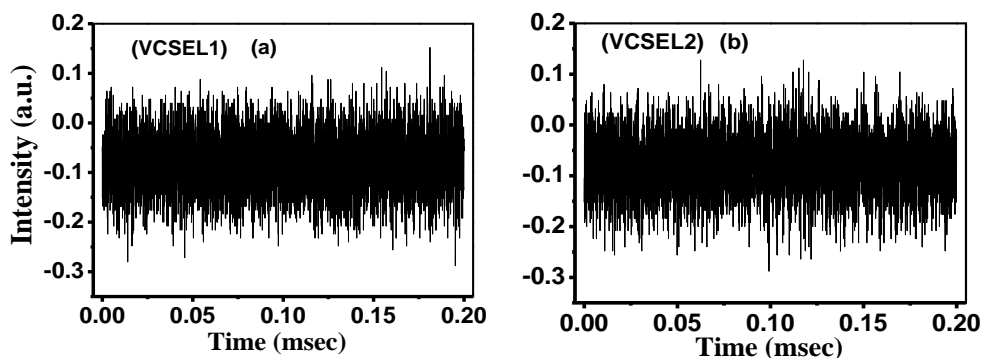
Figure 3.11:   Time traces of intensity of VCSEL 1, VCSEL 2 with CPOI at
bias current 5 mA and 4 mA respectively using AC coupled photodetector.

For both VCSELs there is a range of frequency detuning (from about 20 GHz to -50 GHz) where the injected light beam can influence the lasing threshold current, (see figure 3.12). Similar measurements have been made for linearly polarised injection. These showed similar characteristics as depicted in figure 3.12.

Parallel and orthogonal optical injection was used to compare the effects of linear polarised optical injection (LPOI) and CPOI on lasing characteristics of the VCSELs.

The influences of LPOI and CPOI on the total output power for both VCSELs are similar. However differences are observed between linearly polarised (LP) optical injection and CPOI in the polarisation- resolved L-I curve characteristics.
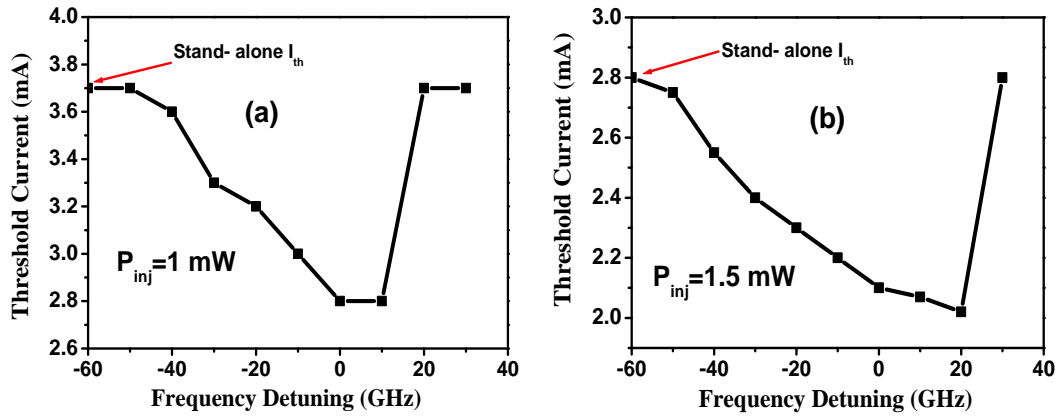

Figure 3.12: Lasing threshold current as a function of Δv using CPOI for a) VCSEL 1 when P_{inj} = 1 mW, b) VCSEL 2 when P_{inj} = 1.5 mW.

3.5 Polarisation resolved output under CPOI

In this section the polarisation resolved output power of VCSELs under CPOI are investigated and compared to linearly polarised optical injection. Figure 3.13 shows polarisation resolved L–I curve of VCSEL1 and VCSEL2 with (a1, b1) CPOI, (a2, b2) LP orthogonal and (a3, b3) LP parallel optical injection.

The optical injection power (P_{inj}) is 1 mW and 1.5 mW for VCSEL1 and VCSEL2 respectively, Δv is -10 GHz in all measurements. black and Red curves represent x and y polarised components of VCSELs respectively.

It can be seen that CPOI influences and enhances both the x polarisation (black line) and y polarisation (red line) modes for VCSEL 1 and VCSEL 2, especially below and near the threshold of stand-alone VCSELs. However, in contrast to CPOI, linear orthogonal (y) polarised optical injection affects mainly the y–polarisation component of VCSELs, as shown in figs. 3.13(a2, b2). On the other hand parallel (x) polarised injection as shown in figs. 3.13(a3, b3) mainly affects the x polarisation component of the VCSEL emission. Figure 3.13 also shows that the lasing characteristics of VCSEL 1 are more affected by optical injection than those of VCSEL 2.
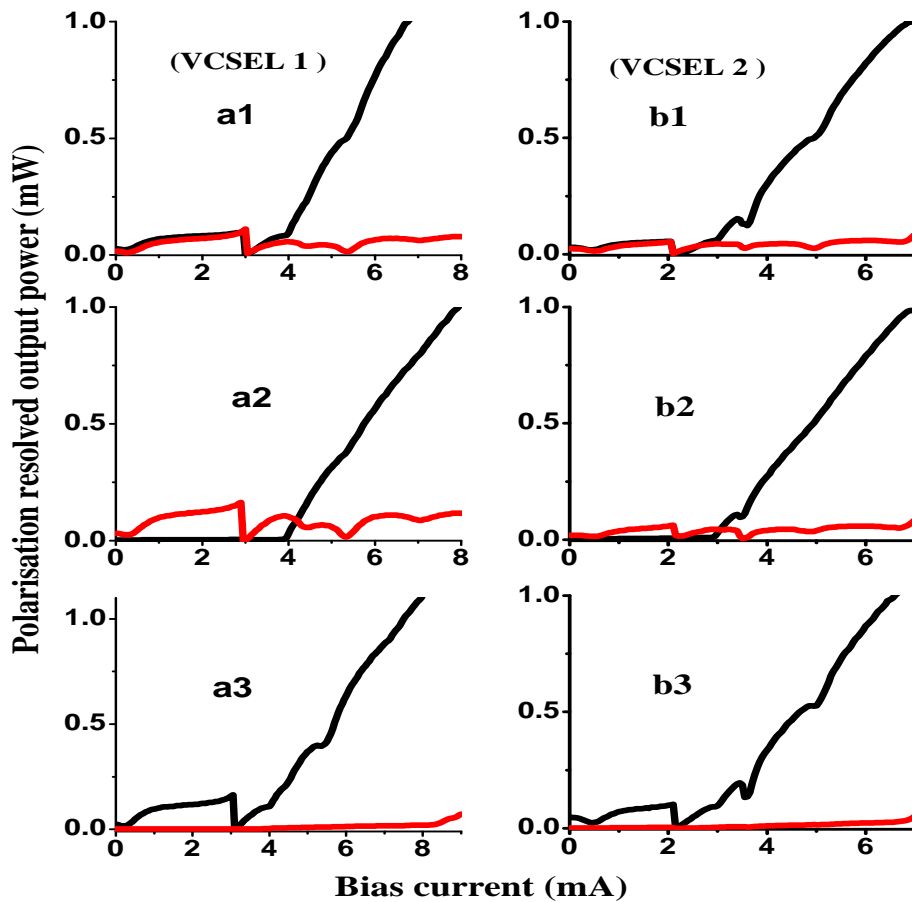
Figure 3.13: Polarisation resolved L–I curve of VCSEL1 and VCSEL2 using (a1, b1) CPOI, (a2, b2) LP orthogonal and (a3, b3) LP parallel. Red and black curves represent x and y polarised components of VCSELs respectively.

3.6 Summary and Conclusion

In this chapter the first experimental investigations of the effects of circularly polarised optical injection (CPOI) on the lasing characteristics of the VCSELs have been described. Two different short-wavelength VCSELs with linearly polarised output were used in the experiments. The results show that the output polarisation of electrically pumped VCSELs can be strongly influenced by CPOI.

The linear polarisation of VCSELs emission become circularly polarised for bias current below or near the stand-alone VCSEL threshold current. The degree of circular polarisation was dependent on the VCSELs bias current and decreased with increasing VCSELs bias current. Below threshold both VCSELs emission were characterised with high degree of left/right circularly polarised under CPOI. Optically injected field at this bias current regime mainly determined the polarisation of the both VCSELs emission through injection locking. While far above threshold degree of circular polarisation decreases dramatically

and the polarisation of the VCSEL emission is determined mainly by the structure of laser. These experimental results have been confirmed by recently theoretical work reported in [7].

Furthermore, lasing threshold reduction in optically injected VCSELs has been observed, confirms the theoretical prediction in [14] that the external optical injection can change the gain in semiconductor laser active media, and hence reduce the lasing threshold, the amount of reduction being dependent on the optical injection strength and frequency detuning. CPOI was used as an additional means to investigate physical mechanisms occurring in VCSELs.

In the next chapter the influence of the circularly polarised optical feedback on the polarisation of the VCSELs emission investigated experimentally.

References:

[1] **Z. G. Pan,** S. Jiang, and M. Dagenais, "Optical injection induced polarisation bistability in vertical-cavity surface-emitting lasers," Appl. Phys. Lett. vol. 63, pp. 2999-3001, **1993**.

[2] **T. B. Simpsony,** J M Liuz, K F Huangx and K Taix, "Nonlinear dynamics induced by external optical injection in semiconductor lasers," Quantum Semiclass. Opt., vol. 9, pp. 765–784, **1997**.

[3] **S. Bandyopadhyay,** Y. Hong, P. S. Spencer, and K. A. Shore, *"VCSEL Polarisation Control by Optical Injection,"* J. Lightwav. Technol., vol. 21, pp. 2395-2303, Oct. **2003**.

[4] **I. Gatare,** M. Sciamanna, J. Buesa, H. Thienpont, and K.Panajotov, "Nonlinear dynamics accompanying polarisation switching in vertical-cavity surface-emitting lasers with orthogonal optical," Appl. Phys. Lett. vol. 88, pp. 101106, **2006**.

[5] **A. Hurtado,** A. Quirce, A. Valle, L. Pesquera, and M. J. Adams,"Nonlinear dynamics induced by parallel and orthogonal optical injection in 1550 nm vertical-cavity surface-emitting lasers (VCSELs)," Optic. Exp. vol. 18, pp. 9423- 9428, Apr. **2010**.

[6] **A. A. Qader,** Yanhua Hong and K.Alan Shore, "Lasing characteristics of VCSELs subject to circularly polarised optical injection," IEEE, J. of Lightwav. Tech., vol. 29, pp. 3804-3809, Dec. **2011**.

[7] **R. Al-Seyab,** K. Schires, A Hurtado, I D. Henning and M. J. Adams , "Dynamics of VCSELs subject to optical injection of arbitrary polarization," IEEE J. Selec. Top. of Quantum Electron., vol. 19, no. 4, pp. 1700512, Jul./Aug **2013.**

[8] **T. Ackemann** and M. Sondermann, "Characteristics of polarization switching from the low to the high frequency mode in vertical-cavity surface-emitting lasers," Appl. Phys. Lett., vol. 78, pp. 3574-3576, Jun. **2001.**

[9] **M. Travagnin,** "Linear anisotropies and polarization properties of vertical cavity surface-emitting semiconductor lasers," Phys. Rev. A, vol. 56, pp. 4094-4105, Nov. **1997**.

[10] **M. Sondermann,** T. Ackemann, S. Balle, J. Mulet, K. Panajotov, "Experimental and theoretical investigations on elliptically polarised dynamical transition states in the polarzation switching of vertical-cavity surface- emitting lasers," Optic. Commun., vol. 235, pp421–434, Feb. **2004.**

[11] **M. Travagnin,** M. P. Van Exter, A. K. Jansen van Doorn, and J. P. Woerdman, "Role of optical anisotropies in the polarisation properties of surface-emitting semiconductor lasers," Phys. Rev. A, vol. 54, pp. 16471660, Aug. **1996**.

[12] **S. Hovel,** N. C Gerhardt, C. Bernner, M. R. Hofmann. F.-Y. Lo, D. Reuter, A D. Wieck, E. Schuster, and W. Keune, "Spin-controlled LEDs and VCSELs," Phy. Stat. Sol. A, vol 204, pp. 500-507, Feb. **2007.**

[13] **S. Jiang,** Z. Pan, M. Dagenais , R. A. Morgan, and K. Kojima, "Influence of external optical feedback on threshold and spectral characteristics of Vertical-Cavity Surface-Emitting Lasers," IEEE Photo. Tech. Lett., vol. 6, pp. 34-36, Jan. **1994.**

[14] **L. Li,** "Static and Dynamic Properties of Injection-Locked semiconductor Lasers," IEEE J. of Quantum Electron. vol. 30, pp. 1701-1708, Aug. **1994**.

[15] **S. Sivaprakasam** and R. Singh, "Gain change and threshold reduction of diode laser by injection locking," Optic. Commun. vol. 151, pp. 253–256, Jun. **1998**.

CHAPTER FOUR

OPTICAL FEEDBACK EFFECTS ON THE EMISSION POLARISATION OF VCSELS

In chapter three, optical injection configurations were used to investigate experimentally the polarisation properties of VCSELs. The results obtained with CPOI motivated further experimental investigations described in this chapter where use is made of optical feedback schemes. A new optical feedback scheme named circularly polarised optical feedback (CPOF) has, in particular, been used in the experiments.[1] It is shown that the stable linear polarisation of VCSEL emission may to some extent, be changed to circular polarisation (CP). The degree of circular polarisation acquired by the VCSEL emission is determined by the feedback power ratio and the VCSEL bias current. The effects of CPOF have been compared to the influence of different kinds of linearly polarised optical feedback (LOPF).

The contents of this chapter are organised as follows:

 In section 4.1 a brief introduction to optical feedback techniques in semiconductor lasers is presented. Section 4.2 includes the most common used feedback schemes as well as the new scheme of feedback - CPOF. In section 4.3 details of the experimental setup used to produce CPOF are provided. Section 4.4 the effects of CPOF on the polarisation state of VCSEL are examined. In section 4.5 the effects of LPOF on polarisation state of VCSEL are investigated and compared to those due to CPOF. Finally, section 4.6 includes a summary and the main conclusions from this work.

4.1 Introduction

Optical feedback (OF) is a widely used technique to explore and amend the properties of semiconductor lasers including VCSELs. In VCSELs a particular use for optical feedback arises in the context of controlling their emission polarisation. OF is a particularly important technique as it enables strong influence to be exerted on the polarisation properties of VCSELs. Several feedback schemes have been used experimentally and theoretically [1, 2]. Using these feedback schemes large numbers of experimentally investigation have been performed [1-3].

---

[1]*This chapter is based on the paper:*
A. A. Qader, Y. Hong and K. A. Shore, IEEE, Photo. Tech. Lett., vol. 24, pp. 1200-1202, Jul. 2012.

Most of the previous studies are concerned with linear polarisation, however, a few studies described elliptical polarisation in electrically pumped VCSELs [3-5]. It was predicted by Masoller [6], that VCSELs subject to orthogonal OF exhibit slightly elliptical polarisation. There have been theoretical studies of the influence of polarised OF on VCSELs including examination of elliptically polarised emission and rotated optical feedback [5-8].

Recently a laser diode with external cavity laser (ECL) has been used to produce circularly polarised (CP) emission [9-10]. The utilized ECL included a Bragg grating and quarter wave plate, which resulted in the production of a high degree of circularly polarised emission from the ECL which operated at long wavelength regime. In [10] a laser diode with an external cavity containing QWP and a chiral mirror used for generating circularly polarised emission. The output circular polarisation ratio was observed near the threshold current.

Interest in circularly polarised emission is in particular stimulated by activities in the area of spintronics where high-speed optical switching may be achieved. All previous studies for VCSELs subject to externally feedback were performed with linear polarisation. In this chapter, a new scheme has also been used namely circularly polarised optical feedback (CPOF) as an additional means to influence and control the polarisation characteristics of VCSELs. Therefore, circular polarised feedback scheme was used here in VCSELs for the first time.

4.2 Optical feedback configurations:

In the previous section, the most commonly used external optical feedback schemes were presented. The feedback strength, external feedback cavity length and the feedback polarisation are the main optical feedback parameters. The feedback parameters are the key point for accessing various feedback schemes. Depending on the external feedback cavity length (time delay), three main types of feedback schemes were found:

1- Long external cavity feedback:

This configuration is characterised by the round trip time of the external cavity being longer than reciprocal of the relaxation oscillation frequency (ROF) of the semiconductor lasers [11].

Round trip time $$(t_r) = \frac{2L_{ext.}}{c}$$ Where L is external cavity length

c is the speed of light

2- Short external cavity feedback

$$t_r \approx 1/ROF$$

3- Extremely short external cavity feedback [11].

$$t_r << 1/ROF$$

In addition, depending on the polarisation of the feedback light optical feedback schemes can be classified in to two groups:

1- Linearly polarised optical feedback (LPOF) schemes. This includes x- parallel OF, y-orthogonal OF and angles of polarisation between 0°-90°.

2- Circularly polarised optical feedback (CPOF) schemes. This includes left/right CPOF and other elliptical polarised optical feedback scheme. Figure 4.1 shows the most common linearly polarised optical feedback schemes compared to CPOF scheme.

Figure 4.1 (a) shows polarisation preserved OF where the polarisation of feedback light is the instantaneous polarisation of VCSEL emission. If the external cavity laser mirror is polarisation sensitive, therefore always modify the polarisation of the reflected light. Polarisation preserved OF is the simplest optical feedback scheme. Early studies of semiconductor lasers subject to optical feedback used this configuration for exploring the spectral characteristics.

Figure 4.1 (b) shows polarisation rotated optical feedback scheme using a quarter wave plate; this configuration may also called rotated polarisation feedback. For this scheme the QWP is inserted into the external cavity with its fast axis making an angle 45° with the incoming polarisation direction. This is will change the incoming x-direction linearly polarised light to circularly polarised (CP) light. As mentioned previously, the external mirror changes left CP to right CP, and then passing again the QWP, it changes back to linearly polarised but in y-polarised direction. Therefore, the light returned into the semiconductor laser is orthogonally polarised to the initial polarisation of the laser emission [2].

Figure 4.1 (c) shows polarisation selective-optical feedback. Here a polarisation beam splitter (PBS) and half wave plate (HWP) are included in the external cavity. Polarisation selective means that one or other of the polarisation components will be selected and re-injected into the laser. With this configuration either x-polarised feedback or y polarised feedback can be accomplished. Polarisation–selective optical feedback has been previously used to induce different dynamical states (including chaotic states and low frequency

fluctuations) [12] PS suppression in VCSELs emission has also been observed using such a configuration [13].
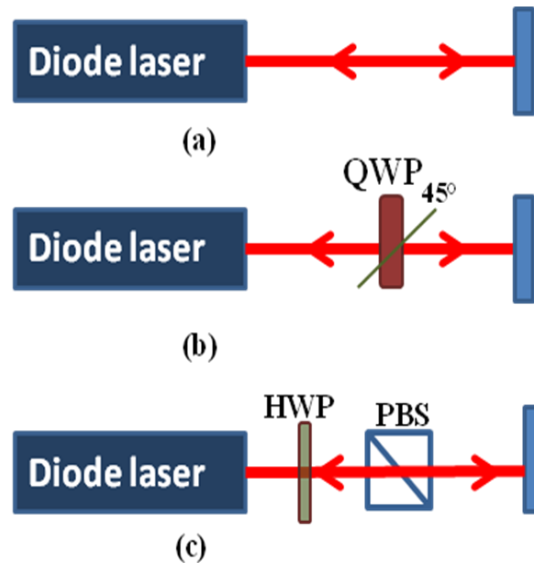

Figure 4.1: common optical feedback schemes: (a) preserved optical feedback, (b) rotated optical feedback, (c) polarisation selective optical feedback.

Circular feedback polarisation configuration:

Figure 4.2 shows the new feedback scheme CPOF used to perform the experimental work of this chapter. The scheme is constructed by inserting both a QWP and a PBS into the external cavity. Emitted light having linear polarisation in the x-direction passing through the QWP with its fast axis making an angle 45° with the incoming polarisation direction. The x-linear polarised changes to a CP beam. When CP beam passes through the PBS it changes back to linear polarisation and then the beam reflected by the external mirror without modifying its polarisation. When the linearly polarised reflected beam passes through the QWP with its fast axis making an angle 45°, becomes circularly polarised. Therefore, in this simple way circular polarisation optical feedback is obtained [14].

Figure 4.2: circularly polarised optical feedback.

Other optical feedback schemes have also been used, e.g. interferometer optical feedback which consists of two channel feedback [15], and a feedback scheme named ring cavity optical feedback [16].

4.3 Experimental setup

The experimental setup is shown in figure 4.3. A commercial oxide-confined VCSEL with an operating wavelength around 850 nm and lasing threshold of 3.7 mA was used in this work. Further details of the characteristics of VCSEL can be found in chapter 3 (see VCSEL1 in section 3.3). The VCSEL was driven by a programmable DC source and was temperature controlled with a thermoelectric temperature controller (TED 200) to within 0.01^0C. The VCSEL emission was collimated using an antireflection coated laser diode objective lens. A non-polarising beam splitter was used to separate the output power of the VCSEL into two channels. One channel is used for OF by the use of a mirror at a distance of about 29 cm, and the other channel is for performing diagnostics. The external mirror position was adjusted to obtain the best mode-matched feedback under the criterion of identifying the maximum influence on the
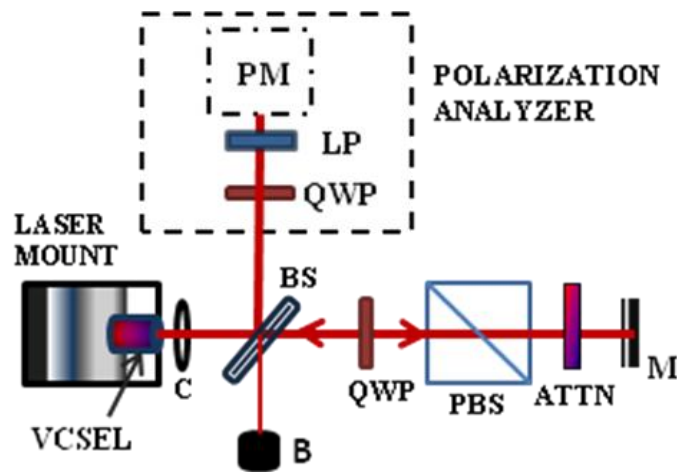
Figure 4.3: *Experimental setup. VCSEL laser; C– laser diode objective lens; BS—beam splitter; QWP—Quarter wave plate; PBS—polarised beam splitter; ATTN—variable optical attenuator; M—mirror; B—Removable beam block; LP—linear polariser; PM—power meter.*

emitted output power in the vicinity of stand-alone VCSEL threshold (i.e. maximum threshold lasing reduction). A quarter wave plate (QWP) and polarisation beam splitter (PBS) were employed to change the linear polarisation of the re-injected light to circular polarisation. A variable optical attenuator (ATTN) was used to control the level of the optical feedback into the VCSEL.

An optical power meter (Anritsu) was used to record the output power. The strength and state of polarisation of the feedback light are measured at the position of the removable beam block (B).

The feedback strength is quantified with the so called feedback power ratio, which given by:

$$\text{Feedback power ratio} = 10 \log_{10}(\frac{P_f}{P_t})$$ .... (1)

Where P_f is the feedback power coupled into the laser cavity, P_t is the total output power of VCSEL
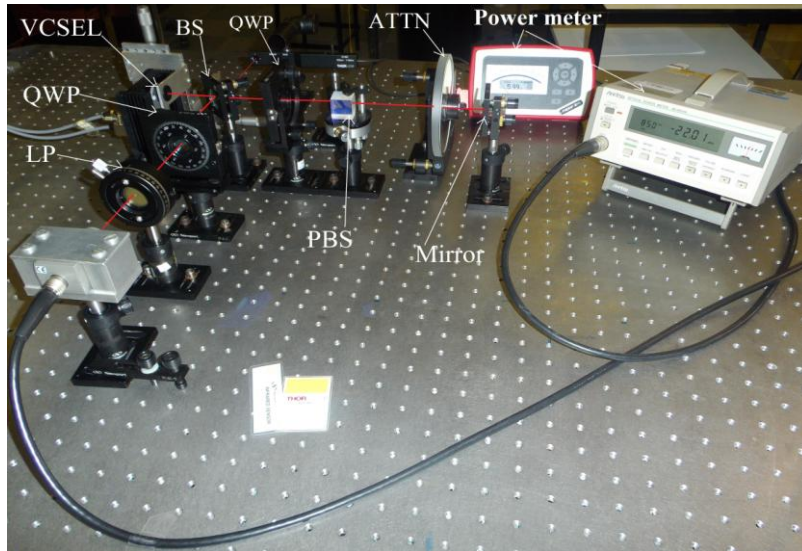

Figure 4.4: *A view picture of the experimental setup. Terms are defined in figure 4.3.*

4.4 CPOF effects on polarisation state of VCSEL:

The experimental set up in 4.3 was used to investigate the polarisation state of the VCSEL emission with CPOF. The degree of circular polarisation (DoCP) was measured as a function of the VCSEL bias current and optical feedback ratio. The feedback ratio is defined as the ratio of the re-injected feedback power to the total output power of the VCSEL subject to optical feedback. It is noted that the lasing threshold of the VCSEL reduced by more than 10% using OF. In addition the feedback will increase the total output power (Pt) of the VCSEL for low bias current ($\sim I_{th}$), while for high bias current ($> I_{th}$) Pt decrease with feedback. The polarisation switching between the orthogonal fundamental modes of the VCSEL is deemed to have occurred when the suppressed (y) mode takes %85 of the total output power.

4.4.1 Measurements with varying bias current

The Stokes parameters for the stand-alone VCSEL emission in both feedback channel and detection channel were measured, and indicate that the polarisation properties of the

VCSEL in the external cavity are not affected by the beam splitter. Details of the Stokes polarisation parameters measurement were described in chapter two (section 2.5). In figure 4.5 the DoCP of the VCSEL emission as a function of the VCSEL bias current has been plotted.
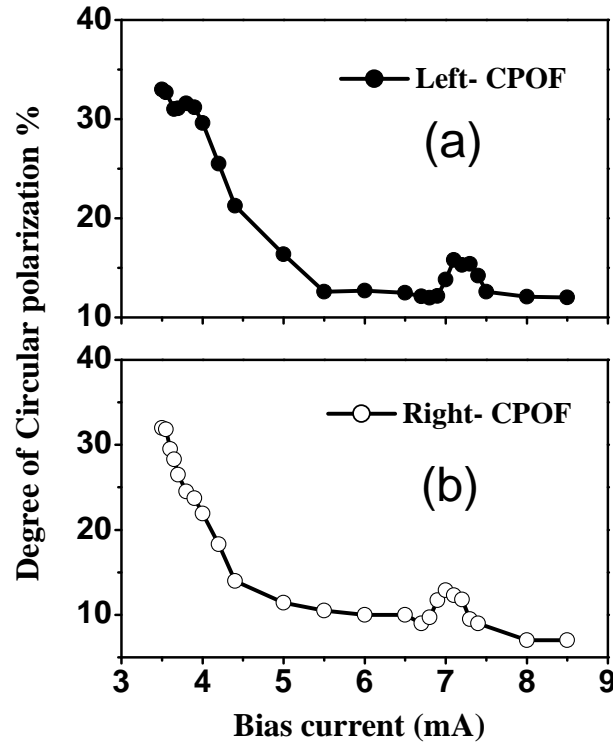

Figure 4.5: DoCP as a function of VCSEL bias current, using a) left CPOF (filled circle) and b) right CPOF (open circle), with optical feedback ratio -10.5 dB.

The OF power ratio was fixed at -10.5 dB, left and right CPOF were used in figures 4.5(a) and (b), respectively. The feedback ratio is not real power reflected into the VCSEL cavity, due to absorption by laser diode objective lens and high reflectivity at the surface of output coupler.

It can be seen that the influences of both left and right CPOF on the polarisation of the VCSEL emission are similar albeit with slightly higher DoCP for left-CPOF. In the vicinity of the lasing threshold of the stand-alone VCSEL both schemes have a relatively high DoCP, but the DoCP decreases with increasing bias current.

For low bias current the polarisation of the VCSEL emission will be mainly determined by the polarisation of the optical feedback, while far above threshold the polarisation of the laser emission is determined mainly by the VCSEL structure. In [10] using circularly polarised external cavity laser diode, a rapid increase of the laser diode output CP ratio near

threshold current has been observed. The obtained CP lasing behaviour of the laser diode results from the buildup of a resonant CP mode in the external cavity.

In figure 4.5 the VCSEL emission under CPOF has small DoCP up to a bias current reach of about 7 mA and then starts to increase again for both left and right CPOF. It is considered that the increase of the DoCP between 6.9 mA and 7.3 mA is may be associated with the excitation of the higher order mode. In section 5.4.1 will be seen that the spectral characteristics of this VCSEL show a single transverse mode for bias current $I < 7$ mA, while a higher transverse mode with orthogonal polarisation to the fundamental mode starts lasing above 7 mA.

Furthermore, the polarisation resolved output power L-I curve, has been recorded using CPOF with feedback ratio -10.5 dB. Figure 4.6 shows the effect of the CPOF on the polarisation resolved output power. It can be seen that the feedback induced enhancement power in y polarised mode. In addition the CPOF reduce the threshold point for both polarisation modes.
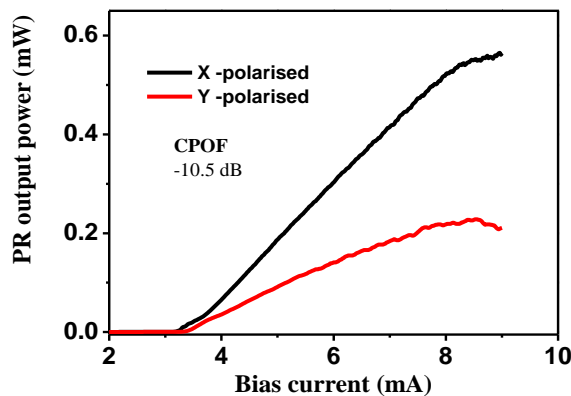
Figure 4.6: Polarisation resolved L-I curve as a function of VCSEL bias current using CPOF with feedback ratio -10.5 dB.

4.4.2 Measurements of DoCP with varying feedback ratio

In this section analysis of the degree of circular polarisation of the VCSEL emission with varying feedback ratio is undertaken. Figure 4.7 shows the DoCP as a function of the feedback power ratio for fixed bias current. Using left-CPOF figures (a1, b1, c1) and right-CPOF figures (a2, b2, c2) for bias currents of 3.5mA, 3.6 mA and 3.7 mA respectively.

The figures show that the DoCP will increase with increasing feedback up to a certain range of OF, then start to decrease for higher OF. This decrease in the DoCP with high optical feedback level can be explained by the fact that with high optical feedback the VCSEL enters the coherence collapse regime, which is characterised by broaden the linewidth and degradation in polarisation degree of the emitted. For a bias current of 3.5

mA decrease of the DoCP has not been observed for both left / right CPOF, this is possibly due to the lower output power and hence lower optical feedback power at this bias current.
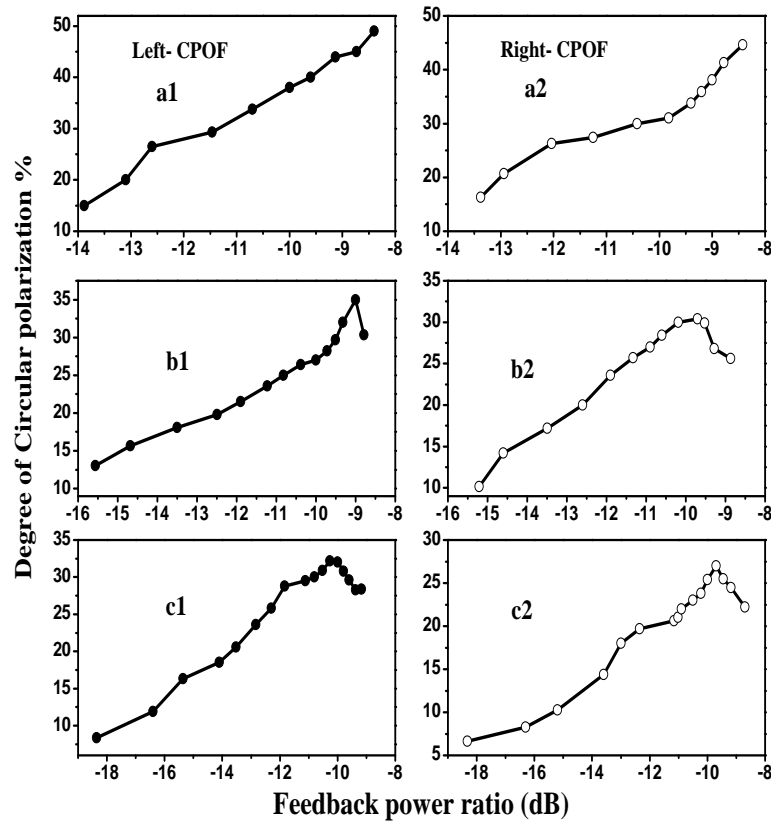

Figure 4.7: Degree of circular polarisation using left (a1, b1, c1), right (a2, b2, c2) CPOF as a function of feedback level, with VCSEL biased at 3.5 mA, 3.6 mA and 3.7 mA respectively.

4.5 LPOF effects on polarisation state of VCSEL:

The influences of the left/right CPOF on the polarisation state have been compared to those of linearly polarised including preserved, Y-polarised selective and polarisation rotated optical feedback. Figure 4.8 shows the various linear OF schemes effects on the
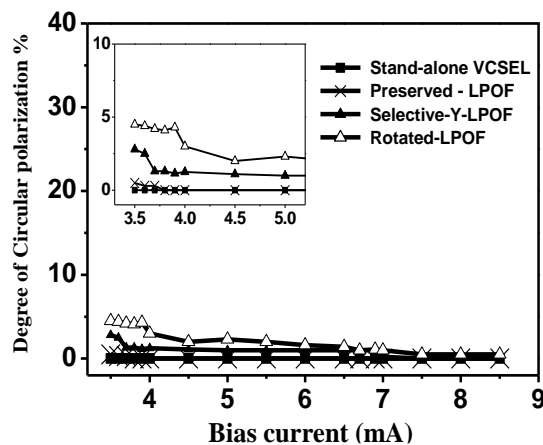
Figure 4.8: DoCP as a function of VCSEL bias current, using various linear polarised optical feedback schemes when feedback ratio is -10.5 dB.

polarisation of the VCSEL emission with OF ratio -10.5 dB.

It can be seen that the preserved OF does not affects the polarisation state of the VCSEL at any bias current. However, for Y-selective polarised and polarisation rotated OF a small DoCP near lasing threshold has been observed.

This observation confirms a theoretical prediction made by Masoller [6], that VCSELs can exhibit a slightly elliptical polarisation state with rotated OF using a QWP, the results for orthogonal LPOF are in a good agreement with reported simulation in [6].

4.6 Summary and conclusion

In this chapter, the effects of the circularly polarised optical feedback on the polarisation characteristics of the VCSEL emission have been presented. It is shown that using CPOF in electrically pumped VCSELs offers a new scheme of OF with potential for enhancing the degree of circular polarisation of VCSEL emission.

Despite the fact that the stand-alone VCSEL emission is linearly polarised, however using optical feedback an elliptically polarised state has been predicted theoretically [6, 7]. Using left/right CPOF the results in section 4.4 of experimental measurements shown that depending on the VCSEL bias current and the feedback power ratio the VCSEL emission can be made to exhibit a degree of circular polarisation.

Using the feedback scheme the DoCP decreases significantly with increasing VCSEL bias current, which similar to observed CP ratio using external cavity laser diode [10]. The DoCP increases with increasing feedback level for a certain range of feedback power. The change of linear polarisation state of the VCSEL emission to circular polarisation can be explained as follow: for low bias currents the external feedback will determine the polarisation of VCSEL output, while for increasing bias current the polarisation state is determined mainly by the VCSEL structure. The effects of CPOF were compared to the effect of various linearly polarised OF including preserved, selective and rotated polarisation OF.

This chapter has emphasised the effects of the circularly polarised optical feedback on the polarisation state of the VCSEL emission. In the next chapter a detailed experimental study of the role of suppressed mode in the polarisation switching characteristics of polarised optically injected VCSELs will be addressed.

References:

[1] **Y. Hong,** P. S. Spencer, and K. Alan Shore, "Investigation of polarization bistability in vertical-cavity surface emitting lasers subjected to optical feedback," IEEE J. of Quantum Electron., vol. 41, pp. 619–624, May **2005.**

[2] **R. Ju,** Y. Hong and P.S. Spencer, "Semiconductor lasers subject to polarisation-rotated optical feedback," IEE Proc.-Optoelectron., vol. 153, pp 131-137, Jun. **2006.**

[3] **S. Ramanujan,** G. P. Agrawal, J. M. Chwalek, and H. Winful, "Elliptical polarization emission from GaAlAs laser diodes in an external cavity configuration," IEEE J. Quantum Electron., vol. 32, Feb. **1996.**

[4] **M. Sondermann,** T. Ackemann, S. Balle, J. Mulet, K. Panajotov, "Experimental and theoretical investigations on elliptically polarised dynamical transition states in the polarization switching of vertical-cavity surface- emitting lasers," Optic. Commun., vol. 235, pp421–434, Feb. **2004.**

[5] **D. Chen,** Z. Fang, H. Cai, and R. Qu, "Polarization characteristics of an external cavity diode laser with Littman–Metcalf configuration," IEEE Photo. Tech. Lett., vol. 21, pp 984-986, Jul. **2009.**

[6] **C. Masoller** and N. B. Abraham, "Polarization dynamics in vertical –cavity surface emitting lasers with optical feedback through a quarter- wave plate," Appl. Phys. Lett., vol. 74, pp. 1078-1080, Feb. **1999.**

[7] **S. Xaing,** W. Pan, L. Yan, B. Luo, X. Zou, N. Jiang and K. Wen, " Variable- polarization optical feedback induced hysteresis of the switching in vertical-cavity surface-emitting lasers," J. Opt. Soc. Am. B, vol. 27, pp 5212-5217, Dec. **2010.**

[8] **S. Xaing,** W. Pan, L. Yan, B. Luo, N. Jiang, K. Wen, X. Zou, and L. Yang "Polarization degree of vertical-cavity surface-emitting lasers subject to optical feedback with controllable polarization," J. Opt. Soc. Am. B, vol. 27, pp 476-483, Mar. **2010.**

[9] **R. K. Kim,** J. H. Song, Y. Oh, D.-Hoon Jang, J. R.Kim, and K. S. Lee, "Circularly polarised external cavity laser hybrid integrated with a polyimide quarter-wave plate on planar lightwave circuit," IEEE Photo. Tech. Lett., vol. 19, pp. 1048-1050, Jul. **2007.**

[10] **F. Zhang,** J. Xu, A. Lakhtakia, T. Zhu, S. M. Pursel, and M. W. Horm, "Circular polarization from an external cavity diode laser," Appl. Phys. Lett. vol. 92, pp. 111109, **2008.**

[11] **S. Ura,** S. Shoda, K. Nishio and Y. Awatsuji, "In- line rotation sensor based on VCSEL behavior under polarization- rotating optical feedback," Optic. Expres. vol. 19, pp 23683-23688, Nov. **2011.**

[12] **H. Aoyama,** S. Tomida, R. Shogenji and J. Ohtsubo, "Chaos dynamics in vertical-cavity surface-emitting semiconductor lasers with polarization-selected optical feedback," Optic. Commun., vol. **284**, pp 1405-1411, **2011.**

[13] **K. Panajoto,** M. Arizaleta, M. Camarena, H. Thienpont, H. J. Unold, J. M. Ostermann, and R. Michalzik, " Polarization switching induced by phase change in extremely short external cavity vertical-cavity surface-emitting lasers," Appl. Phy. Lett., vol. 84, pp 2763-2765, Apr. **2004.**

[14] **A. A. Qader,** Y. Hong and K. Alan Shore, "Circularly polarised optical feedback effects on the polarization of VCSEL Emission," IEEE Photo. Tech. Lett., vol. 24, pp 1200-1202, Jul. **2012.**

[15] **Y. Liu** and J. Ohtsubo, "Dynamics and chaos stabilization of semiconductor laser with optical feedback from an interferometer," IEEE J. Quantum Electron., vol. 33, Jul. **1997**.

[16] **R. Ju** and Paul S. Spencer, "Dynamic regimes in semiconductor lasers subject to incoherent optical feedback," IEEE J. Lightwav. Tech., vol. 23, pp. 2513-2523, Aug. **2005.**

CHAPTER FIVE

THE ROLE OF THE SUPPRESSED MODE IN POLARISATION SWITCHING OF OPTICALLY INJECTED VCSELS

◆━━━━━━━━━━━━━━━━━━━━━━━━━━━━━━━━━━━━━━◆

In the two previous chapters the outcome of experimental investigation of the polarisation states of VCSELs subject to circularly polarised optical injection and optical feedback were described. In this chapter, various linearly polarised optical injection schemes have been used to investigate the polarisation switching (PS) characteristics of birefringent VCSELs. Through this work the role of the suppressed mode of VCSELs in reducing the injected optical power required for polarisation switching has been identified.[1] For orthogonal optical injection the minimum optical injection power to induce PS was found to occur at a frequency detuning corresponding to the VCSEL birefringence. The value of the minimum injected optical power to effect PS reduced significantly with increasing bias current. The frequency detuning for PS is found to be independent of the VCSEL bias current, injected power level and a defined range of polarisation angles of the injected light. Furthermore, the influence of the polarised optical injection on the VCSELs spectral characteristics of the suppressed mode was investigated. These influences have been compared to those obtained using polarised selective optical feedback.

The contents of this chapter are organised as follows:
In section 5.1 an introduction to PS phenomena in VCSELs is presented. Section 5.2 includes the details of the experimental setup used to demonstrate the role of the suppressed mode in the PS characteristics of VCSELs subject to polarised optical injection. In section 5.3 the optical spectra of the stand-alone VCSELs including the transverse mode behaviour and birefringence of the VCSELs are provided. In section 5.4 polarisation switching characteristics performed using orthogonal optical injection and various polarised angle of injected light are described. Section 5.5 includes the polarisation switching behaviour of VCSELs subject to parallel optical injection. Section 5.6 describes the frequency detuning for polarisation switching using various polarisation angles of optical injection. In section 5.7 polarisation-resolved optical spectra of VCSELs subject to

---

[1]*This chapter is based on the paper:*
A. A. Qader, Y. Hong and K. A. Shore, IEEE, J. Quantum Electron., vol. 49, pp. 205-209, Feb. 2013.

orthogonally polarised optical injection are analysed. Polarisation resolved output power and polarisation switching using optical feedback have been investigated in section 5.8. Section 5.9 includes spectral characteristics of VCSELs subject to polarised selective optical feedback. Finally section 5.10 summarizes the main conclusions derived from the experimental results.

5.1 Introduction

Although VCSELs emission is typically linearly polarised along one of two orthogonal crystal directions, it is commonly observed that due to changes in operating conditions such as bias current or device temperature [1-3] the polarisation of stand-alone VCSELs will switch to the orthogonal linear polarisation. The physical mechanisms responsible for the polarisation switching (PS) are complex and seemingly involve a number of factors as discussed in chapter 2 section 2.2.

Previous studies have shown that it is possible to induce PS in VCSELs subject to optical injection [4], optical feedback [5] and current modulation [6]. Optical injection can be used to significantly decrease the linewidth of laser emission, creation of complex dynamic behaviour (chaotic dynamics) and increase the modulation bandwidth of the device. Optical injection has also been used to induce various nonlinear dynamics e.g. limit cycle, periodic dynamics and deterministic chaos [7]. Another interesting consequence of optical injection in VCSELs is to effect PS. It has been shown that PS in VCSELs emission can be induced by orthogonal optical injection [3]. PS using both orthogonal and parallel optical injection with variation in frequency detuning has been reported by Hong et al. [7].

Recently PS in long wavelength VCSELs subject to orthogonal optical injection has been investigated theoretically and experimentally [8]. That work indicated that the optical injected power (P_{inj}) required for PS increases with the VCSELs bias current, and the minimum injected power for PS was obtained in the region of negative frequency detuning or near the frequency of the lasing mode frequency in the stand-alone VCSEL [8, 9]. More recently an experimental study showed that the frequency detuning (FD) required for the suppression of the parallel polarised depends on the optical injected power [10]. The route to PS and nonlinear dynamics accompanying PS in VCSEL has been studied [11, 12].

In [13] it was predicted that the minimum optical power for polarisation switching occurs when the frequency of orthogonally-polarised injected light coincides with that of the orthogonal mode of VCSEL i.e. with the frequency detuning being the VCSEL birefringence. Despite the fact that numerous studies have been conducted of orthogonal/

parallel optical injection [7]-[12], little attention has been paid to the role of the suppressed VCSEL mode in the PS of optically injected VCSELs. This chapter addresses that issue.

5.2 Experimental setup

The experimental setup used in this work shown in figure 5.1. A tunable single-frequency laser diode (model SDL-TC10), with a centre wavelength of 850 nm and wavelength tuning range of about 20 nm was used as the master laser (ML) to inject light into a VCSEL slave laser (SL). Two commercially available oxide-confined VCSELs named VCSEL1 and VCSEL2 with operating wavelengths around 850 nm were used as slave lasers. Further details of the characteristics of both VCSEL1 and VCSEL2 can be found in chapter 3 (see section 3.3). There are some similarities between the experimental setup shown in figure 5.1 and the one shown in figure 3.2 (chapter 3, section 3.2). The key difference is that the isolators before Fabry–Pérot interferometer have been removed. Also two polarisation beam splitter have been inserted into the setup, therefore the new setup enables the measurement of the birefringence of the VCSELs and observe both X and Y polarised mode spectrum simultaneously.

The VCSEL was driven by a laser diode controller DC source (Tektronix LDC 202) and was temperature controlled with a thermoelectric temperature controller (TED 200) to within 0.01^0C. Two optical isolators (each providing >40 dB isolation) were used to ensure that the ML is free from the effects of any reflected light. A variable optical attenuator (ATTN) was used to change the strength of the optical injection into the VCSEL slave laser. Three half-wave plates (HWP) were used to change the polarisation direction. HWP1 used to align the polarisation of the ML with the polarisation direction of the VCSEL emission, while HWP2 and HWP3 were used before polarised beam splitter (PBS2) to change the desired amount of slave laser output to either optical spectrum analyzer (OSA) or Fabry–Pérot interferometer (FPI).

An optical spectrum analyzer (OSA) with resolution of 0.06 nm was used to record the laser spectra. A FPI with a free range of 30 GHz and a finesse of 150 was used to observe the spectral modes of master and slave lasers. Two PBS included in the setup was used to observe the spectral intensity of both lasing and suppressed mode simultaneously. A slightly misaligned FPI was used to avoid the effect of strong feedback into the VCSEL. A digital phosphor oscilloscope (Tektronix TDS 7404) with high bandwidth (4 GHz) was used to record the spectral intensities and frequency detuning between

master and slave lasers. The OSA and oscilloscope were connected to personal computer through General-Purpose Interface Bus (GPIB). The polarisation and optical injection power level were monitored at the position of the removable beam block. The PS between two fundamental polarised modes of the VCSEL was monitored with the components indicated in the dotted rectangle which includes a PBS and digital power meter [14].
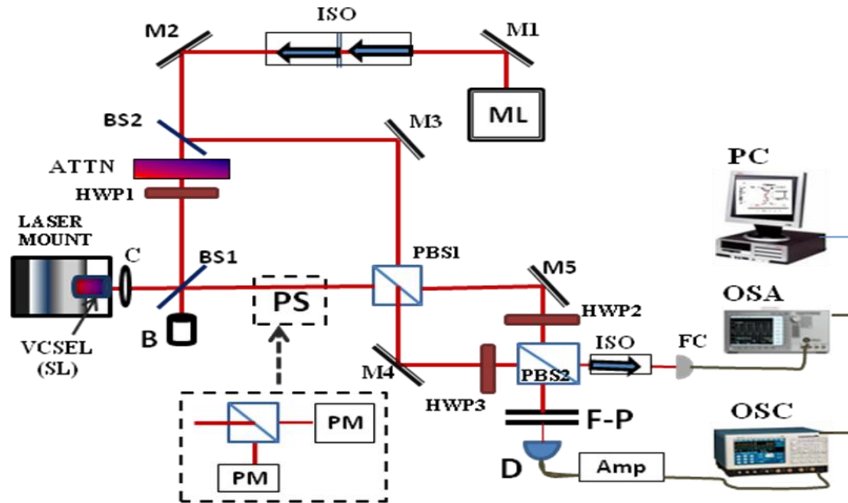

Figure 5.1: Experimental setup

5.3 Spectral characteristics of stand-alone VCSELs

An optical spectrum analyzer (Agilent 8614xB) was used to record the optical spectra of the stand-alone VCSELs. The limitation of this device is its poor spectral resolutions (0.06 nm or about 24 GHz at 850 nm), but it is useful for finding the absolute wavelengths of the laser, a measurement which cannot be performed using a Fabry-Perot interferometer. The wavelength of both VCSELs changes by ~ 0.32nm per 1 mA.

Figures 5.2 show the optical spectra of the VCSEL1 at different bias currents, a) I=5mA, b)
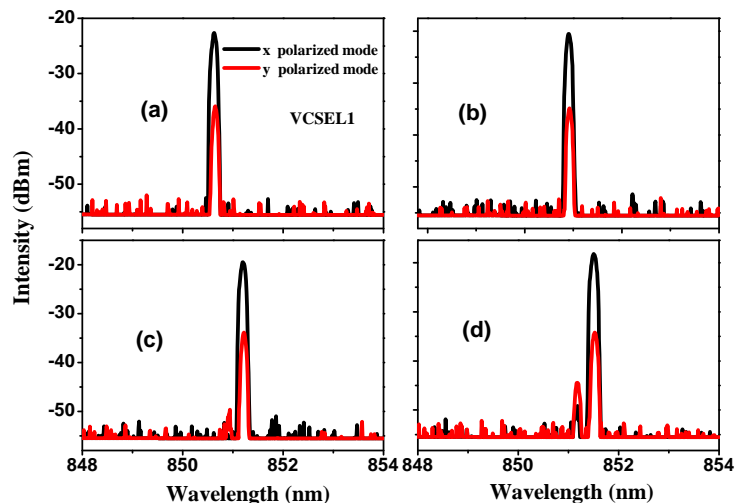
Figure 5.2: The optical spectra of the stand-alone VCSEL1 for bias current a) I=5mA, b) I=6mA, c) I=7 mA, d) I =8mA.

I=6mA, c) I=7 mA, d) I =8mA. The figures indicate that the higher transverse mode starts lasing for bias currents above about 7 mA. The higher order transverse mode is found to have a polarisation direction which is orthogonal to the polarisation direction of the fundamental mode. The higher order mode is at optical frequency which is higher than the fundamental transverse mode frequency. Figure 5.3 shows the optical spectra of the VCSEL2 for different bias current a) I=4mA, b) I=6mA, c) I=7 mA, d) I =8mA. Similar to VCSEL1 the polarisation direction of the higher order mode in VCSEL2 is orthogonal to the polarisation direction of the fundamental mode and it is at optical frequency which is higher than the fundamental transverse mode frequency. Figure 5.3d is for I= 8 mA, where it is illustrated that PS occurred in the stand-alone PR-output power.
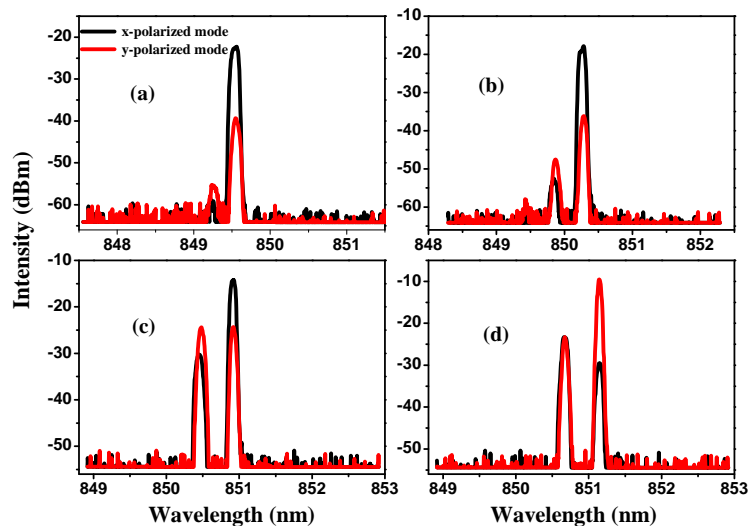
Figure 5.3: *The optical spectra of the stand-alone VCSEL2 for bias current a) I=4mA, b) I=6mA, c) I=7 mA, d) I =8mA.*

5.4 Orthogonal optical injection

In this set of experiments use has been made of orthogonal optical injection to investigate the role of the suppressed mode in PS, and to determine the minimum P_{inj} and frequency detuning required for PS.

5.4.1 Polarisation resolved output power of VCSELs:

Figure 5.5 shows the polarisation resolved (PR) output characteristics of the VCSEL when subject to orthogonally polarised optical injection when the VCSEL1 was biased at 6 mA and P_{inj} is 100 μW. VCSEL2 was biased at 4.5 mA and P_{inj} of 50 μW was used to investigate PS.

It is seen that PS occurs between the lasing mode (black filled squares) and the suppressed mode (red open circles) at a FD of about -11 GHz. This FD represents the frequency

difference (birefringence) between the lasing mode and the suppressed mode of the VCSEL (see the figure 5.4). Using orthogonal optical injection in both VCSEL1 and VCSEL2 a single sharp PS occurs near the suppressed mode frequency.
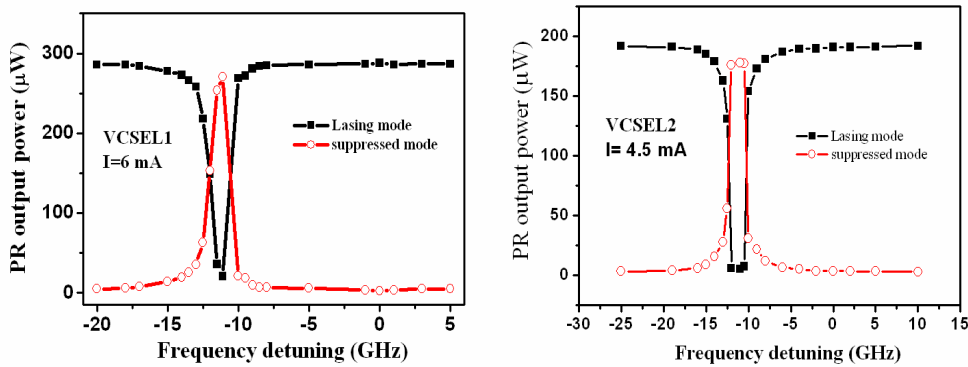

Figure 5.5: *Polarisation resolved output power of VCSEL vs. FD. When bias current I = 6 mA and P_{inj} 100 µW for VCSEL1, bias current I=4.5 mA and P_{inj} 50 µW for VCSEL2.*

Figure 5.6 show the polarisation resolved output power of VCSEL1 as a function of the bias current. The figure indicates that the power in the suppressed mode increases with increasing bias current. There is a notable increase in power, when the bias current reaches I=8 mA, which appear to be related to the excitation of the orthogonally polarised higher order transverse mode.
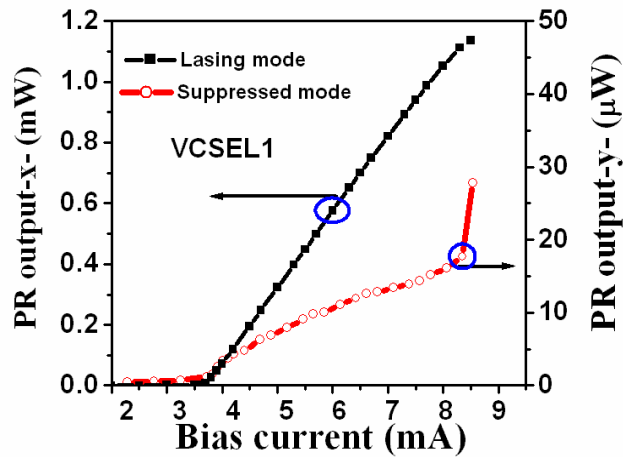
Figure 5.6: *Polarisation resolved output power as function of bias current for stand-alone VCSEL1.*

On the basis of the results in Figure 5.3 and Figure 5.6 it would be expected that the injected optical power needed for switching decreases with injection current and this is confirmed in figure 5.7. Figure 5.7a shows the minimum injected power required to induce the PS as a function of bias current for VCSEL1. It is seen that the required injected power

to induce PS decreases significantly with increased bias current, especially near the bias current which is seemingly related to the excitation of the orthogonal polarised higher transverse modes.

Similar measurements have been made in the polarisation-stable bias current regime of VCSEL2 (which has different structure with VCSEL1). For VCSEL2 the injected power for PS was recorded for the stable polarisation regime of bias current. The injected power for PS decreases significantly with increasing bias current. Figure 5.7b shows the minimum injected power to induce the PS as a function of bias current in VCSEL2.

It is noted that the observed dependence (of the minimum P_{inj} on the slave laser bias current) was not experimentally observed in [6]. Reference [6] does not include detailed spectral measurements of the devices used in their experiments but it is supposed that those VCSELs exhibited contrasting spectral features to those shown in figures 5.2 and 5.3. In particular the higher order mode may be parallel in contrast to VCSELs 1,2 when they are orthogonal.
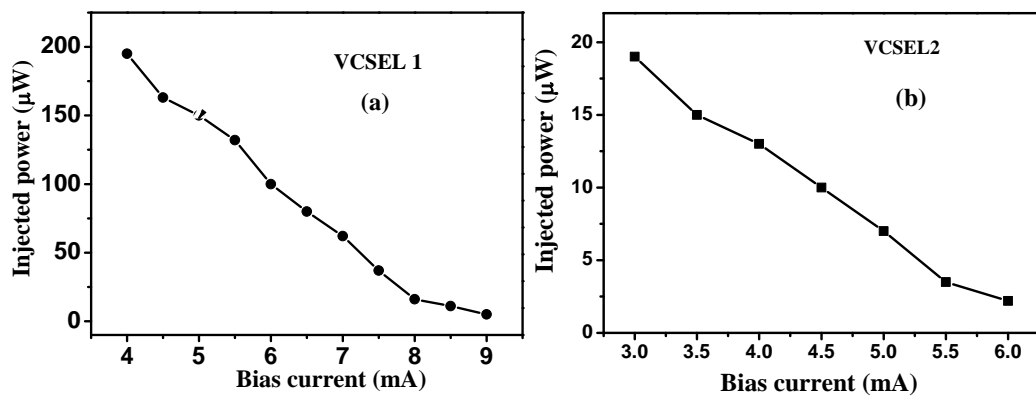
Figure 5.7: *Minimum optical injected power P_{inj} for PS as a function of VCSEL bias current, a) VCSEL1 with FD= -11 GHz, b) VCSEL2 with FD= -10.5 GHz.*

5.4.2 Frequency detuning for polarisation switching:

 Figure 5.8 shows the FD (blue filled triangles) at which PS in the VCSEL occurs as a function of bias current. The FD was scanned in decreasing direction until PS occurred. From the figure it is apparent that the PS occurs at a FD around -11 GHz for all operating bias currents.

It can be seen that the FD for polarisation switching to occur is independent of the VCSEL bias current using orthogonal optical injection. Orthogonally optically injected light into the VCSEL has been used to compare the roles of the suppressed mode frequency and the lasing mode frequency in PS. Figure 5.9a shows that when the FD was fixed at -11 GHz the PS occurs near 100 µW for increasing and decreasing P_{inj}.
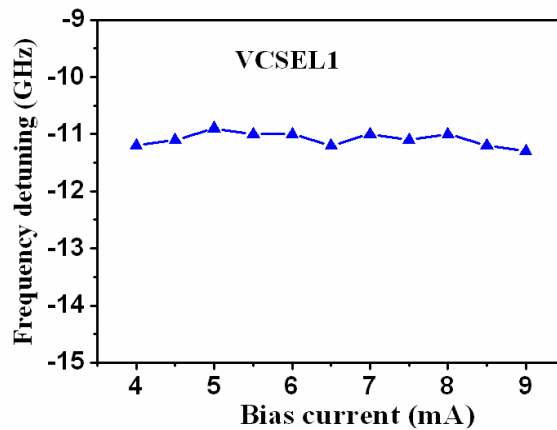
Figure 5.8: Frequency detuning for PS as a function of VCSEL1 bias current.

However, it can be seen in figure 5.9b that no PS was observed with orthogonal optical injection when the injected light frequency was at the frequency of the lasing mode, even for relatively high levels of P_{inj} greater than 2 mW. These results confirm the predictions of [13] that the minimum optical injected power required for PS is located around the frequency of the suppressed mode.
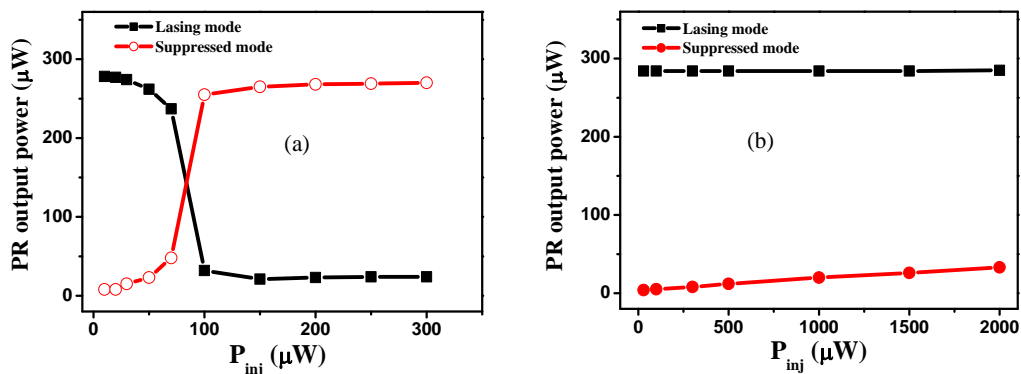

Figure 5.9: PR output power of VCSEL1 as a function of optical injected power, using orthogonal optical injection at bias current I= 6 mA. a) FD= -11 GHz, b) FD= 0 GHz.

Figure 5.10 shows the FD for polarisation switching as a function of optical injection power when VCSEL1 is subject to orthogonal optical injection at a bias current 6 mA. It can be seen that the FD for PS is independent of the level of injected power. The PS occurs around -11 GHz for large range of P_{inj}. In contrast it was reported by Quirce et al. [10] that the FD for PS depends on the optical injection power. The results in figure 5.10 agree with theoretical calculations included in [10] which indicated that the polarisation switching occurs at a frequency defined by the VCSEL birefringence. It is noted that the authors of [10] attribute differences in this respect between their theoretical and experimental results to thermal effects.
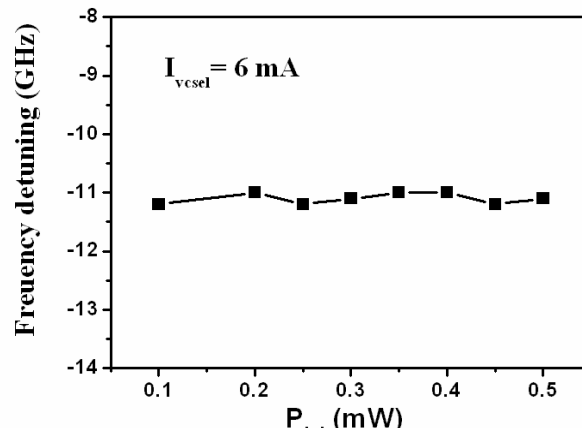
Figure 5.10: *Frequency detuning as a function of optical injected power (P_{inj}) for VCSEL1 with bias current of 6 mA.*

Additional measurements have been made in the polarisation-stable bias current regime of VCSEL2 (see section 3.3 stand- alone VCSEL2 characteristics figures 3.2, b1 and b2) in chapter three. The measurements made with this second device showed similar characteristics as those in figure 5.10 and thus are again in agreement with the theoretical results included in [10].

5.5 Parallel optical injection

In this section both polarisation resolved output power and FD for PS in VCSELs are investigated using parallel optical injection.

5.5.1 Polarisation resolved output power of VCSELs

Parallel optical injection has also been used to obtain the FD and optical injection power required for polarisation switching. The results show that using parallel optical injection the PS will normally occur at a positive FD for a wide range of VCSEL bias currents and P_{inj}. Figure 5.11 shows the PR output as a function of FD
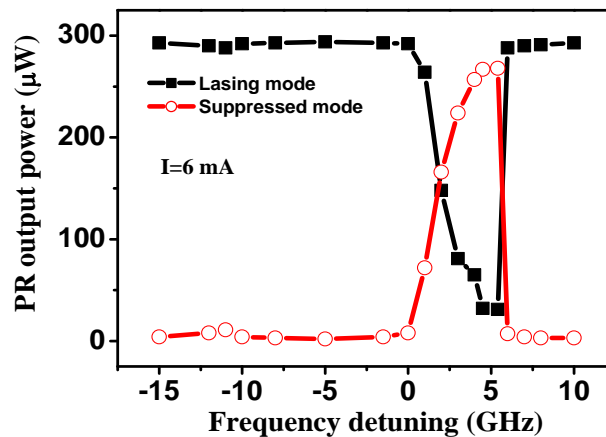

Figure 5.11: *Polarisation resolved output power of VCSEL1 as a function of FD when bias current is 6 mA and injection power is 350 μW.*

using parallel optical injection when the VCSEL1 biased at 6 mA and Pinj= 350 µW. FD ranges scanned from +10 GHz to -20 GHz.

Figure 5.12 shows the PR output power as a function of FD when the VCSEL1 was biased at 8 mA and P_{inj} is 500 µW. It can be seen that, in this case where the FD ranges scanned from +10 GHz to -20 GHz, PS occurs at positive detuning (around 7 GHz) and also close to the suppressed mode frequency (around -11 GHz). Abruptly PS occurred at FD of +5 GHz and then switched back to x-polarised mode gradually, which is considered to be related to optical injection locking.

The FD for PS changed with the optical injection power. This double switching scenario was observed only with the use of relatively high power parallel optical injection. However, it is emphasized that using orthogonal optical injection only a single switching point was observed near the suppressed mode frequency.
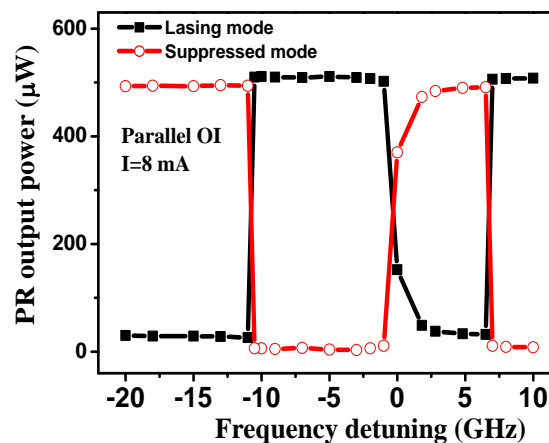

Figure 5.12: *Polarisation resolved output power of VCSEL1 as a function of FD, when bias current I = 8 mA and injection power 500 µW.*

5.5.2 Frequency detuning for polarisation switching:

In this section, the FD for PS to occur in VCSEL1 subject to parallel optical injection is investigated experimentally. Figure 5.13 shows the FD for PS as a function of P_{inj} for two fixed values of the bias current 6 mA and 8.5 mA. When the VCSEL1 is biased at 6 mA the FD for PS decreases with increasing optically injected power. However, for higher bias current 8.5 mA the FD for PS will increase with increasing P_{inj}.

As in the case of orthogonal optical injection, in parallel optical injection the optical injected power (P_{inj}) decreases with increasing VCSEL bias current, but for parallel optical injection the minimum optical injected power is between two to three times higher - depending on the bias current. For both schemes wide hysteresis is observed at high bias

currents ($> 2I_{th}$), while no hysteresis is observed for low bias currents. For parallel optical injection the FD for PS changes for different values of P_{inj} or bias current.
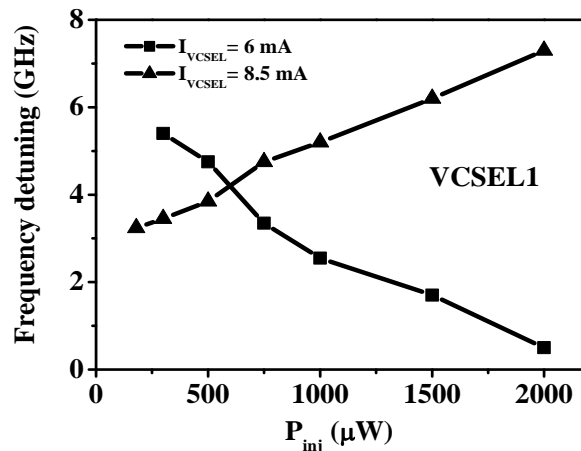

Figure 5.13: Frequency detuning as a function of optically injected power for VCSEL1, using parallel optical injection, for bias current 6 mA (filled squares) and 8.5 mA (filled triangle).

Similar PS characteristics in figure 5.13 were obtained for VCSEL2. Figure 5.14 shows that the positive FD for PS as a function of P_{inj}. When VCSEL2 is biased at 5 mA the FD for PS decreases with increasing optically injected power. However for VCSEL2 no FD (for PS to occurs) increase with increasing optically injected power has been observed.
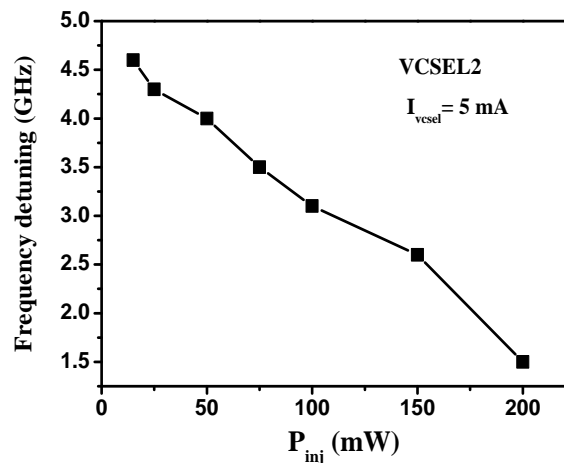

Figure 5.14: Frequency detuning as a function of optically injected power, using parallel optical injection, for bias current 5 mA.

Figure 5.15 shows the minimum optically injected power P_{inj} required for PS as a function of bias current. The figure show that using parallel optical injection the P_{inj} decreases with increasing bias current up to 8 mA and then starts to increase again. As noted earlier, for currents greater than 8 mA the VCSEL supports a higher- order transverse mode. It is considered that the increase in P_{inj} above 8 mA is related to the excitation of higher order modes. Using parallel optical injection the PS occurs at different detuning with increasing

VCSEL bias current. This is due to the FD dependence on injected power for parallel injection.
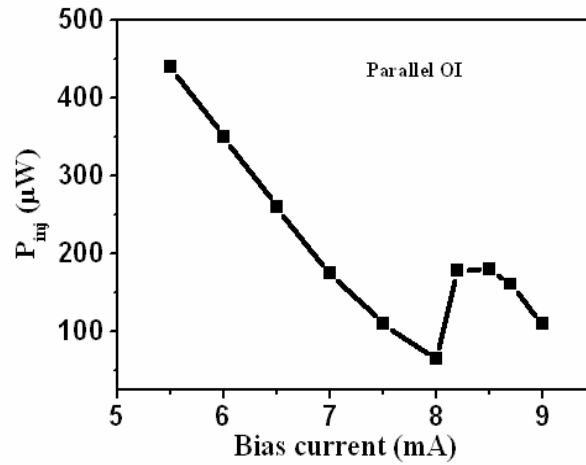

Figure 5.15: Optical injected power (P_{inj}) required for PS as a function of bias current for VCSEL1, using parallel optical injection.

Figure 5.16 show the minimum injected power required for PS using parallel optical injection for VCSEL2. The injected power decreases with increasing bias current, however, for VCSEL2 the increase of injected power at high bias current has not been observed.
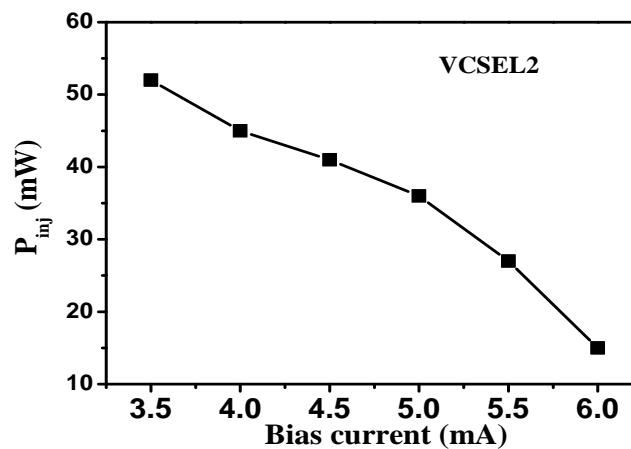

Figure 5.16: Optical injected power (P_{inj}) required for PS as a function of bias current for VCSEL2, using parallel optical injection.

5.6 Using various polarisation angles of optical injection

Figure 5.17 shows FD as function for several values of polarisation angle of injected light when the VCSEL1 was biased at 6 mA and P_{inj} =500 µW, VCSEL2 biased at 3.5 mA and P_{inj} =20 µW. The polarisation angle is the angle between polarisation of the injected light and polarisation of the lasing mode. Various polarisation angle of the injected light is obtained by using HWP1 in figure 5.1. For angles 90°, 75°, 60°, 45°and 30° it is clear that the PS occurs around the frequency of the suppressed mode, while for a polarisation angle

of 15° the polarisation switching is possible both near lasing mode frequency (positive FD) and around the suppressed mode frequency (negative FD). For an angle 0° which correspond to parallel optical injection the PS occurs only for positive FD.
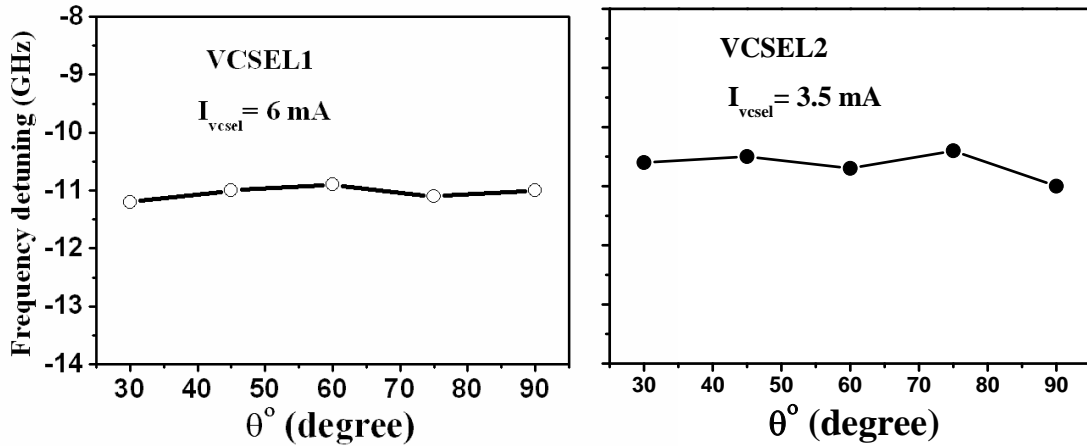

Figure 5.17: Frequency detuning as a function of polarisation angle of injected light for VCSEL1 and VCSEL2.

5.7 Polarisation-resolved optical spectra of optically injected VCSELs

In the previous section the role of the suppressed mode in polarisation switching in single mode optically injected VCSEL1 and VCSEL2 were presented. In this section, the polarisation–resolved optical spectra of VCSEL1 subject to orthogonal optical injection are investigated. The measurements were performed using the experimental setup detailed in figure 5.1.

Figure 5.18 shows the optical spectra of VCSEL1 subject to orthogonally optical injection with varying FD but fixed optical injection power (500 µW). The figure shows that the optical spectra of the suppressed mode are very similar to the optical spectra of the lasing mode, but with different intensity level (for clarity the intensity of lasing mode was reduced with HWP3 in the experimental setup figure 5.1). The figure shows the changes of the spectral characteristics with scanning FD. It can be seen that different spectral behaviours of device have been obtained in this FD range. In Figure 5.18(a), the detuning was -8.13 GHz the optical spectra of the suppressed mode begins to have an effect. The coexistence of the lasing mode and the injected light beam gives rise to a spectral peak near the frequency of the injected beam.

With further decreasing of the FD in figures 5.18 (b, c, d) (where the frequency detuning are -9.08 GHz, -9.56 GHz and -10.2 GHz respectively) the spectra of the suppressed mode exhibit are essentially identical to that of the lasing mode. In figure 5.18(b) when the FD is

-9.08 GHz, two groups of peaks coexist in the optical spectra of VCSEL1. The two peaks have different polarisation directions, one is in the x-polarisation direction (which is also the polarisation direction of the lasing mode near threshold) and the other peak is in the orthogonal y-polarisation direction (which is the polarisation direction of the suppressed mode). Decreasing the FD to -10.2 GHz, as in figure 5.18 (d), it is observed that two identical lasing peaks exist each with two very small side modes. Continued decreases of the FD in figure 5.18(e) show the spectral characteristics of the VCSEL1; the PS occurs, when the detuning was -11.1 GHz. Further decreasing FD to the -12.8 GHz the VCSEL1 output switches back to x polarised mode as shown in figure 5.18(f).
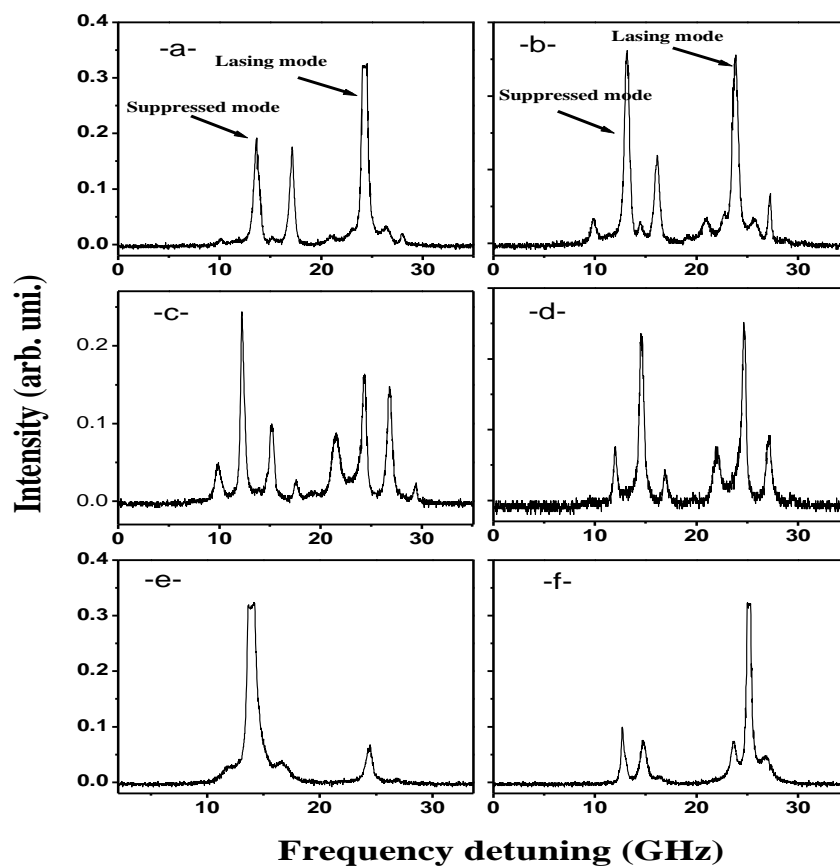

Figure 5.18: *Changes in spectral characteristics with FD for VCSEL1 using constant orthogonal optical injection power of 500μW. Frequency detuning FD: a) FD= -8.13 GHz, b) -9.08 GHz, c) -9.56 GHz, d) -10.2 GHz, e) -11.1 GHz, f) -12.8 GHz. For bias current 4.5 mA and temperature stabilised at 20° C.*

Figure 5.19 shows the spectral characteristics of the optically injected VCSEL1 when the optical injected power is varied for fixed detuning (-10 GHz). It can be seen that in the figures 5.19 (a, b) low injection power generates two strong peaks which represent the lasing mode and the suppressed mode.

For both peaks the two small side peaks, with frequency difference to the main peaks ~2.3 GHz, correspond to the undamped relaxation oscillation. With further increase of the orthogonal polarisation injection power to 500 μW, the optical spectra of the VCSEL became more complicated and a few peaks are excited as in figure 5.19(c). In figure 5.19(d) using 1000 μW injection power, show that the spectra of the lasing mode and suppressed mode are no longer identical.
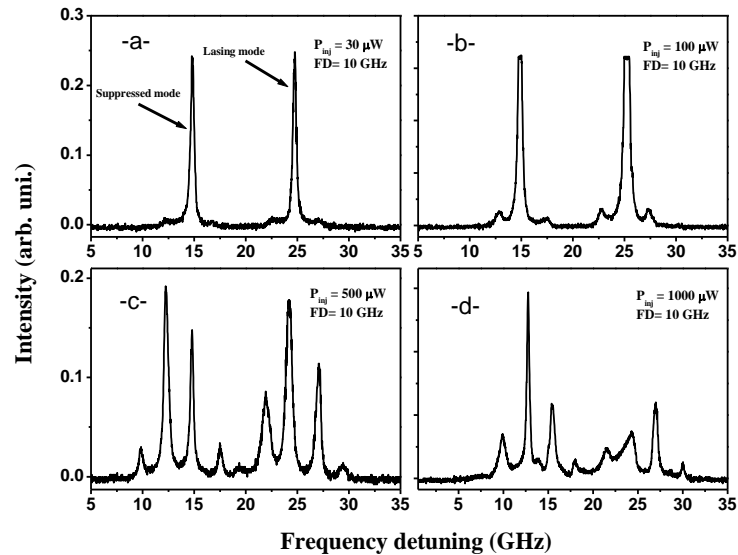

Figure 5.19: *Optical spectral changes with injection power for VCSEL1 using orthogonal optical injection, with fixed FD= -10 GHz. Injection power P_{inj}: a) $P_{inj} = 30$ μW, b) 100 μW, c) 500 μW, d) 1000 μW.*

Figure 5.20 shows the dynamical behaviour of the power in the x-polarised and y-polarised modes of the VCSEL biased at 4.5 mA, for a FD of -10 GHz and optical injection power of 1000 μW. AC coupling photodetector was used to record the time series. The figures indicate that the output power is stable.

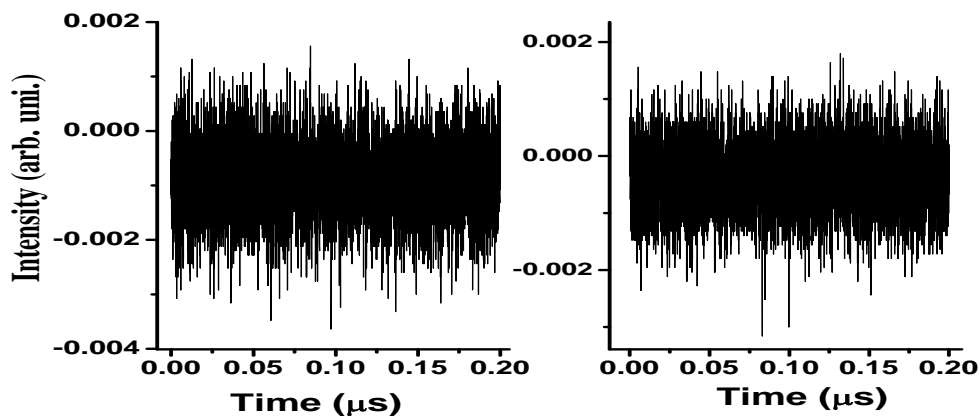**Figure 5.20:** *Time series of the polarisation-resolved output power of the VCSEL using optical injection power 1000 μW at detuning -10 GHz recorded using AC coupling photodetector.*

5.8 Polarisation resolved output power and polarisation switching using optical feedback.

In the previous sections the effect of polarised optical injection on VCSEL1 output power and spectral characteristics has been presented. In this section the effect of optical feedback on polarisation resolved output power, polarisation switching and spectral characteristics are investigated.

The experimental setup which has been used to perform the measurements in section 5.1 has been amended to use optical feedback, as shown in Figure 5.21. For the optical feedback experiments, the feedback ratio was defined as the ratio of the feedback power to the total output power of the VCSEL1. The polarisation and feedback power level of the re-injected light were measured just after the beam splitter (BS1). The dotted rectangle includes a PBS and optical power meter (Anritsu) which were used at position A to record the PR output and PS of the VCSEL. More details about the experimental setup and the characteristics of the stand-alone VCSEL1 can be found in section 5.3, and chapter 3 section 3.3 respectively.
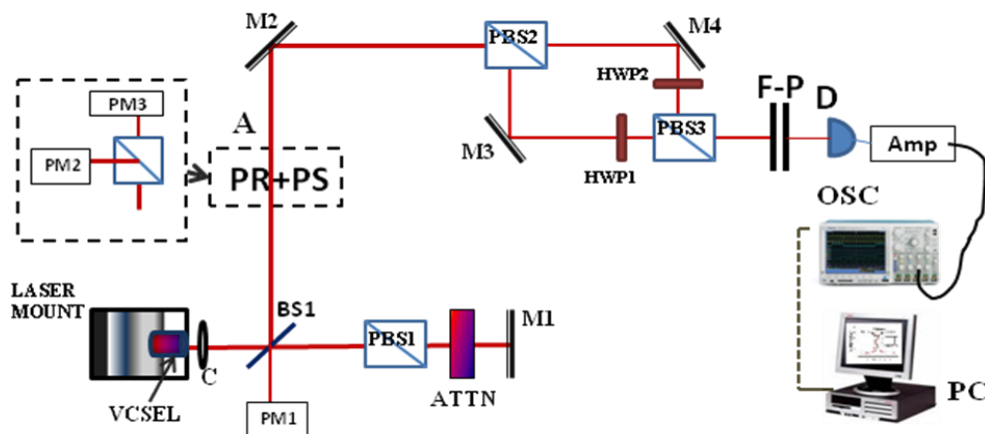

Figure 5.21: *Experimental setup : VCSEL laser; C– laser diode objective lens; BS– beam splitter; PBS– polarised beam splitter; ATTN – variable optical attenuator; M – mirror; PM– power meter; HWP – Half wave plate; F-P– Fabry–Pérot interferometer; D– detector; Amp– amplifier; OSC– oscilloscope; PC– personal computer.*

Figure 5.22 shows the PR output power as a function of the bias current of the VCSEL1 subject to y-selective polarised optical feedback. Figure 5.22(a) shows the PR output power measured with a constant optical feedback ratio of -35.2 dB.

It can be seen that the stable PS with this low feedback ratio only occurs above bias currents of about 6.55 mA (~ $1.8I_{th}$). This is explained by the fact that at high bias current the VCSEL requires a lower feedback ratio for PS to occur.
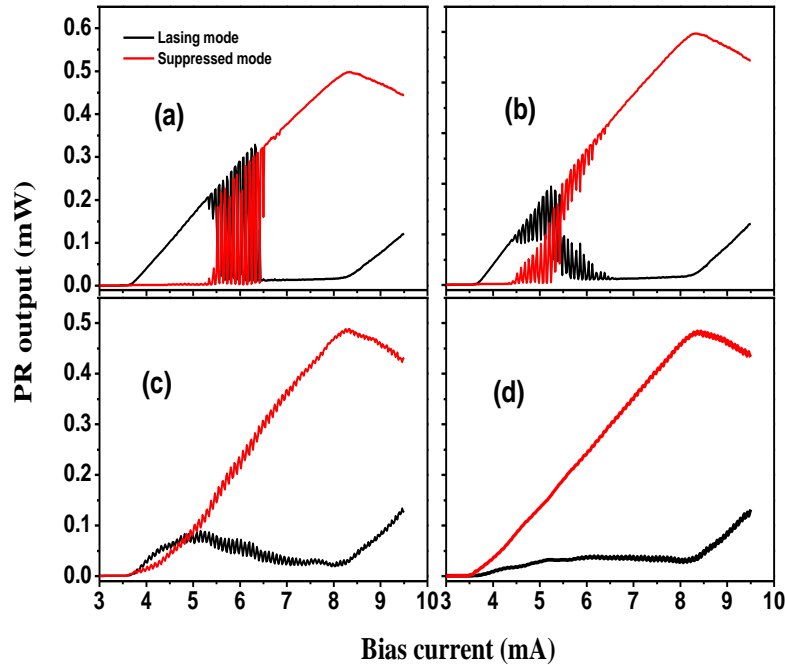

Figure 5.22: *Polarisation-resolved L-I curve of the VCSEL subject to y- polarized selective OF. The black curve and red curve correspond to lasing mode (parallel polarised light) and suppressed mode (orthogonal polarised light), respectively. The feedback ratios are a) -35.2 dB, b) -30 dB, c) -18.2 dB, d) -16 dB.*

In addition, weak optical feedback induces multiple polarisation switching between x-parallel polarised and y-orthogonal polarised modes. When the feedback ratio was increased to -30 dB, as shown in figure 5.22(b), the PS occurred at a lower bias current (~ 6.25 mA) than the bias current in the case of the smaller feedback ratio of -35.2 dB. With further increase of the feedback ratio to -18.2 dB, as shown in figure 5.22(c), the PS point moves to a lower bias current around 5.5 mA accompanied by a fluctuation in the output power of the VCSEL. The lasing mode (x-polarised light) was completely suppressed a higher feedback ratio of -16dB, as illustrated in figure 5.22(d). For this feedback ratio the VCSEL emits y-polarised light for the entire range of bias currents.

The polarisation switching points as a function of the VCSEL bias current have been obtained in figure 5.23. It can be seen that the feedback ratio required for PS decreases significantly with increased bias current. For high bias current 7.8 mA (which is more than $2I_{th}$) the feedback ratio for PS is as low as -37 dB. It is worth noting that the trend of the obtained results using selective optical feedback is similar to that obtained using orthogonal

optical injection in [14]. With both optical feedback and optical injection the power required for PS between the fundamental modes decreases significantly with increasing VCSEL bias current.

5.9 Spectral characteristics of VCSEL1 subject to optical feedback

In this section, the influence of the various feedback levels on optical spectra of the suppressed mode was investigated experimentally using orthogonal and parallel polarised selective optical feedback.

Figure 5.24 shows the optical spectra of the suppressed mode using orthogonally polarised selective optical feedback. The VCSEL1 was biased at 5 mA ($I>2I_{th}$) and the feedback ratio was -25.18 dB. The figure shows that the optical spectra of the suppressed mode are essentially identical to the lasing mode spectra for this feedback ratio. In the figure, two main peaks coexist in the optical spectra of the VCSEL1. Each main peak is accompanied by two very small side peaks with frequency differences of about 2.6 GHz to the main mode. For further increase of the feedback ratio the optical spectra of the lasing mode and the suppressed mode are no longer identical.
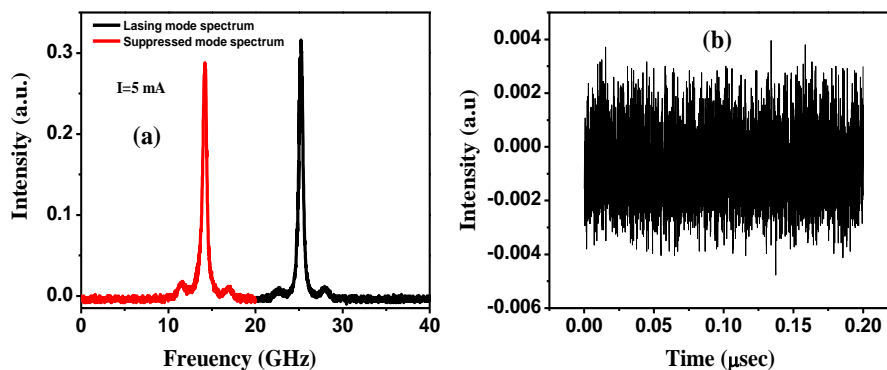

Figure 5.24: *Optical spectra and time series of VCSEL1 subject to y-polarision selective optical feedback. The bias current is 5 mA and the feedback ratio is -25.18 dB.*

Figure 5.25 show the influence of selective x-polarised feedback on the optical spectra of the suppressed mode when the VCSEL is biased at 8 mA using different feedback ratios. Similarities between the suppressed mode and lasing mode spectra have been found for the defined range of the feedback ratios.

The time traces of the polarisation resolved emission are shown in figure 5.25(c, d). It can be seen that for high feedback level the VCSEL shows some instabilities in the time traces of the x- polarised mode. However, for y- polarised mode such instabilities were not observed perhaps due to the very low level of the mode power.
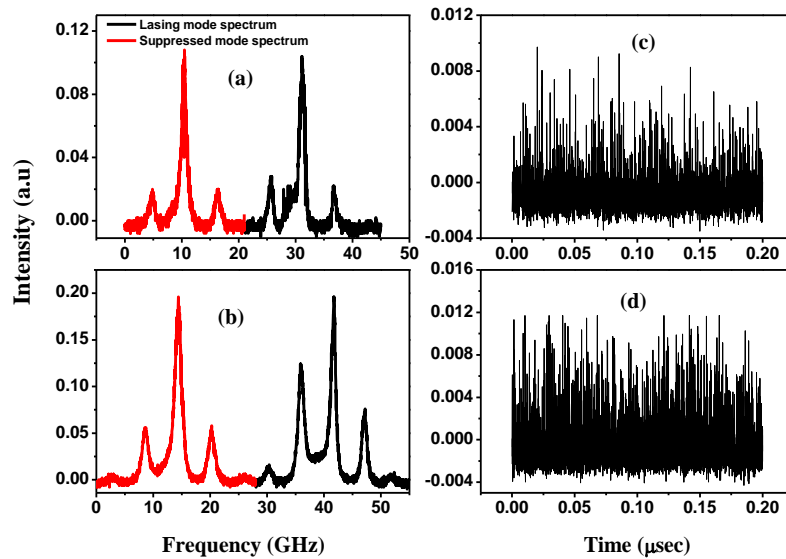
***Figure* 5.25:** *Optical spectra and time series of VCSEL1 subject to x-polarisation selective optical feedback. The bias current is 8 mA and the feedback ratios are a) -20 dB, b) -18.5 dB.*

5.10 Summary and Conclusion

Experimental investigations of the polarisation switching and spectral characteristics in optically injected have been presented. Specific attention has been given to the role of the suppressed lower order transverse mode in polarisation switching and spectral characteristics of optically injected VCSELs.

The physical mechanism underlying the optical injection induced PS in VCSELs is considered simply to be the change in local gain and hence modal gain caused by the optical injection. As such the injected light (regardless of its polarisation angle within a certain range) will induce switching between the fundamental modes.

The results show that the FD for PS is close to the VCSEL birefringence and is independent of the VCSEL bias current, optical injection power and a defined range of polarisation angles. For both VCSEL1 and VCSEL2 the minimum P_{inj} for PS using orthogonal optical injection was found at a FD of -11 GHz, and 10.5 GHz respectively. This FD represents the frequency difference (birefringence) between the lasing mode and the suppressed mode of the VCSEL. In contrast to measurements reported in [10], P_{inj} is found to decrease significantly with increasing bias current.

For parallel optical injection the FD for PS is positive, and is dependent on P_{inj} and the VCSEL bias current and is considered to be consistent with injection locking. For VCSEL1 the FD for PS decreases with increasing P_{inj} for a bias current of 6 mA (I< 2Ith), while FD

for PS   increases with increasing P_{inj} for higher bias current 8.5 mA (I> 2Ith). For VCSEL2 the FD for PS also decreases with increasing $P_{inj.}$ However, for VCSEL2 the increase of FD for PS with increasing P_{inj} has not been observed.

The influences of varying the FD and optical injection level for polarised optical injection on the optical spectra of the suppressed mode were also investigated. For a defined range of FD and injection power, the VCSEL suppressed mode possesses essentially identical optical spectra to that of the lasing mode spectra. Similar spectral characteristics of the device have been found using polarisation selective optical feedback.

From the above discussion and experimental results in this chapter and those included in chapter three it is apparent that optical injection can influence the polarisation state selection and control the polarisation switching between fundamental modes. The more control of the polarisation behaviour of the VCSELs which can be exercised will broaden potential device applications.

In the next chapter, irreversible polarisation switching in optically injected VCSELs will be addressed.

References:

[1] **M. San Miguel,** Q. Feng, and V. Moloney, "Light –polarization dynamics   in surface-emitting semiconductor lasers," Phys. Rev. A. vol. 52, pp. 1728-1739, Aug. **1995**.

[2] **J. Martin-Regalado,** S. Balle, M. S. Miguel, A. Valle, and L. Pesquera, "Polarization and transverse-mode selection in quantum-well vertical-cavity surface-emitting lasers: Index- and gain-guided devices," Quantum Semiclass. Opt., vol. 9, pp. 713–736, **1997**.

[3] **Z. G. Pan,** S. Jiang, M. Dagenais, R.A. Morgan, K. Kojima, M. T. Asom, R.E. Leibenguth, G. D. Guth, and M. W. Focht, "Optical injection induced polarization bistability in vertical-cavity surface-emitting lasers," Appl. Phys. Lett. vol. 63, pp. 2999-3001, **1993**.

[4] **W. L. Zhang,** W. Pan, B. Luo, M. Y. Wang, and X. H. Zou, "Polarization switching and hysteresis of VCSELs with time-varying optical injection," J. of Selec. Top. in Quantum Electron., vol. 14, pp. 889-894, May/Jun. **2008.**

[5] **J. Houlihan,** L. Lewis, and G. Huyet, "Feedback induced polarisation switching in vertical cavity surface emitting lasers," Optic. Commun., vol. 232, pp. 391–397, **2004.**

[6] **J. Paul,** C. Masoller, Y. Hong, P. S. Spencer, and K. Alan Shore, "Experimental study of polarization switching of vertical-cavity surface-emitting lasers as a dynamical bifurcation," Optic. Lett., vol. 31, pp. 748-750, Mar. **2006.**

[7] **Y. Hong,** P.S.Spencer, S. Bandyopadhyay, P. Rees and K. Alan Shore, "Polarization-resolved chaos and instabilities in a vertical cavity surface emitting laser subject to optical injection," Optic. Commun. vol. 216, pp. 185-189, **2003**.

[8] **M. Torre,** A. Hurtado, A. Quirce, A. Valle, L. Pesquera, and M. Adams, "Polarization switching in long-wavelength VCSELs subject to orthogonal optical injection," IEEE, J. of Quant. Electron. vol. 47, no. 1, pp. 92-98, Jan. **2011**.

[9] **I. Gatare,** J . Buesa, H . Thienpont, K .Panajotov, and M. Sciamanna, "Switching bistability and dynamics in vertical-cavity surface-emitting laser under orthogonal optical injection," Optical and Quantum Electron., vol. 38, pp. 429–443, **2006**.

[10] **A. Quirce,** J. R. Cuesta, A. Valle, A. Hurtado, L. Pesquera, and M. Adams, "Polarization bistability induced by orthogonal optical injection in 1550-nm multimode VCSELs," IEEE J. of Selec. Top. in Quantum Electron., vol. 18, no. 2, pp. 772-777, Mar./April **2012**.

[11] **M. Sciamanna** and K. Panajotov, "Route to polarization switching induce by optical injection in vertical cavity surface emitting lasers," Phys. Rev. A, vol. 73, pp.023811, **2006**.

[12] **I. Gatare,** M. Sciamanna, J . Buesa, H . Thienpont,and K .Panajotov, "Nonlinear dynamics accompanying polarization switching in vertical cavity surface emitting lasers with orthogonal optical injection" Appl. Phy. Lett. vol. 88, pp. 101106, **2006**.

[13] **J. Martin-Regalado,** F.Prati, M. S. Miguel, and N. B. Abraham, "Polarization properties of vertical-cavity surface-emitting lasers," IEEE J. Quantum Electron., vol. 33, no. 5, pp. 765–783, May **1997**.

[14] **A. A. Qader,** Y. Hong and K. Alan Shore, "Role of suppressed mode in the polarization switching characteristics of optically injected VCSELs," IEEE J. Quantum Elect., vol. 49, pp. 205-209, Feb. **2013**.

CHAPTER SIX

IRREVERSIBLE POLARISATION SWITCHING

IN OPTICALLY INJECTED VCSELS

◆━━━◆

Chapter 5 focused on investigating polarisation switching (PS) of optically injected VCSELs in the single mode regime and the role of suppressed mode in PS was identified. In this chapter, PS characteristics of two-mode VCSELs subject to polarised optical injection are addressed. In the two-mode regime robust and irreversible PS were observed with changes in frequency detuning and optical injection power.[1] Robust irreversible means that the PS was maintained over a wide range of a number of control parameters including: bias current and device temperature. The results of PS characteristics in two mode regime were compared to the experimental observation in single mode regime.

The content of this chapter are organised as follows:
 In section 6.1 gives a brief introduction to PS characteristics of multi-mode VCSELs. Section 6.2 describes the experimental setup used to demonstrate the PS characteristics in VCSELs supporting precisely two modes. Section 6.3 includes the frequency-detuning-induced irreversible PS using parallel and orthogonal optical injection. In section 6.4 injected optical power-induced irreversible PS is demonstrated in two mode emission operation and multi-mode operation. Section 6.5 investigates the range of the control parameters where irreversible PS was maintained. Finally section 6.6 summarises the main conclusions drawn from the experimental results.

6.1 Introduction

The PS characteristics of single mode VCSELs have been widely investigated experimentally and theoretically [1-4], however, PS in multi-mode VCSELs has not received much attention. The excitation of higher orders modes in VCSELs with increasing bias current makes their emission characteristics more complex. In the multi-mode regime PS and bistability have been investigated experimentally [5] and theoretically [6, 7]. Despite the fact that such studies have been conducted of PS in multi-mode VCSELs, little

_____

[1]*This chapter is based on the paper:*
 A. A. Qader, Y. Hong and K. A. Shore, IEEE, Photo. Tech. Lett., vol. 25, pp. 1173-1176, Jun. 2013.

attention has been paid to the robustness of the PS when a control parameter is changed. The polarisation bistable operation is highly desirable in realising VCSELs with high switching speed. However, one of the main drawbacks to its practical utilisation is the dependence of bistable operation on the device temperature.

In the present chapter, experimental observations are described which indicate means by which VCSEL PS persists even when values of the control parameters are reversed. This behaviour is termed here 'irreversible Polarisation switching' (IPS). The output power of the VCSEL scanned with increasing and decreasing frequency detuning (FD). FD is the frequency difference between the master laser frequency and slave laser frequency (frequency of the lasing mode). In as much as the behaviour is obtained with a number of control parameters including bias current and device temperature, it is considered that the phenomenon is robust.

6.2 Experimental setup

The experimental setup used in this work is illustrated in figure 6.1. Optical injection is achieved by means of an external cavity tunable single-frequency master laser (model SDL-TC10), with a centre wavelength of 850 nm and wavelength tuning range of about 20 nm.
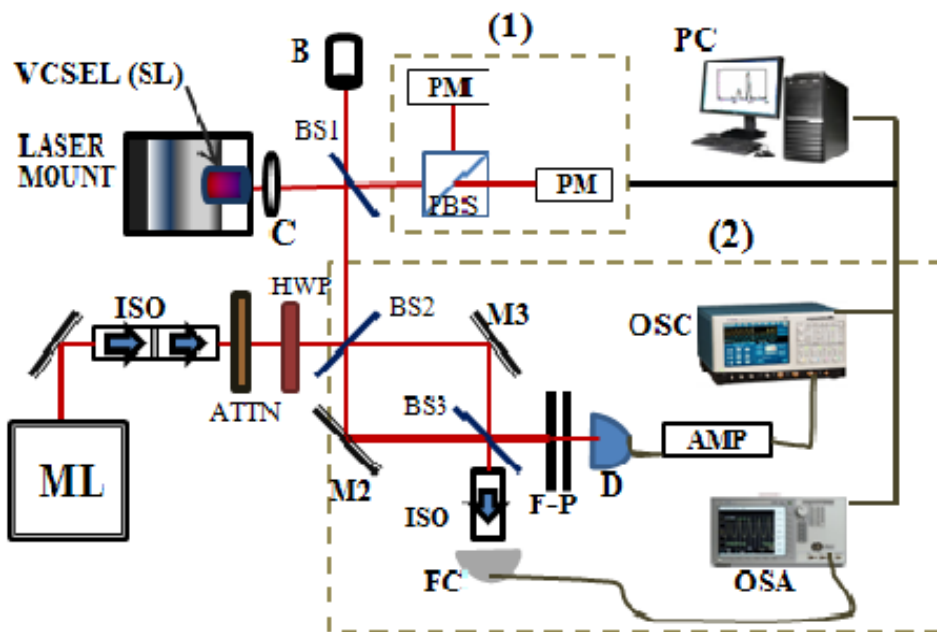

Figure 6.1: Experimental setup: SL – slave laser; C– laser diode objective lens; BS –beam splitter; ML – master laser; M –mirror; ISO –optical isolator; ATTN – variable optical attenuator; HWP–Half wave plate; F-P –Fabry–Pérot interferometer; D–detector; Amp– amplifier; FC–fibre coupling; OSA– optical spectrum analyser; OSC–oscilloscope; PC– personal computer; B– Removable beam block; PBS– polarised beam splitter; PM– power meter.

A commercially available oxide-confined quantum well VCSEL (which was termed VCSEL1 in chapter3) was used as the slave laser (SL) in this work. Figure 6.2 show a photograph of the optical components included in the experimental setup. The experimental setup is similar to that in figure 5.1, however, several optical components have been re-organised for more efficient optical injection scheme. Further explanation of the optical components is provided in association with figure 5.1.
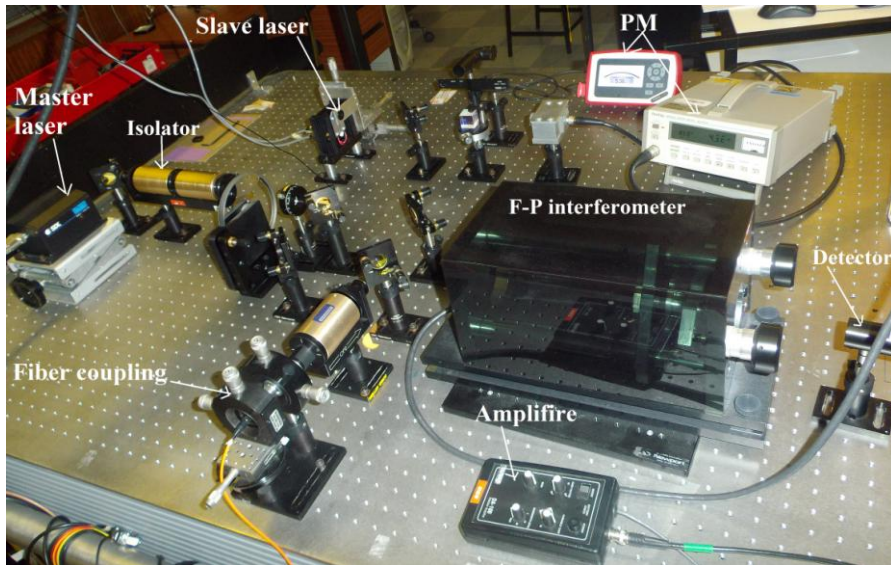

Figure 6.2: *Photograph of the experimental setup.*

Figure 6.3 shows the optical spectrum of the VCSEL with a bias current of 8.5 mA, indicating two-transverse mode emission. The orthogonally Polarisation higher order mode is shifted 0.37 nm to the short wavelength side of the fundamental mode.
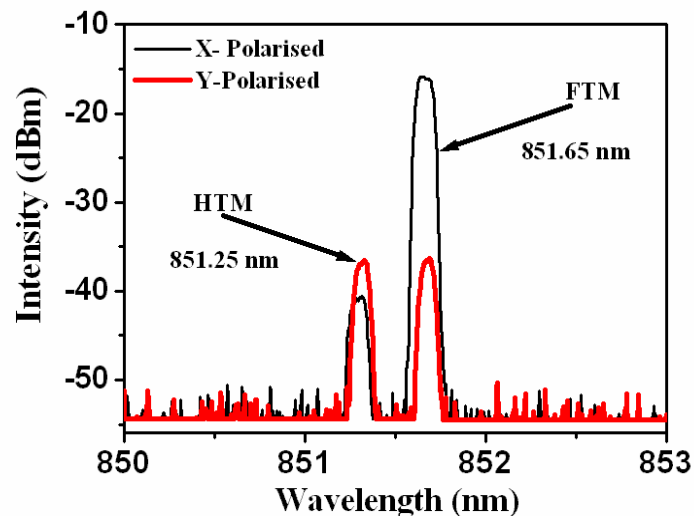

Figure 6.3: *Optical spectra of the stand-alone VCSEL for bias current I= 8.5 mA, showing fundamental transverse mode (FTM) and higher transverse mode (HTM).*

6.3 Frequency detuning induced irreversible polarisation switching:

In this section, new characteristics of the PS in multi-mode VCSELs unveiled. Both parallel and orthogonal polarised optical injections were used to explore the irreversible PS characteristics in two mode regime. The optical spectrum of VCSEL1 in chapter 5, figure 5.2 shows that the device start supports two lasing modes when the bias current exceeds 8 mA.

6.3.1 Using parallel optical injection

The PS characteristics in multi-mode regime of VCSEL1 were investigated using parallel optical injection when the device was biased at 8.5 mA. Figure 6.4 shows PS of the VCSEL (orthogonal Polarisation- $P\perp$) as a function of FD, when the FD is first decreased (red line) and then increased (black line) with fixed optical injection power $P_{inj} = 4$ μW.

It can be seen that for decreasing FD two PS points are found: near zero and in the negative detuning region; the device exhibited a small hysteresis cycle (see the inset figure in Fig. 6.4). For increasing FD, the first PS occurred at about -9.5 GHz, with further increase of the FD, the Polarisation of the VCSEL switched back to X-Polarisation at about -7 GHz.
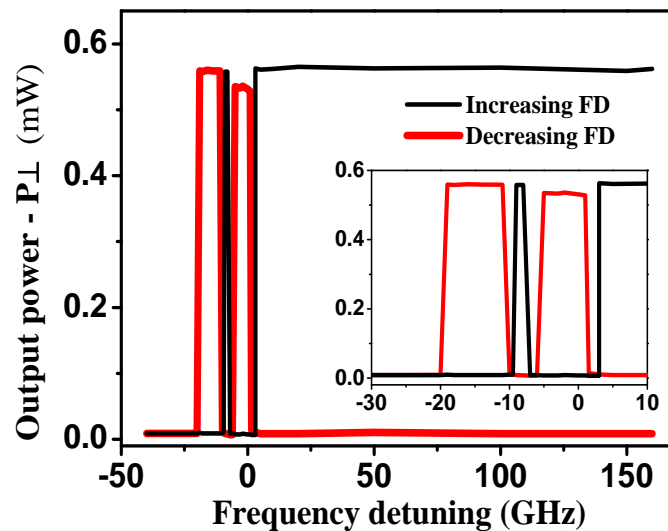

Figure 6.4: PS in the output power (orthogonal polarisation) as a function of FD. Using parallel optical injection when FD decreased red thick line and then increased black line.

With continued increase of the FD to about 3 GHz, the VCSEL switched to the orthogonal polarisation mode and continued emitting in that mode (no switchback is observed for large positive detuning range). The device thus exhibits irreversible polarisation switching (IPS). Similar results have been obtained for parallel injected power levels up to 1 mW.

In [6] it was observed experimentally and predicted theoretically that VCSELs in the multi-mode regime were characterised by another minimum switching power near the frequency of the higher order mode. No such switching point was observed in the performed experiments using parallel optical injection

6.3.2 Orthogonal optical injection

Orthogonal polarised optical injection has also been used to experimentally investigate PS in multi-mode VCSELs. Using orthogonal optical injection three types of PS are observed. First when low optical power injection is used ($P_{inj} < 20$ µW), PS occurred at negative detuning with a small hysteresis cycle, no IPS is observed for such low P_{inj}. Increasing P_{inj} above 20 µW a second type of PS, similar to the results in figure 6.5, was obtained. The intensity spectra of the VCSEL indicate that both fundamental and higher order modes are involved in the PS in the two mode regime.

Figure 6.5 shows IPS in the VCSEL output power (orthogonal Polarisation) as a function of FD using orthogonal optical injection. In figure 6.5 a P_{inj} of 25 µW has been used when the FD first decreased (thick - red line) and then increased (black line).

It can be seen that a single PS occurred when the FD decreased while for increasing FD a double PS occurred with no switch back observed for the second PS (see the inset in figure 6.5). The third type of the PS was observed when P_{inj} increased above 50 µW. For the latter case the VCSEL output power will switch back to parallel Polarisation around the frequency of the higher order mode, thus exhibiting an ultra-wide hysteresis cycle.
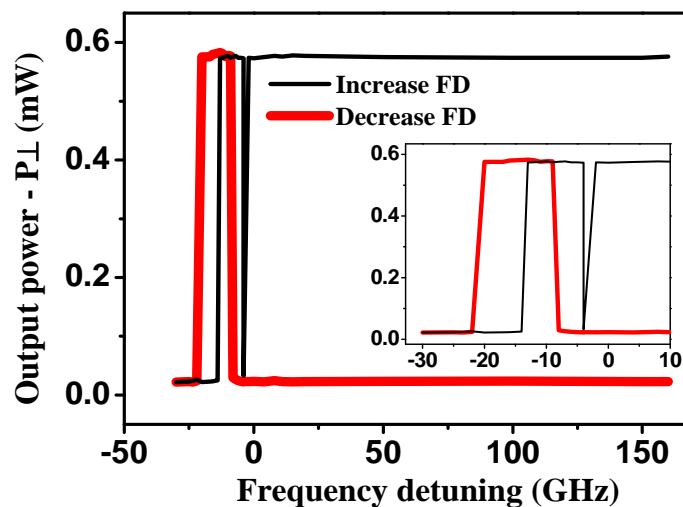

Figure 6.5: *PS in the output power (orthogonal polarisation) as a function of FD. Using orthogonal optical injection when FD decreased red thick line and then increased black line.*

Characterization of this ultra-wide hysteresis will be investigated in chapter 7. No such ultra-wide hysteresis is observed with parallel optical injection scheme even for high injection power >1mW.

It noted that no such irreversible PS was observed in work reported in [5-7]. The device used in [5] is a multi-transverse mode, long wavelength (1550 nm) VCSEL. It is characterised by a large frequency separation between the two orthogonal Polarisation modes (60 GHz) and parallel Polarisation emission for the two transverse modes. In contrast, the device used in this work supports a single transverse mode for bias currents up to about 8 mA, and the excited higher-order transverse mode has its Polarisation orthogonal to that of the fundamental mode (see figure 5.2). References [6, 7] do not describe in detail the device used in their experiments but it is expected that those VCSELs possess contrasting spectral features to the devices used in the experiments described here.

6.4 Intensity Induced irreversible polarisation switching

Intensity-induced PS has been investigated for both parallel and orthogonal optical injection schemes. Intensity-induced PS occurs when the injection power first is increased and then decreased for a fixed FD. Figure 6.6 shows the intensity induced PS when the VCSEL is biased at 8.5 mA with a fixed FD of -11 GHz for orthogonal optical injection and a FD of +2 GHz for parallel optical injection.

It can be seen that for both parallel and orthogonal optical injection the VCSEL continues to emit in the orthogonal Polarisation even when the injected power is decreased to zero. This represents another case of IPS. This behaviour of VCSEL is considered to be related to the excitation of higher order transverse modes.

It was observed experimentally in [8, 9] that the VCSELs emission remain in orthogonal polarisation after PS occurred using orthogonal optical injection. The VCSELs were used in their work was characterised by polarisation unstable. However, no detail was given about the optical spectra of the VCSELs. The VCSELs were biased in a bistable region and very high injected power was used (a few mW) and the behaviour of the VCSELs was attributed to characteristics of the bistable region.

Intensity induced PS in multi-mode regime when VCSEL biased at I=9.5 mA have also been investigated here. At this bias current the optical spectra shows that additional higher order modes are excited. Figure 6.7 shows the intensity induced PS in VCSEL subject to orthogonal optical injection at a fixed FD of - 11 GHz. It can be seen that when the optical injection power increased the PS occurred at P_{inj}= 3 µW. For decreasing injection power

the VCSEL output power switches back to parallel polarisation at $P_{inj}=2$ μW, thus exhibited only a small hysteresis.
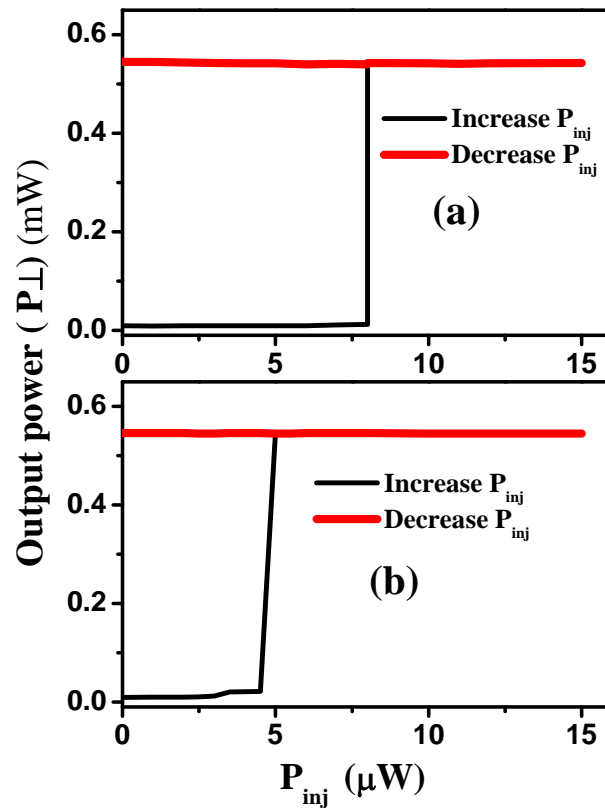

Figure 6.6: PS in the output power (orthogonal mode) of the VCSEL as a function of injection power. For a) parallel optical injection, b) orthogonal optical injection.

These characteristics of intensity induced PS are similar to those of the single mode regime. Therefore, it is considered that the IPS behaviour is the characteristics of two mode emission regime only.
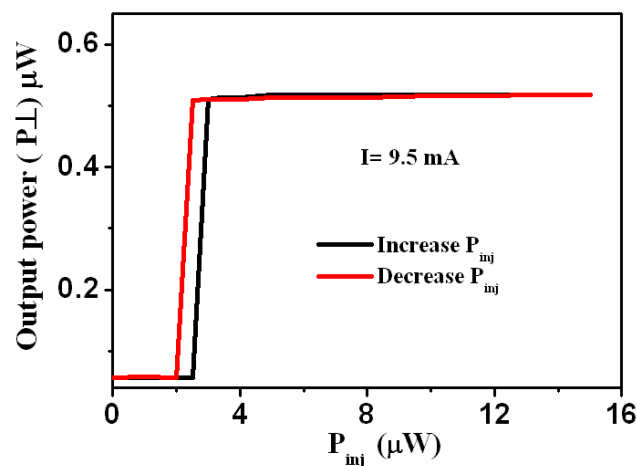

Figure 6.7: PS in the output power (orthogonal mode) of the VCSEL as a function of injection power. Using orthogonal optical injection when VCSEL bias at 9.5 mA and the FD was fixed at -11 GHz.

6.5 VCSELs control parameters for irreversible polarisation switching

This section addresses the range of values of two control parameters: the bias current and the device temperature, where irreversible PS was maintained using optical injection. First the polarisation resolved output as a function of the VCSEL bias current and device temperature have been obtained. Furthermore, the results were compared to the single mode PS characteristics under optical injection.

6.5.1 VCSEL bias current range

In figure 6.8 polarisation resolved output power as a function of VCSEL bias current using parallel optical injection illustrating the current of which the PS is maintained.

In order to obtain the bias current range where the PS was maintained, the device biased at 8.5 mA. The FD was fixed at +2 GHz with respect to this bias current of the SL and the injected power was 50 μW.

When the PS was obtained the optical injection power was removed completely. Then the VCSEL bias current was scanned up starting from 8.5 mA, the VCSEL emission switched back to x-polarised mode at 9.2 mA. For scan down the VCSEL was biased again at 8.5 mA and injected with 50 μW, when the PS occurred the optical injection power was removed completely. Then the current was scanned down starting from 8.5 mA, the VCSEL emission remained in y polarisation mode until bias current 7.65 mA, when switched back to the x-polarised mode. Therefore, a large range of the bias current (more than 1.5 mA) was obtained over which the output power of the VCSEL remains in the orthogonal Polarisation direction after PS occurred.
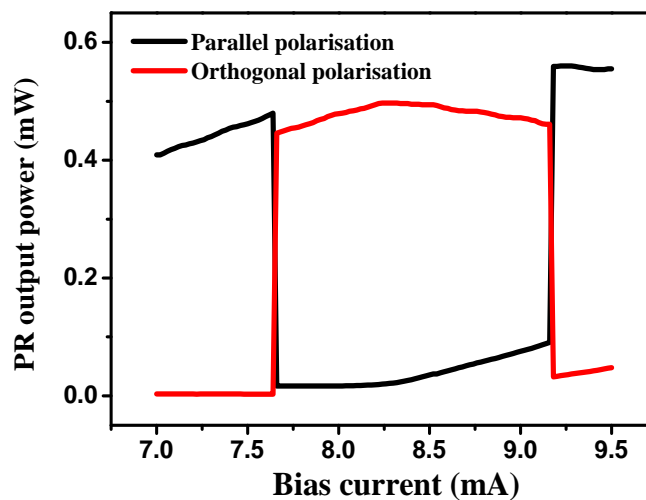

Figure 6.8: PR output power of VCSEL 1 as a function of bias current using parallel optical injection. I=8.5 mA, P_{ini} =50 μW and FD= +2 GHz.

The polarisation resolved output power as a function of bias current in single mode regime was also investigated. The results show that no such wide range of bias current for maintaining PS is observed for single mode regime. The hysteresis and polarisation resolved output power of VCSEL under optical injection is discussed further in the next chapter- section 7.4.

6.5.2 Temperature range

Device temperature is one of the most important control parameters of VCSELs emission. The stability of emission characteristics of VCSELs over a wide range of device temperature is of great importance for some applications including optical switching. PS characteristics as a function of operating temperature have been investigated in multi-mode optically injected VCSELs. Figure 6.9 shows the polarisation resolved output power as a function of device temperature in the VCSEL1. In both figure 6.8 and 6.9 the injected power is removed completely after the occurrence of the PS. The persistence of this PS behaviour for a range of control parameter values leads to term such behaviour in the VCSELs emission as robust.

In the experiments, parallel polarised optical injection has been used, the VCSEL1 biased at 8.5 mA, P_{inj}= 50 µW, and FD = +2 GHz. Range of the device temperature (from 10^oC to 30^oC) where the output power of the VCSEL continues emitting in the orthogonal Polarisation after the PS occurred.
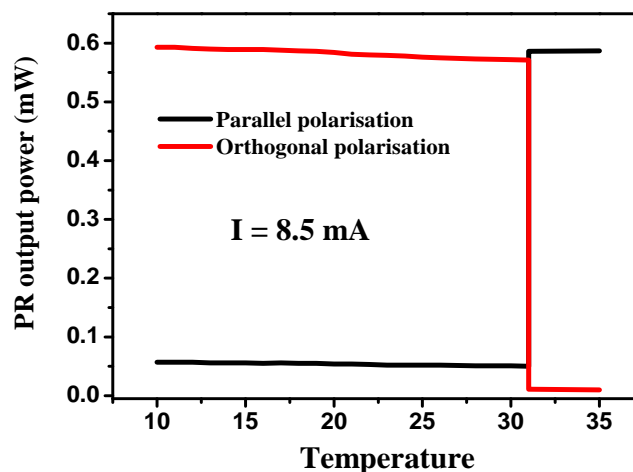
.

Figure 6.9: *PR output power as a function of the device temperature using parallel optical injection shows the temperature range of the stable IPS. I= 8.5 mA, P_{inj}= 50 µW, and FD = +2 GHz.*

The temperature range where the PS maintained in single mode regime has also been investigated Figure 6.10 shows the polarisation resolved output power (orthogonal mode) as a function of device temperature, when the VCSEL1 biased at 6 mA (single mode regime operation), device temperature was 20°C, using optical injection power 100 µW, and FD = +3.5 GHz. After PS occurred the device temperature scanned up and remains in y polarisation just to the temperature 21°C then switched back to x polarisation mode. For scanned down the VCSEL 1 was fixed first at device temperature 20°C then PS occurred and remained in y polarisation until device temperature 19°C. For single mode operation it can be seen that the PS in the VCSEL1 is maintained within a very small temperature range (19°C– 21°C). Therefore, the robust IPS occurs only in a two-mode regime.
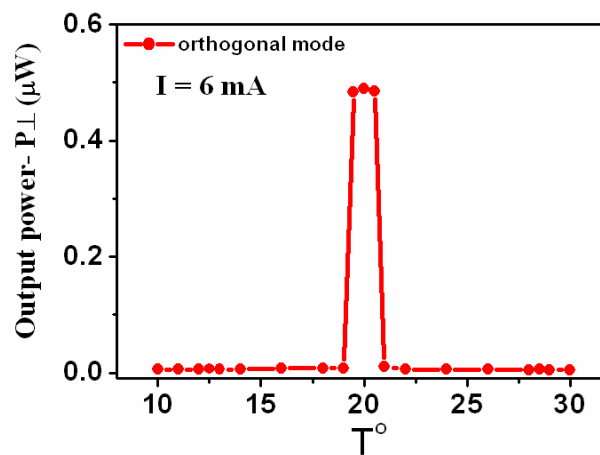

Figure 6.10: *Polarisation resolved output power (orthogonal polarisation) as a function of the device temperature using parallel optical injection. I= 6 mA, P_{inj}= 100 µW, and FD = +3.5 GHz.*

Furthermore, for the specific device used here, in the bias current range 7.7 mA- 9.2 mA both FD-induced IPS and intensity induced IPS were observed. In this bias current range two modes are supported - as shown in figure 5.2 chapter 5. For lower bias currents single mode operation regime whilst for higher bias current additional higher order modes are excited. In both cases IPS is not observed outside this bias current range (7.7 mA- 9.2 mA). In consequence was considered that the observed behaviour is a feature of the regime of two-mode operation. Furthermore, in the present work several VCSELs have been investigated and have shown the same IPS characteristics when subject to parallel/ orthogonal optical injection.

6.6 Summary and conclusion

This chapter has focused on the observation of robust irreversible Polarisation switching in optically injected VCSELs operating in the multi-mode regime. The results show that using both parallel and orthogonal optical injection VCSELs may exhibit irreversible PS for decreasing and increasing FD. The intensity-induced Polarisation switching has also been found in the two-mode regime, showing intensity-driven irreversible PS for both parallel/orthogonal optical injections. The PS was found to persist for a wide range of the control parameters including bias current and device temperature (from 10°C to 30°C).

Using orthogonal optical injection only for small range of the optical injection power, VCSEL 1 exhibited irreversible PS, with high injection power the VCSEL 1 move to the ultra-wide hysteresis bistability.

Furthermore, the PS in single mode operation (I < 2Ith) of VCSELs was also investigated using both parallel and orthogonal optical injection. The results show that no irreversible PS was observed in this operation regime. In addition, at very high bias current where the additional higher order modes excited the VCSEL no longer exhibited irreversible PS. In consequence it is considered that the irreversible PS is a feature of the regime of two-mode operation. Robust irreversible PS in VCSELs has potential for implementing optical mono-stables.

Having explored the polarisation switching in two mode operation VCSELs in this chapter, the next chapter includes the bistability and ultra-wide hysteresis in the two mode operation of VCSELs.

References:

[1] **M. Sciamanna** and K. Panajotov, "Route to Polarisation switching induce by optical injection in vertical cavity surface emitting lasers," Phys. Rev. A, vol. 73, pp.023811, **2006**.

[2] **K. H. Jeong,** K. H. Kim, S. H. Lee, M. H. Lee, B. S. Yoo, and K. Alan Shore, " Optical injection-induced Polarisation switching dynamics in 1.5-µm wavelength single-mode vertical-cavity surface-emitting lasers," IEEE Photon. Tech. Lett., vol. 20, pp. 779-781, May **2008.**

[3] **M. Torre,** A. Hurtado, A. Quirce, A. Valle, L. Pesquera, and M. Adams, "Polarisation switching in long-wavelength VCSELs subject to orthogonal optical injection," IEEE, J. of QuantumElectron. vol. 47, pp. 92-98, Jan. **2011**.

[4] **A. A. Qader,** Y. Hong and K. Alan Shore, "Role of suppressed mode in the polarisation switching characteristics of optically injected VCSELs," IEEE, J. of Quantum Electron. vol. 49, pp. 205-209, Feb. **2013.**

[5] **A. Quirce,** J. R. Cuesta, A. Valle, A. Hurtado, L. Pesquera, and M. Adams, "Polarisation bistability induced by orthogonal optical injection in 1550-nm multimode VCSELs," IEEE J. of Selected Topics in Quantum Electron., vol. 18, pp. 772-777, Mar./April **2012.**

[6] **A. Valle,** I. Gatare, K .Panajotov, and M. Sciamanna, "Tranverse mode switching and locking in vertical-cavity surface-emitting lasers subject to orthogonal optical injection," IEEE, J. of Quantum Electron. vol. 43, pp. 322-333, Apr. **2007.**

[7] **K. Panajotov**, I. Gatare, A. Valle, H. Thienpont, and M. Sciamanna, "Polarisation- and transverse mode dynamics in optically injected and gain-switched vertical-cavity surface-emitting lasers," IEEE, J. of Quantum Electron. vol. 45, pp. 1473-1481, Nov. **2009**

[8] **I. Gatare,** J. Buesa, H. Thienpont, K. Panajotov, and M. Sciamanna, "Polarisation switching bistability and dynamics in vertical-cavity surface-emitting laser under orthogonal optical injection," Optical and Quantum Electron., vol. 38, pp. 429-443, **2006.**

[9] **J. B. Altes,** I. Gatare, K. Panajotov, H. Thienpont, and M. Sciamanna, "Mapping of the dynamics induced by orthogonal optical injection in vertical-cavity surface-emitting lasers," IEEE, J. of Quantum Electron. vol. 42, pp. 198-206, Feb. **2006.**

CHAPTER SEVEN

POLARISATION BISTABILITY AND HYSTERESIS IN OPTICALLY INJECTED TWO-MODE VCSELS

◆━━━━━━━━━━━━━━━━━━━━━━━━━━━━━━━━━━━━◆

In the previous chapter the polarisation switching characteristics in two-mode VCSELs subject to polarised optical injection were presented. The results obtained there motivated further experimental investigations described in this chapter which emphasises a scheme of orthogonal optical injection. The scheme has been used to investigate bistability and hysteresis accompanied by polarisation switching in two-mode VCSELs. It has been found that for orthogonal optical injection an ultra-wide hysteresis (~155 GHz) can be obtained with the VCSEL.[1] The results are compared to those obtained for single mode operation. The widths of the hysteresis in two-mode operation are dependent on the target laser bias current and on the optical injected power. In addition, hysteresis in the polarisation resolved output power of optically injected VCSELs has been observed.

The content of this chapter are organized as follows:

 In section 7.1 an introduction to polarisation bistability and hysteresis phenomena in VCSELs is presented. Section 7.2 includes the experimentally measure polarisation bistability and hysteresis behaviour of VCSELs subject to orthogonal optical injection in both the single mode regime and the two-mode regime. Section 7.3 describes the dependence of the hysteresis with bias current and optical injection power. In section 7.4 polarisation resolved output power is investigated in two mode VCSELs subject to orthogonal optical injection and compared to that in the single mode regime. Finally section 7.5 summarizes the main conclusions derived from the experimental results.

7.1 Introduction

Polarisation bistability (PB) in optically injected VCSELs has been widely investigated in single mode operation both experimentally [1-4] and theoretically [5, 6]. PB is often observed together with polarisation switching (PS) in VCSELs as has been investigated experimentally and theoretically [7]. PS with hysteresis has been obtained experimentally using parallel optical injection [8] and orthogonal optical injection [9].

―――――――――――――

Previous studies have indicated that for low optical injection power the hysteresis width fluctuates around a constant level, while for high injection power the hysteresis width is found to be reduced [10]. On the other hand, Hong et al. [3] observed an increase of the hysteresis width with increasing injection power, albeit that for high optical injection powers the hysteresis width was found to decrease. The hysteresis cycles obtained had widths of about 1.65 GHz for parallel injection [10] and 37 GHz for orthogonal optical injection [11, 12].

Reported experimental results indicate that the hysteresis in VCSELs depends on the frequency detuning and the injection power level [10, 13]. The FD is defined as the frequency difference between the master laser frequency and the slave laser lasing mode frequency ($\Delta \upsilon = \upsilon_{ml} - \upsilon_{sl}$). In [11] the widening of the hysteresis cycle associated with the existed PB at high bias current was explained by the physical phenomenon of dispersive nonlinearity. Recently Zhang et al [14] have predicted that the hysteresis width depends on the sweep rate of frequency detuning (FD) and the injection power.

In [4] polarisation bistability in multi-mode VCSELs induced by orthogonal optical injection was investigated experimentally. For fixed frequency detuning, the hysteresis width increases with increasing bias current. Compare to the single mode devices, the multimode emission property from VCSELs adds new functionalities [4].

Most of the previous studies of PB and hysteresis in VCSELS were conducted in the regime of single mode operation [9-14], In the present chapter, experimental observations of an ultra-wide hysteresis cycle in VCSEL subject to orthogonal optical injection whilst operating in a two mode regime are described. Pure frequency induced PB and associated ultra-wide hysteresis was obtained by increasing and decreasing the FD.

7.2 Polarisation bistability and hysteresis in different operation regime.

In this section PB and hysteresis in single mode and two mode regimes of optically injected VCSELs are investigated. The detailed description of the experimental setup was presented in chapter 6, section 6.2. Polarisation resolved L-I curve characteristics and optical spectra of the stand-alone VCSEL are given in chapter 3, section 3.3. The device termed VCSEL1 was used for experimental work of this chapter. The frequency of the orthogonal fundamental mode is 11.1 GHz lower than that of the parallel fundamental mode (as shown in the inset of the Fig. 2b), while the frequency of the higher order mode is about 160 GHz higher than that of the parallel fundamental mode.

Measurements of the output powers in the orthogonal (P⊥) and parallel (P$_{ll}$) polarisation as a function of the FD have been performed. These measurements were made at the position of rectangle (1) of the figure 6.1, recording the power in P⊥ and P$_{ll}$ while scanning the FD with fixed optical injection power (P$_{inj}$).

7.2.1 Polarisation bistability in single mode operation (I < 2I$_{th}$):

The polarisation resolved output power (orthogonal polarisation) in single mode regime when VCSEL1 biased at 7 mA was investigated using orthogonal optical injection. Figure 7.1 show the orthogonal mode power as a function of frequency detuning for a constant optical injection power P$_{inj}$ of 50 µW. It can be seen that for decreasing FD the PS occurs around -11 GHz.
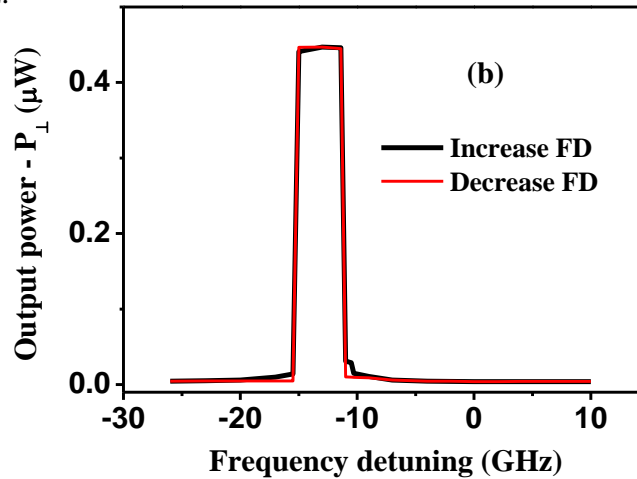

Figure 7.1: Bistability in optical output power (orthogonal polarisation) of the VCSEL as a function of FD for bias current 7 mA with P$_{inj}$= 50µmW.

With continued decrease of FD the VCSEL still emits in the orthogonal polarisation until -15.2 GHz, then switches back to parallel polarisation. With increasing FD the PS occurred again around -15.2 GHz, and the emission switches back to parallel polarisation near a FD of -11 GHz.

Intensity induced PS and bistability for a fixed frequency detuning value of -11 GHz using orthogonal optical injection were also investigated at this bias current. Figure 7.2 shows the polarisation resolved (PR) output power as a function of optical injected power for VCSEL1 when biased at 7 mA. It can be seen that the PS occurred at an injection power of 37 µW for increasing injection power and no hysteresis observed with decreasing injection power.
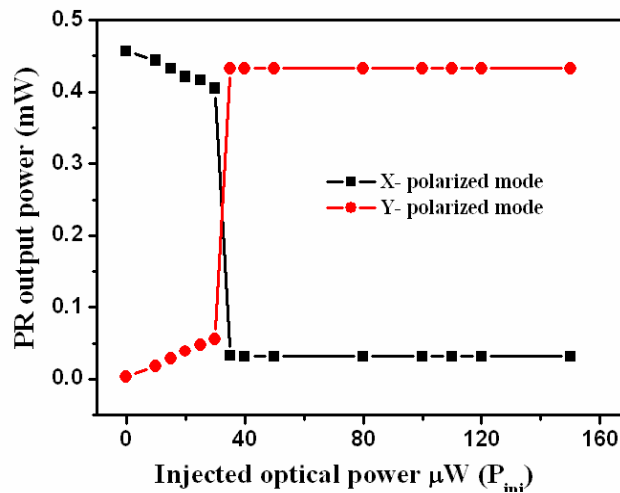
Figure 7.2: Polarisation resolved (PR) output power as a function of optical injection power. The VCSEL1 biased at 7 mA, FD= -11 GHz, the temperature was fixed at 20°C.

7.2.2 Polarisation bistability in two mode operation ($I > 2I_{th}$):

Although the VCSEL used was characterised by single mode for bias currents up to 7 mA, however, first order transverse mode excited above that bias current. Using low optical injection power P_{inj}= 4 µW for I=8.5 mA ($I>2I_{th}$), it is shown in figure 7.3 that only two small bistable regions, both for negative FD, were obtained. The measured value of the hysteresis width was about 3 GHz when the FD was decreased (thick red line) and then increased (black line). However, by utilizing larger values of P_{inj} the behaviour of the VCSEL is changed and two bistable regions and associated hysteresis cycles are obtained. The first hysteresis cycle (termed H1) is located at positive FD and the second hysteresis cycle (termed H2) is found for negative FD.
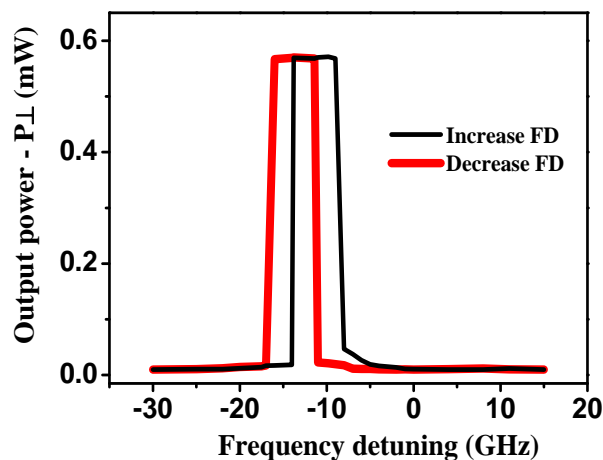

Figure 7.3: Bistability and related hysteresis in optical output power (orthogonal polarisation) of the VCSEL as a function of FD for bias current 8.5 mA with P_{inj}= 4 µW.

Figure 7.4 shows the results for four different values of the P_{inj}, figures 7.4(a), 7.4(b), 7.4(c), and 7.4(d) corresponding to P_{inj} = 50 µW, 100 µW, 300 µW, 500 µW, respectively. In figure 7.4(a), when the FD is increased, two PSs (corresponding to PS from parallel to the orthogonal polarisation) are observed, the first one is near a FD of about -11.1 GHz (the frequency difference between the parallel and orthogonal polarisation of the fundamental mode) and the second PS at a FD of about -2 GHz. The second PS is not observed for high P_{inj}. After the second PS the VCSEL emission remains in the orthogonal polarisation maintaining almost constant power up to a positive FD of about 158 GHz, and then switches back to the parallel polarisation.

As can be seen from figure 6.3, in chapter 6, the FD of 158 GHz is close to the frequency space between the fundamental mode and the higher order mode. The ultra-wide hysteresis in the positive detuning regime in figure 7.4 is explained by the frequency of the higher order mode being at a higher frequency than that of the fundamental mode (parallel mode).
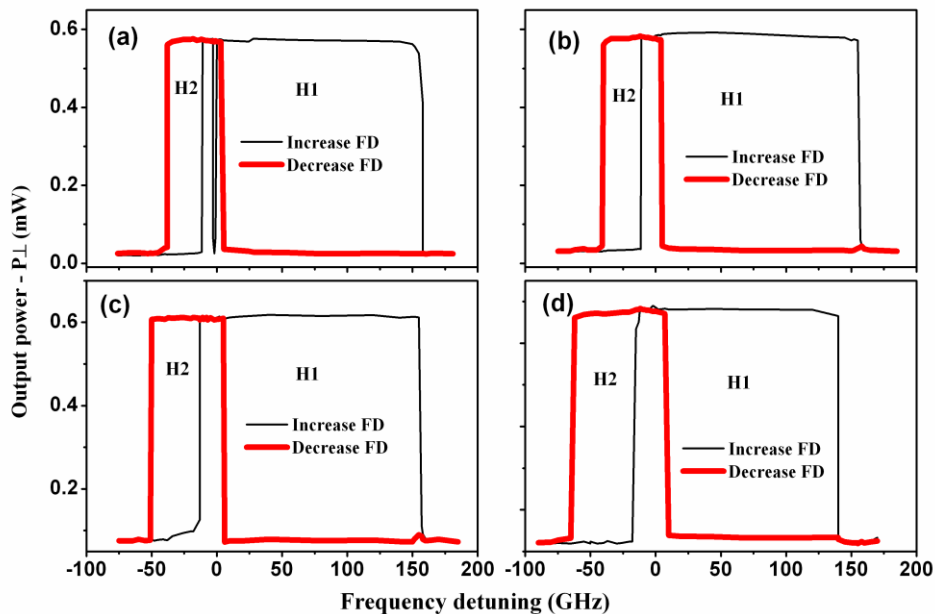

Figure 7.4: Hysteresis in the output power (orthogonal polarisation) of the VCSEL as a function of FD when increasing (black line) and decreasing (thick red) ML frequency. For P_{inj} a) 50 µW, b) 100 µW, c) 300 µW, and d) 500 µW.

For decreasing FD, the VCSEL switches to the orthogonal polarisation at a FD of about 3.2 GHz, and thus an ultra-wide hysteresis cycle of 154.8 GHz was obtained (H1). A second hysteresis (H2) was obtained for negative FD. Here the PS occurs at about -11.1 GHz for increasing FD and switches back for decreasing FD at -38.4 GHz in this way a hysteresis width of about 27.3 GHz was obtained. In optically injected VCSELs, the second minimum

switching power is located near the frequency space between the fundamental and the first order modes of the stand-alone VCSEL [15]. This explains a very wide hysteresis of H1 when VCSEL subject to orthogonal optical injection.

The results show that both the fundamental mode and the first order mode were involved in the PS. Figure 7.5 illustrate the optical spectra of the VCSEL when first FD is decreased (a, b) and then increased (c, d). Figure 7.5a shows the change of the spectra of the higher transverse mode when PS occurred for decreased FD near 3 GHz (in figure 7.4b), and is considered that the PS occurred between fundamental modes. In figure 7.5b the optical spectra show that the VCSEL emission switched back to parallel mode for decreased FD which is represented by PS at FD of -38.4 GHz in figure 7.4b. Figures 7.5 (c, d) show optical spectra when PS occurred and the polarisation switched back for increased FD, is considered that the PS occurred in this region between higher order mode and fundamental mode. The latter resulted in producing an ultra-wide hysteresis bistability.
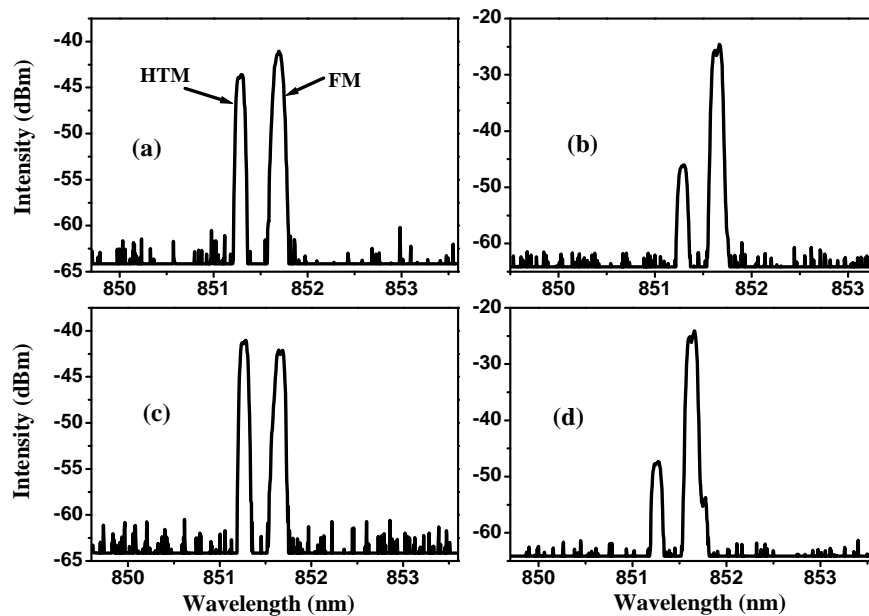

Figure 7.5: Optical spectra of the VCSEL subject to orthogonal optical injection indicate involve higher transverse mode (HTM) in polarisation switching: a) and b) when the frequency detuning decreased, c) and d) when frequency detuning increased. P_{inj}= 100 µW, VCSEL biased at 8.5 mA.

7.3 Hysteresis width change with injection power and bias current

The characteristics of both hysteresis H1 and H2 obtained in the previous section were investigated in detail with changing injection power and bias current. Figure 7.6 summarizes the measured widths of H1 and H2 as a function of P_{inj} for the VCSEL biased at 8.5 mA. The figure shows that the widths of H1 (black squares) are constant for a range

of P_{inj}, and then start to decrease for very high P_{inj}. While the widths of H2 (black triangles) continue to increase with increasing P_{inj} for the same range of P_{inj}. It was predicted by Gatare et al. 2007 that the hysteresis width increases with increasing injection power. Therefore, the obtained results for H2 confirmed the theoretical result in [15].

In addition, the dependence of the hysteresis width on the bias current for two mode regime was investigated. In figure 7.7 we plot the hysteresis widths as a function of the VCSEL bias current for $P_{inj} = 250$ µW. It can be seen that both measured widths of H1 (black squares) and H2 (black triangles) increase with increasing VCSEL bias current. The figure shows the change of hysteresis H1 when the bias current increased: for 7.7 mA the width of H1 is about 129 GHz and increases with increasing bias current to about 155 GHz for 8.5 mA. However, the widths of the H2 begin to increase with increasing bias current, but start to decrease at a bias current of about 8.8 mA, then increased again for bias current of 9 mA.
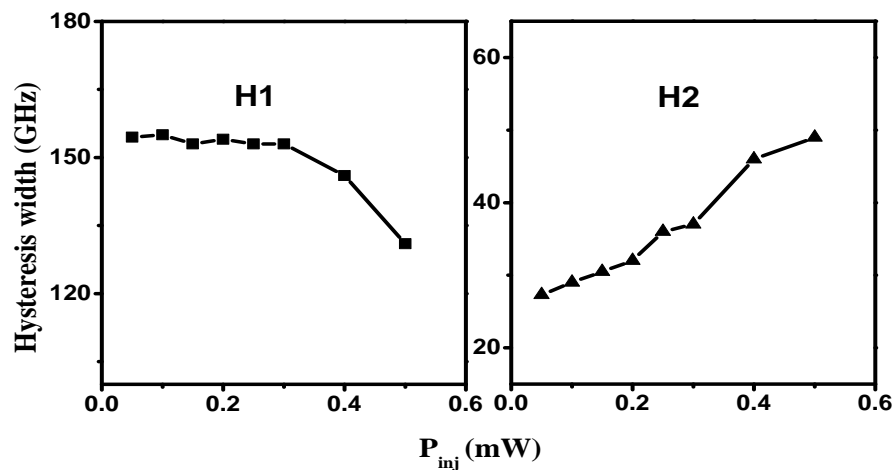

Figure 7.6: Frequency width of the hysteresis cycle H1 and H2 as a function of optical injected power P_{inj} when the VCSEL biased at 8.5 mA.
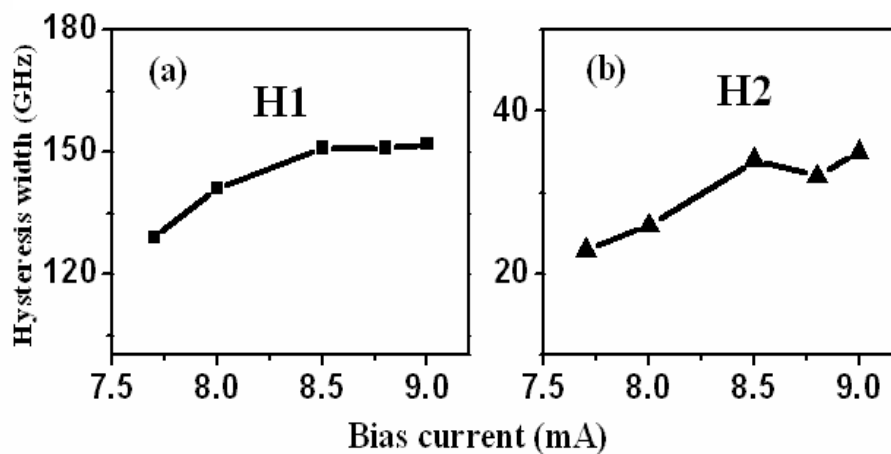

Figure 7.7: Frequency width of the hysteresis cycle H1 and H2 as a function of bias current.

7.4 Bistability in polarisation resolved output power of VCSELs subject to orthogonal optical injection

In this section the polarisation resolved output power of VCSELs subject to orthogonal optical injection is investigated in the multi-mode regime. The difference between the experiments performed in chapter 6 section 6.5.1 and the present section is that the experiments here is to illustrate the PB region and the hysteresis regions in term of bias current. The experiments in the present section are performed with keeping the optical injection power from the ML. However, the experiments in section 6.5.1 performed with removing the injection power from ML after PS occurred.

As seen from figure 3.4(a) in chapter 3, the polarisation resolved output power of the stand-alone VCSEL1 is characterised by stable polarisation. However, when the device is subject to orthogonal optical injection it exhibited a PS with a large bistability and hysteresis in the bias current. The polarisation resolved output power as a function of bias current of the VCSEL1 subject to orthogonal optical injection is shown in figure 7.8. The VCSEL1 was biased at 7.7 mA, injection power was 40 μW, and the FD was fixed at -11 GHz with respect to the bias current of the SL at I = 7.7 mA.

As it can be seen from the figure, first PS occurred at bias current 7.67 mA, then the VCSEL1 power switches back to parallel mode at bias current 7.76. Continuing increase the slave laser bias current the second PS occurs at bias current 7.8 mA, then the VCSEL1 output emitting in orthogonal mode until reach bias current 9.12 mA then switches back to parallel mode. Thus the VCSEL1 show two region of polarisation bistability.
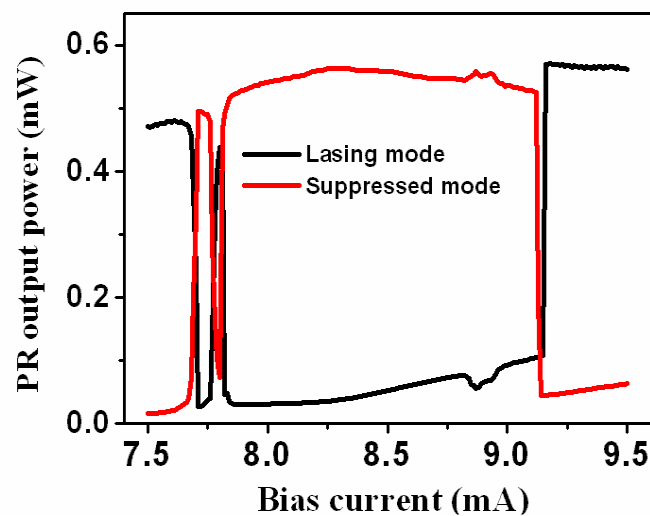

Figure 7.8: *Polarisation resolved (PR) output power as a function of VCSEL bias current when the P_{inj}= 40 μW*

 Furthermore, polarisation bistability and hysteresis were investigated in the two mode regime with first increased and then decreased bias current. Figure 7.9 shows the power in the orthogonal polarisation as the bias current was increased (black line) and then decreased (red line). The injected power into the slave laser was fixed at 50 µW and FD was fixed at -11 GHz with respect to the bias current of the SL at I = 8.5 mA. It can be seen that when the bias current increased the PS occurred at 8.44 mA and switched back to parallel polarisation at bias current 9.1 mA. However, for decreased bias current the PS occurred at 8.82 mA and switched back to parallel polarisation at bias current 8.3 mA. Therefore, two hysteresis regions of the bias current were found on either side of 8.5 mA. It is observed that due to the bias current dependence of the emission frequency of the VCSEL this hysteresis can also be represented as a FD hysteresis.
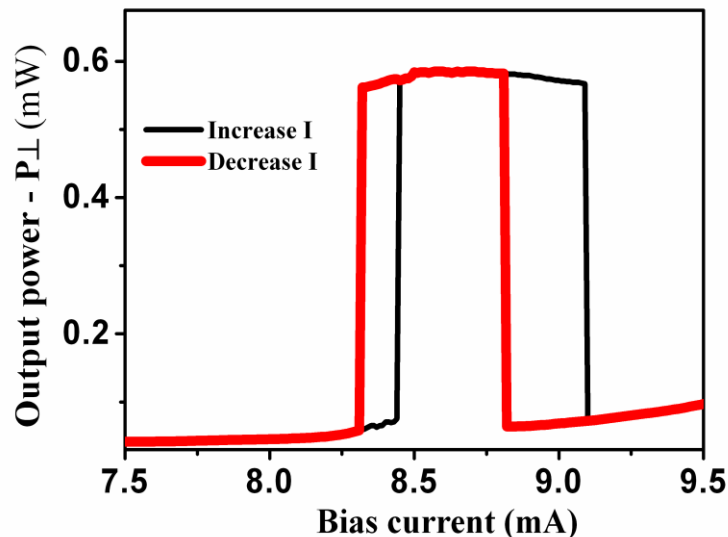
Figure 7.9: Output power of the orthogonal mode as a function of VCSEL bias current when the P_{inj}= 50 µW and the FD was -11 GHz with respect to the bias current of the SL at I= 8.5 mA.

In addition, the single mode operation characteristics of the VCSEL1 under orthogonal optical injection were investigated. Figure 7.10 shows the polarisation resolved output power (orthogonal polarisation) as a function of bias current. The FD was fixed at -11 GHz with respect to the bias current of the SL at I = 5 mA (left panel) and I=7 mA (right panel). The figures show that no hysteresis is found in this bias current regime using orthogonal optical injection.

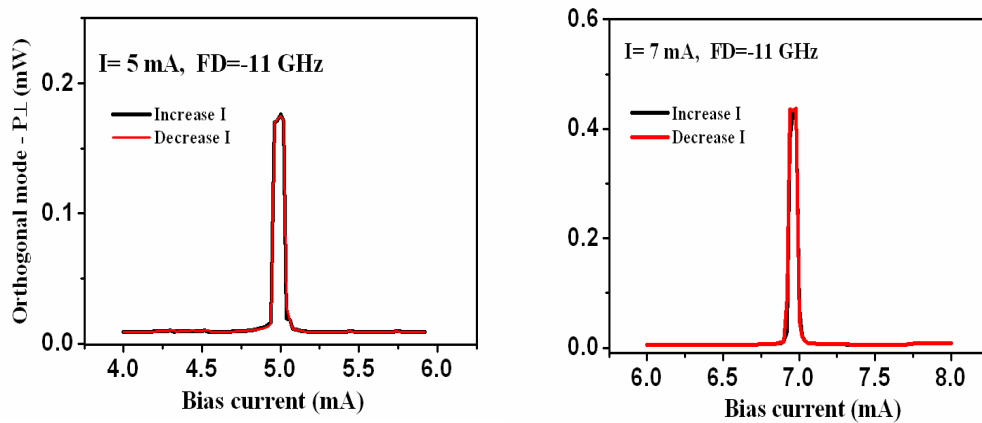**Figure 7.10:** *Output power of the orthogonal mode as a function of VCSEL bias current when the FD was -11 GHz with respect to the bias current of the SL at I= 5 mA and I=7 mA.*

7.5 Summary and Conclusion

 Polarisation bistability and hysteresis have been studied in two-mode VCSELs using orthogonal polarised optical injection. Experimental observations were made of ultra-wide frequency hysteresis in VCSELs subject to orthogonal optical injection. The VCSEL1 was biased at high current I> 2Ith, where two mode operation occurs. In this regime pure frequency induced-polarisation bistability has been obtained by increasing and decreasing the FD.

Two types of PB and associated frequency hysteresis cycle have been observed. The first type of the hysteresis cycle was found for positive detuning, and is characterised by being ultra-wide – 155 GHz – thus having a frequency hysteresis width which is four times larger than that the previously reported largest hysteresis [11, 12]. The second type of hysteresis cycle was found for negative detuning region and has a smaller hysteresis width of about 38 GHz. Both hysteresis types are optical injection power and target laser bias current dependent.

Furthermore, the polarisation resolved output power of VCSEL1 subject to orthogonal optical injection was investigated. The VCSEL also exhibited two regions of bistability and hysteresis in terms of the target laser bias current depending on the injected light frequency with respect to the target laser frequency.

The results of the present chapter may be useful for further understanding the basic condition for very wide hysteresis in VCSELs output power. Polarisation bistability and hysteresis are useful for many polarisation dependent applications including Doppler

velocimetry with polarisation bistable VCSELs [16], optical switching, and optical signal processing [17].

In the next chapter dynamical hysteresis and thermal effect in VCSELs subject to direct current modulation will be investigated experimentally and theoretically.

References:

[1] **H. Kawguchi,** "Bistable laser diodes and their applications: state of the art," IEEE J. of Selec. Top. in Quantum Electon., vol 3, pp.1254-1270, Oct. **1997.**

[2] **X. Tang,** J. P. van der Ziel, B. Chang, R. Johnson, and J. A. Tatum, "Observation of bistability in GaAs quantum-well vertical-cavity surface-emitting lasers," IEEE, J. of Quantum Electron. vol. 33, pp. 927-932, Jun. **1997.**

[3] **Y. Hong,** K. A. Shore, A. Larsson, M. Ghisoni and J. Halonen, "Pure frequency-polarization bistability in vertical cavity surface-emitting semiconductor laser subject to optical injection," Elect. Lett. vol. 36, pp 2019-2020, Nov. **2000.**

[4] **A. Quirce,** J. R. Cuesta, A. Valle, A. Hurtado, L. Pesquera, and M. Adams, "Polarization bistability induced by orthogonal optical injection in 1550-nm multimode VCSELs," IEEE J. of Selec. Top. in Quantum Electron., vol. 18, pp. 772-777, Mar./Apr. **2012.**

[5] **P. L. Neo,** S. F.Yu, and T. D. Wilkinson, "Theoretical studies of polarization bistability in birefringent ARROW VCSELs," IEEE, J. of Quantum Electron. vol. 42, pp. 1107-1114, Nov. **2006.**

[6] **M. F. Salvide,** M. S. Torre, A. Valle, and L. Pesquera, "Transverse mode selection and bistability in vertical-cavity surface-emitting lasers induced by parallel polarised optical injection," IEEE, J. of Quant. Electron. vol. 47, pp. 723-730, May **2011.**

[7] **Y. Hong**, R. Ju, P.S. Spencer, and K. A. Shore, "Investigation of polarization bistability in vertical-cavity surface-emitting lasers subject to optical feedback," IEEE, J. of Quantum Electron. vol. 41, pp. 619-624, May **2005.**

[8] **A. Quirce,** A. Valle, A. Hurtado, C. Gimenez, L. Pesquera, and M. J. Adams, " Experimental study of transverse mode selection in VCSELs induced by parallel polarized optical injection," IEEE, J. of Quantum Electron. vol. 46, pp. 467-473, Apr. **2010.**

[9] **A. Valle,** M. Gomez-Molina, and L. Pesquera, " Polarization bistability in 1550 nm wavelength single-mode vertical-cavity surface-emitting lasers subject to orthogonal optical injection," IEEE J. of Selected Topics in Quantum Electron., vol. 14, pp. 895-902, May./Jun. **2008.**

[10] **Y. Hong,** P.S. Spencer, and K. A. Shore, "Power and frequency dependence of hysteresis in optically bistable injection locked VCSELs," Elect. Lett. vol. 37, pp 569-570, Apr. **2001.**

[11] **A. Hurtado,** A. Quirce, A. Valle, L. Pesquera, and M. J. Adams, "power and wavelength polarization bistability with very wide hysteresis cycles in a 1550nm-VCSEL subject to orthogonal optical injection." Opt. Expre. vol. 17, pp 23637-23642, Dec. **2009**

[12] **A. Quirce,** A. Valle, and L. Pesquera, "Very wide hysteresis cycles in a 1550nm-VCSEL subject to orthogonal optical injection." IEEE Photon. Tech. Lett., vol. 21, pp. 1193-1196, Sep. **2009.**

[13] **I. Gatare,** K .Panajotov, and M. Sciamanna, "Frequency-induced polarization bistability in vertical-cavity surface-emitting lasers with orthogonal optical injection," Phy. Rev. A, vol. 75, pp. 023804, **2007.**

[14] **W. L. Zhang,** W. Pan, B. Luo, M. Y. Wang, and X. H. Zou, "Polarization switching and hysteresis of VCSELs with time-varying optical injection," IEEE, J. Selec. Top. in Quantum Electron. vol. 14, pp. 889-894, May/Jun. **2008.**

[15] **A. Valle,** I. Gatare, K .Panajotov, and M. Sciamanna, "Transverse mode switching and locking in vertical-cavity surface emitting lasers subject to orthogonal optical injection," IEEE, J. of Quantum Electron. vol. 43, pp. 322-333, Apr. **2007.**

[16] **J. Albert,** M. C. Soriano, I. Veretennicoff, K. Panajotov, J. Danckaert, P. A. Porta, D. P. Curtin, and J. G. McInerney, "Laser Doppler velocimetry with polarization-bistable VCSELs," IEEE J. of Selec. Top. in Quantum Electon., vol 10, pp.1006-1012, Sep./Oct. **2004.**

[17] **S. H. Lee,** H. W. Jung, K. H. Kim, M. H. Lee, B.S. Yoo, J. Roh, and K. Alan Shore, "1-GHz all-optical flip-flop operation of conventional cylindrical-shaped single-mode VCSELs under low-power optical injection," IEEE Photon. Tech. Lett., vol. 22, pp. 1759-1761, Dec. **2010.**

CHAPTER EIGHT

DYNAMICAL HYSTERESIS AND THERMAL EFFECTS IN DIRECTLY MODULATED VCSELS

◆━━━━━━━━━━━━━━━━━━━━━━━━━━━━━━━━━━━━━━━◆

In the previous chapters, VCSEL emission characteristics under external optical injection and optical feedback have been investigated experimentally. In this chapter, the influence of the frequency of direct current modulation and substrate temperature on the VCSEL threshold current has been studied experimentally.[1] The results show that the modulation frequency has a large impact on the lasing threshold current of long wavelength VCSELs in the high frequency range. Positive hysteresis and negative hysteresis have been observed in turn-on and turn-off currents. The results are compared to the obtained results with theoretical model developed by other.

The contents of this chapter are organised as follows:

In section 8.1 a brief introduction to direct current modulation of semiconductor laser is presented. Section 8.2 illustrates the detail of the experimental setup used for direct current modulation. In section 8.3 the influence of VCSEL substrate temperature on the hysteresis of turn on and turn off discussed. Section 8.4 describes the effect of the modulation frequency on the hysteresis cycle of lasing threshold and compared to numerical results. In section 8.5 experimental results are compared with the theoretical results which are conducted by other. Finally section 8.6 includes the summary and main conclusions.

8.1   Introduction

Semiconductor lasers (SLs) subject to direct current modulation (DCM) have been extensively investigated both theoretically [1, 2], and experimentally [3, 4]. The principal attraction of the DCM technique of SL is its simplicity. Basically, the laser is biased above threshold and a modulation signal will be added to the drive current, then the output power signal of the laser is expected to follow the modulation waveform. Near threshold directly modulated semiconductor laser can generates pulses with high repetition rates [4].

───────────────────────────────

The behavior of modulated semiconductor lasers has been widely reported using modulation parameters including modulation frequency and modulation depth. Depending on the modulated parameters six different dynamical regimes including chaos and period doubling have been observed [2, 5]. The modulation response at high frequency depends on the electrical parasitic of the laser package and chip. Therefore, achievement of high speed operation requires minimization of such parasitic. Two main schemes of SL modulation have been found, direct modulation and external modulation. In the experiments here the use has been made of the direct current modulation. Figure 8.1 shows the principle diagram of the direct modulation scheme.

Recently directly modulated, long-wavelength vertical-cavity surface-emitting lasers (VCSELs) become attractive components for the fast-growing market of high speed optical communication systems [6].
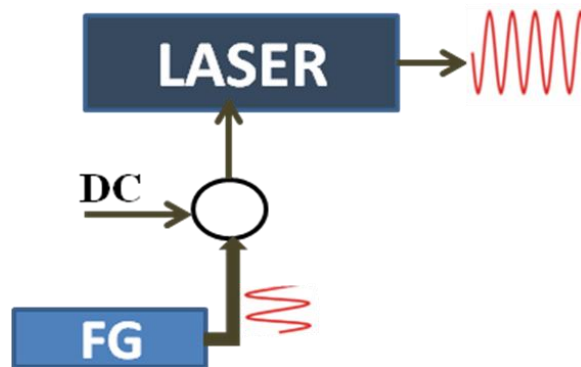

Figure 8.1: *Basic schematic diagram of the direct modulation.*

In contrast to 850 nm VCSELs, for some long-wavelength VCSELs have a relatively large spectral detuning between the gain and the cavity resonance at room temperature [7].This results in increased temperature sensitivity, which can have an impact on the performance of directly modulated devices [8].

A recent numerical study [9] has shown thermally induced hysteresis on the laser switch-on and switch-off points, which depends on the relationship between two time-scales: that of the current modulation, that results in dynamical hysteresis [10, 11] and that of thermal dissipation, that is an additional source of hysteresis which can give either positive or negative [12, 13] hysteresis cycles.

In positive cycles the laser turns on at a higher current value than its turns off; in negative cycles, the turn on occurs at a lower current value than the turn off. Temperature-induced hysteresis depends on the current modulation frequency: if the modulation is too fast, thermal effects do not have time to act; and if the current modulation is too slow, the dynamics is quasi-static and thermal equilibrium is reached before the bias current changes appreciably.

In this chapter the experimental work conducted to investigate the influence of direct current modulation frequency and substrate temperature on VCSEL threshold current. The experimental results are compared to those obtained with numerical simulation; a good qualitative agreement was found.

8.2 Experimental setup.

The experimental setup is shown in figure 8.2. A commercial VCSEL with lasing wavelength of about 1550 nm was used, which operates on a single longitudinal and transverse mode and exhibits no polarization switching over the entire range of bias currents.   The VCSEL was driven by an ultra-low noise current source and was temperature controlled to within 0.01°C. The dc bias current was set at 4 mA and modulation amplitude was 3.7 mA, so the bias current was scanned from 0.3 to 7.7 mA. The output of the VCSEL was collimated by an anti-reflection coated laser diode objective lens. The orthogonal polarization components of the VCSEL were divided by a half-wave plate and a polarization beam splitter.
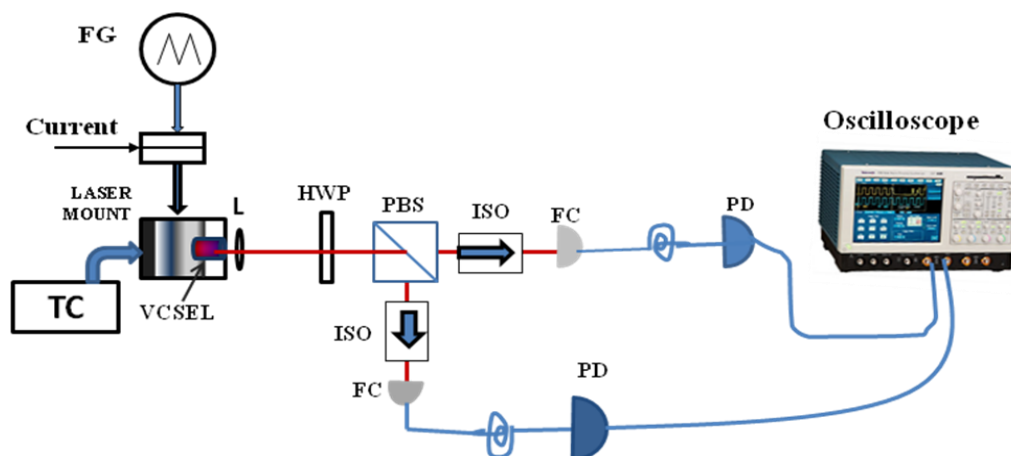

Figure 8.2: *Experimental setup: VCSEL– laser diode; L– collimating lens; PBS– polarization beam splitter; ISO– optical isolator; FC– fibre coupling unit; PD– photodiode; FG– function generator; TC– temperature controller.*

A triangular direct current modulation signal was added to the VCSEL bias current source through a Bias Tee. Two optical isolators with more than -40 dB isolation were used to prevent feedback into the VCSEL. The output of the orthogonal polarization components were recorded simultaneously using 1 GHz bandwidth detectors and were stored in a 4 GHz bandwidth digital oscilloscope.

The polarization resolved output power of stand-alone VCSEL used in the experiments is shown in Figure 8.3. It can be seen that the VCSEL does not exhibit any polarization switching at any bias current.
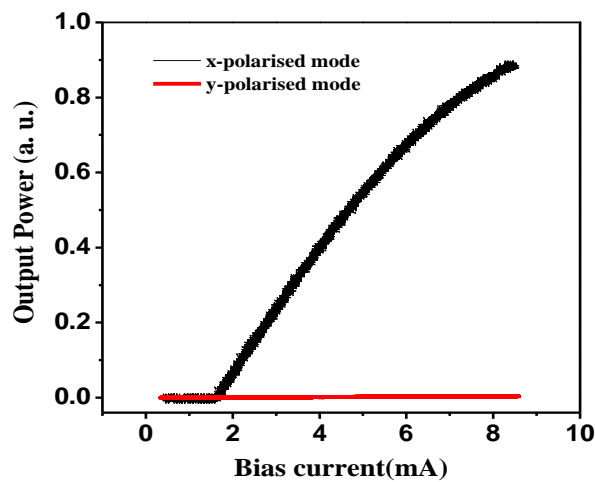

Figure 8.3: Polarisation resolved output power of the long wavelength stand-alone VCSEL.

8.3 Thermal effects on hysteresis of laser turn on and turn off

Figure 8.4 shows the light-current (L-I) curve when the current modulation frequency is 10 kHz and the substrate temperature was 10°C (figure 8.4a) and 60°C (figure 8.4b). Since the VCSEL operates in one linear polarisation, only the output of that lasing polarisation is plotted. In the figure, the black curve is for increasing current and the red curve is for decreasing current. The inset displays in detail the threshold current. It can be seen that the lasing threshold with increasing current, termed the turn-on threshold, I_{on}, does not overlap the threshold with decreasing current, termed the turn-off threshold, I_{off}.

There is hysteresis between I_{on} and I_{off}: in the case of low substrate temperature, $I_{on} > I_{off}$ (this type of hysteresis will be termed positive hysteresis); in the case of high substrate temperature, $I_{on} < I_{off}$ (this type of hysteresis will be termed negative hysteresis).

Figure 8.5 shows the turn-on and turn-off currents as a function of the substrate temperature for various modulation frequencies. It is noticed that both, I_{on} and I_{off} increase

with the substrate temperature, but the rates of variation are different except for the slow 1 Hz modulation frequency, in which these are equal.
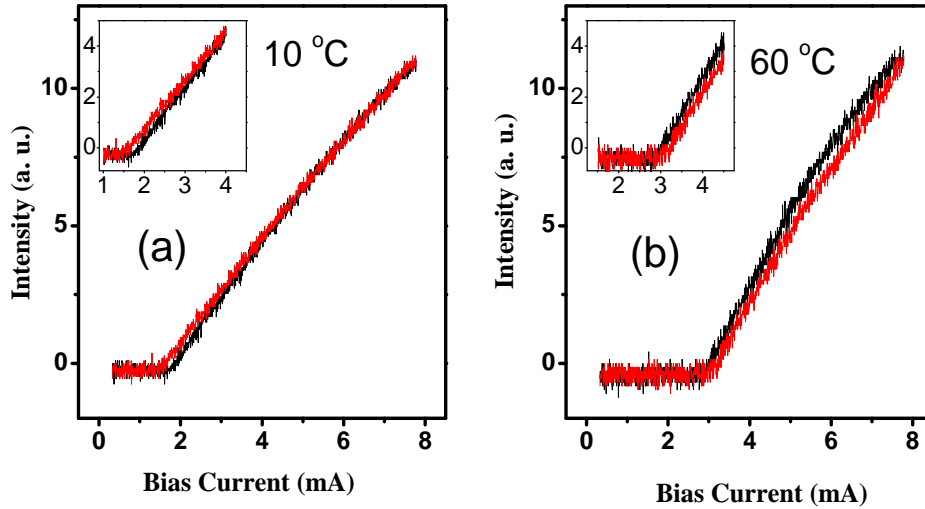
Figure 8.4: *The light–current (L–I) curve of the VCSEL with 10 kHz modulation frequency for (a) 10°C and for (b) 60°C substrate temperature. The black curve is for increasing current, the red curve is for decreasing current. The inset displays a detail of the threshold.*

For 1 Hz modulation frequency, as shown in Figure 8.5 (a), $I_{on} = I_{off}$ within the operation range of the substrate temperatures and correspond to the static threshold current. A parabolic-like dependence of the static threshold with the substrate temperature is observed, in good agreement with previous experimental and theoretical studies [14, 15].

Figure 8.5: *The threshold currents as a function of the substrate temperature for various modulation frequencies. The black circles and the red squares indicate I_{on} and I_{off}, respectively.*

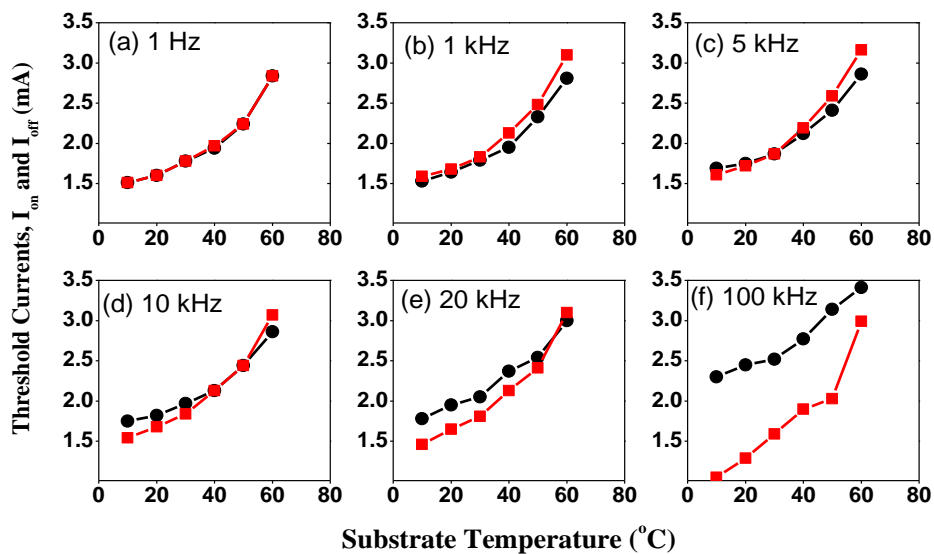When the modulation frequency increases to 1 kHz, as shown in Figure 8.5(b), I_{on} and I_{off} show hysteresis at substrate temperatures higher than 30°C. It is apparent that $I_{on} < I_{off}$, thus there is a negative hysteresis cycle. When the modulation frequency is between 5 kHz and 20 kHz, as shown in Figure 8.5 (c)-(e), $I_{on} > I_{off}$(positive hysteresis) at low substrate temperature and $I_{on} < I_{off}$ (negative hysteresis) at high substrate temperature. With further increase of the modulation frequency to 100 kHz, I_{on} and I_{off} show only positive hysteresis, $I_{on} > I_{off}$.

8.4 Modulation frequency effects on hysteresis of the turn on and turn off of laser

In this section the influence of the modulation frequency on the hysteresis cycle of threshold lasing of the VCSEL investigated. Figure 8.6 shows the width of the hysteresis cycle as a function of the modulation frequency for different substrate temperatures. It can be seen that the curves have similar trends for all substrate temperatures. For lower modulation frequencies, there is no clear hysteresis between the turn-on and turn- off current. When the modulation frequency is increased over a certain value, I_{on} -I_{off} decreases and becomes negative. With further increase of the modulation frequency, I_{on} - I_{off} grows and becomes positive at high frequency.
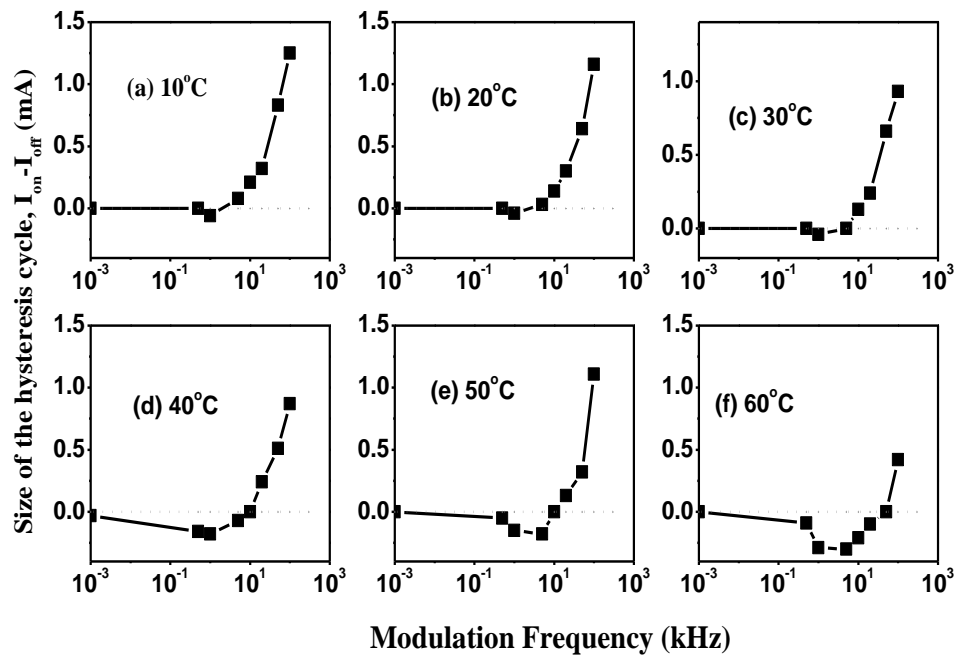

Figure 8.6: *Size of the hysteresis cycle, I_{on} -I_{off}, as a function of the modulation frequency at various values of the substrate temperatures.*

8.5 Theoretical results

The experimental results of the VCSEL subject to direct current modulation were compared to the theoretical results obtained using the rate equation model (see appendix1). The rate equation analysis was performed by Masoller and Torre [16]. The model equations were integrated with typical parameters appropriate for a 1550 nm VCSELs: the room temperature gain-cavity offset, $\delta_0 = -10$ nm, $\gamma_N = 1$ ns^{-1}, $\gamma_T = 1$ μs^{-1}, $Z = 8.5$ x 10^{-3}, $P = 9.2$ x 10^{-5}, and all other parameters as in [9, 14]. The size of the hysteresis cycle vs the modulation frequency at three values of the substrate temperature is displayed in Figure 8.7 and one can notice that there is a qualitatively good agreement with the experimental observations in the previous section.
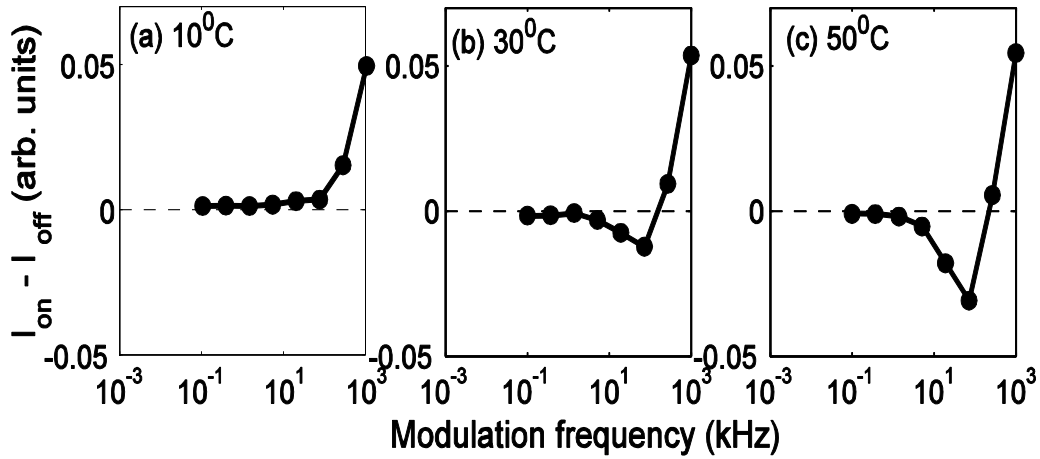
Figure 8.7 numerically calculated size of the hysteresis cycle, I_{on}-I_{off}, vs. the modulation frequency at three values of the substrate temperatures.

8.6 Summary and conclusion

In this chapter, the thermal effects and dynamical hysteresis in the turn-on and turn-off of directly-modulated VCSELs were studied experimentally. The hysteresis in the turn-on and turn-off can be explained in terms of the interplay of dynamical hysteresis (due to current variation), thermal dissipation and device heating. The device heating is an additional source of hysteresis because of the red-shift of both gain peak and the cavity resonance with increasing temperature. At high substrate temperature, the interplay of these effects can give negative hysteresis in a certain range of modulation frequencies; at low frequencies, the dynamics is quasi-static and there is no hysteresis; at high frequencies, slow thermal effects do not have time to act and there is only normal dynamical hysteresis.

The obtained results provide a complete picture of the various timescales on which heating effects come into play and affect the device performance.

The next chapter summarises the experimental results and main conclusions of the thesis. It also includes proposals for future work.

References

[1] **E. Scholl,** D. Bimberg, H. Schumacher and P. Landsberg, "Kinetics of picosecond pulse generation in semiconductor lasers with bimolecular recombination at high current injection," IEEE J. Quantum Electron. vol. 20**,** pp 394-399, Apr. **1984.**

[2] **M. Tang** and S. Wang, "Simulation studies of bifurcation and chaos in semiconductor lasers, " Appl. Phys. Lett. Vol. 48, pp 900-902, Apr. **1986.**

[3] **J. M. Osterwalder** and B. J. Rickett, "Frequency modulation of GaAlAs injection laser at microwave frequency rates," IEEE J. Quantum Electron. vol. 16, pp 250-252, Apr. **1984.**

[4] **S. Tarucha** and K. Otsuka, "Response of semiconductor laser to deep sinusoidal current modulation," IEEE J. Quantum Electron. vol. 17, pp 810-816, May **1981.**

[5] **H. Kawaguchi,** "Optical bistability and chaos in semiconductor laser with a saturable absorber," Appl. Phys. Lett. vol. 45, pp. 1264-1266, **1984**.

[6] **X. Zhao,** B. Zhang, L. Christen, D. Parekh, W. Hofmann, M. C. Amann, F. Koyama, A. E. Willner and C. J. Chang-Hasnain**,** "Greatly increased fiber transmission distance with an optically injection-locked vertical-cavity surface-emitting laser", Optic. Expres., vol. 17, pp. 13785-13791, **2009.**

[7] **S. Mogg,** N. Chitica, U. Christiansson, R. Schatz, P. Sundgren, C. Asplund and M. Hammar, "Temperature sensitivity of the threshold current of long-wavelength InGaAs-GaAs VCSELs with large gain-cavity detuning", IEEE J. Quantum Electron., vol. 40**,** pp.453-462, **2004.**

[8] **Y. Hong,** J. Paul, P. S. Paul and K. A. Shore, "Influence of low-frequency modulation on polarization switching of VCSELs subject to optical feedback," IEEE J. Quantum Electron. vol. 44, pp. 30-35, Jan. **2008.**

[9] **M. S. Torre** and C. Masoller, "Dynamical hysteresis and thermal effects in vertical-cavity surface-emitting lasers," IEEE J. Quantum Electron. vol. 46, pp. 1788-1794, Dec. **2010.**

[10] **J. R. Tredicce,** G. L. Lippi, p. Mandel, B. Charasse, A. Chevalier and B. Picqué, "Critical slowing down at a bifurcation," Am J. Phys. vol. 72, pp. 799-809 Jun. **2004.**

[11] **J. Paul,** C. Masoller, Y. Hong, P. S. Paul and K. A. Shore, "Experimental study of polarization switching of vertical-cavity surface-emitting lasers as a dynamical bifurcation," Optic. Lett. vol. 31, pp. 748-750, Mar. **2006.**

[12] **D. Bromley,** E. J. D'Angelo, H. Grassi, C. Mathis and J. R. Tredicce, "Anticipation of the switch-off and delay of the switch-on of a laser with a swept parameter," Optic. Commun. vol. 99, pp. 65-70, May **1993.**

[13] **S. Sivaprakasam,** D. N. Rao and R. S. Pandher, "Demonstration of negative hysteresis in an injection-locked diode laser," Optic. Commun. vol. 176, pp.191-194, Mar. **2000.**

[14] **C. Masoller** and M. S. Torre, "Modeling thermal effects and polarization competition in vertical-cavity surface-emitting lasers," Optics Express, vol. 16, pp. 21282-21296, Dec. **2008.**

[15] **C. Chen,** P. O. Leisher, A. A. Allerman,K. M.Geib, and K. D. Choquette, "Temperature analysis of threshold current in infrared vertical-cavity surface-emitting lasers," IEEE J. Quantum Electron. vol. 42, pp.1078-1083, Oct. **2006.**

[16] **Y. Hong,** Cristina Masoller, Maria S. Torre, Sanjay Priyadarshi, Abdulqader A. Qader, Paul S. Spencer, and K. Alan Shore, "Thermal effects and dynamical hysteresis in the turn-on and turn-off of vertical-cavity surface-emitting lasers", Optic. Lett. ,vol. 35, no. 21, pp3688 - 3690 Nov. **2010.**

[17] **G. Verschaffelt, J**. Albert, B. Nagler, M. Peeters, J. Danckaert, S. Barbay, G. Giacomelli, and F. Marin, "Frequency response of polarization switching in vertical-cavity surface-emitting lasers," IEEE J. Quantum Electron. vol. 39, pp. 1177-1186, Oct. **2003.**

CHAPTER NINE

CONCLUSIONS AND FUTURE WORK

◆━━━━━━━━━━━━━━━━━━━━━━━━━━━━━━━━━━━━━━━◆

This work has been devoted mainly to the study of the polarisation properties of vertical cavity surface emitting lasers (VCSELs) subject to optical injection and optical feedback. The research has been undertaken to expand understanding of the unique polarisation properties of VCSELs. Special attention has been given to three main aspects of the polarisation properties of VCSELs namely: polarisation state selection; polarisation switching and polarisation bistability. Previous studies had demonstrated that optical injection and optical feedback can efficiently control the direction of polarisation and also influence polarisation switching. Proposals for future work are presented for further experimental investigation of the VCSELs polarisation characteristics. This, in turn, may further enhance understanding of the polarisation control and polarisation bistability of these devices.

9.1 Conclusions

The thesis work has shown that a new scheme of circular polarised optical injection can produce some degree of circularly polarised VCSELs emission. These contributions were described in chapter 3 where the main results obtained are:

1- Using circularly polarised optical injection, linearly polarised of the stand-alone VCSELs is converted into circularly polarised emission. The VCSELs exhibited a high degree of circular polarisation for bias current below and near the lasing threshold of the stand-alone VCSELs. The degree of circular polarisation decreases with increasing VCSELs bias current.

2- Lasing threshold reduction of the VCSELs has been observed when the device is subject to optical injection. The amount of lasing threshold reduction is dependent on the optical injection power and frequency detuning between the injected beam and the target laser.

The results with optical injection motivated the use of circularly polarised optical feedback to influence the polarisation state selection of VCSELs. In chapter 4 circularly polarised optical feedback has been used as a new feedback scheme. Similar results of circular

polarisation emission were obtained as was found in optical injection experiments. For optical feedback the degree of circular polarisation depends on the feedback power ratio. The degree of circular polarisation increases with increasing feedback power ratio. The degree of the circular polarisation was again found to decrease with increasing device bias current.

In chapter 5 the role of the suppressed VCSEL mode in polarisation switching of optically injected VCSELs was addressed. A variety of linear polarisation optical injections have been used to identify the role of the suppressed mode in determining the switching characteristics between the two orthogonal linearly polarised fundamental modes. The main results are:

1- The minimum power for polarisation switching is strongly dependent on the VCSELs bias current. For both orthogonal/ parallel optical injection the switching power was found to be decreases dramatically with increasing bias current.

2- The frequency detuning for polarisation switching to occur is close to the VCSEL birefringence and it was found to be independent of the VCSEL bias current for a defined range of injection power and range of polarisation angle.

3- The influence of frequency detuning and optical injection level on the optical spectra of the suppressed mode was investigated. The suppressed mode possessed an essentially identical spectrum to that of the lasing mode spectra for a defined range of frequency detuning.

Additionally, using parallel optical injection the FD for PS was dependent on the injection power, which is considered to be consistent with injection locking.

In chapter 6 an experimental demonstration of robust irreversible polarisation switching in optically injected two-mode VCSELs was presented. In that chapter it was shown that the VCSELs exhibited such irreversible polarisation switching with both orthogonal/ and parallel optical injection the main results being:

1- Irreversible PS was obtained for decreasing and increasing frequency detuning. It is considered that this switching behaviour is related with the excitation of a higher transverse mode with orthogonal polarisation to the fundamental mode.

2- Intensity induced polarisation switching also showed irreversible polarisation switching in VCSELs operated in two mode regime, for both parallel/ orthogonal optical injection.

3- The PS was found to persist for a wide range of the control parameters including bias current and device temperature and was hence termed to be robust.

Motivated by the need to investigate further the underlying polarisation switching characteristics of VCSEL for the observations reported in chapter 6, the aim of chapter 7 was to characterise polarisation bistability and hysteresis in optically injected two mode VCSELs. The main results are:

1. Using orthogonal optical injection an ultra-wide frequency hysteresis cycle was obtained for two-mode VCSELs. Two type of hysteresis in this operation regime were found. The first type was located at positive frequency detuning and was characterised by an ultra-wide hysteresis cycle, the second one was located at negative frequency detuning and characterised by smaller hysteresis cycle.

2. The obtained hysteresis widths are optical injected power and bias current dependent. For a defined range of injection power the hysteresis width of the first type of hysteresis was relatively constant with value close to the frequency difference between the fundamental mode and the higher order mode. The hysteresis of the first type starts to decrease with very high injection power. However, the widths of the hysteresis of the second type increase with increasing injection power.

3. The hysteresis of both types increases with increasing VCSELs bias current.

For orthogonal optical injection in two-mode operation regime, injected power controls transfer between 'irreversible PS' and 'ultra-wide hysteresis frequency bistability' regions.

Finally, the lasing characteristics in VCSELs subject to direct current modulation were explored in chapter 8. The effects of the frequency of direct current modulation and substrate temperature on lasing threshold have been identified. Hysteresis in the turn-on and turn-off lasing threshold current of the VCSELs were observed. The hysteresis in the turn-on and turn-off can be explained in terms of the interplay of dynamical hysteresis and device heating.

9.2 Original contributions

This thesis includes several original contributions. New approaches namely circularly polarised optical injection and circularly polarised optical feedback were used experimentally for the first time. Using circularly polarised externally optical injection, the output polarisation of electrically pumped VCSELs can be strongly influenced. The linear polarisation of VCSELs emission can become circularly polarised for bias currents below

or near the threshold current of the stand-alone VCSELs. In addition, using a new circularly polarised optical feedback scheme, the VCSELs emission was made to exhibit a degree of circular polarisation. The degree of circular polarisation depends on the feedback power ratio and the VCSEL bias current.

The role of suppressed mode in the polarisation switching characteristics of VCSELs was investigated using different forms of linearly polarised optical injection. The minimum injection power for polarisation switching to occurs has been found to be decreases dramatically with increasing VCSELs bias current. Polarisation switching in multimode VCSELs was investigated using optical injection. Irreversible polarisation switching in two-mode operation VCSELs was observed using parallel/orthogonal optical injection. Furthermore, polarisation bistability and ultra-wide hysteresis were obtained for two-mode operation regime with orthogonal optical injection.

9.3 Proposals for future work

There are two main lines of research arising from this experimental work which should be pursued.

Recent experiments suggest that the polarisation state selection in VCSELs is strongly influenced by circularly polarised optical injection. Despite the fact that numerous studies made of linear (parallel/orthogonal) optical injection, relatively little attention has been given to other types of polarised injection. A theoretical and experimental published work has been reported VCSELs dynamics using elliptical polarised optical injection [1]. Therefore, a first line of research development is to investigate the VCSELs dynamics and spectral characteristics using this new optical injection scheme.

A second line of research development which follows from chapter 6 and chapter 7 is to investigate polarisation bistability and ultra-wide hysteresis in optically injected VCSELs. The study can be extended to investigate the hysteresis cycle width of the VCSELs with different characteristics and structure. Such hysteresis phenomena may be further explored using VCSELs with different frequency separation between the fundamental mode and higher order mode, or devices where the polarisation direction of the higher order mode is parallel to that of the fundamental mode.

References:

[1] **R. Al-Seyab,** K. Schires, A Hurtado, I D. Henning and M. J. Adams , "Dynamics of VCSELs subject to optical injection of arbitrary polarization," IEEE J. Selec. Top. of Quantum Electron. vol. 19, pp. 1700512, Jul./Aug **2013.**

APPENDIX

Rate equation model

In chapter 8 use is made of simulation performed using rate equations which are described briefly here. The rate equation model is an important tool for evaluating the behaviour of semiconductor lasers under direct current modulation. The rate equations describe the interrelation between carrier density and optical field or photon density. Due to stimulated emission the interaction between the charge carriers and photons is inherently nonlinear nature, which makes the laser output oscillates periodically before attaining its steady state. The oscillation is referred to as relaxation oscillations frequency, which is typically in the GHz range and increases with increasing device current. The transient effects play an important role when using direct current modulation at frequencies approaching a few GHz.

The equation for the relaxation oscillation frequency is:

$$\nu_R = \frac{1}{2\pi} \sqrt{\frac{G_N}{ed}(J - J_{th})} \tag{1}$$

The laser dynamics is generally described using a carrier density (equ. (2)) and a photon density (equ.(3)) rate equations. The determination of the frequency modulation response of single mode semiconductor laser is performed with these two equations. Equ.(2) describes the rate of change of the carrier density N. While equ.(3) describes the rate of change of the photon density, S.

$$\frac{dN}{dt} = C - \frac{N}{\tau_N} - A(N - N_O)S \tag{2}$$

$$\frac{dS}{dt} = A(N - N_O)S - \frac{S}{\tau_p} + \frac{\beta N}{\tau_N} \tag{3}$$

Where N is the carrier density, C is the carrier flux or current density, τ_N is the spontaneous carrier lifetime, A is the gain coefficient, N_o is the minimum carrier density required to obtain laser action, S is the photon density, τ_p is the photon lifetime, β is the spontaneous emission factor [1].

The rate equations for a semiconductor laser, incorporating the dynamic variation of the temperature of the active region are [2]:

$$\dot{E} = \frac{1}{2}k(1 + j\alpha)(gN - 1)E + \sqrt{\beta_{sp}\gamma_N}\xi \tag{4}$$

$$\dot{N} = \gamma_N(\mu - N - gN|E|^2) \tag{5}$$

$$\dot{T} = -\gamma_T(T - T_s) + Z(\frac{N}{K} + 1) + P(\frac{\mu}{K} + 1)^2 \tag{6}$$

Where E is the complex slowly varying optical field, N is the normalized carrier density, and the T is the active region temperature. Other parameters are the linewidth enhancement factor, α; the coefficient of spontaneous emissions, β_{sp}; the field decay rate, k, the carried decay rate, γ_N, and the normalized injection current, $\mu = K(I/I_0 - 1)$, where, I is the bias current, I_0 is the current needed to reach transparency and K is a dimensionless constant. In the temperature equation, γ_T takes into account the decay rate to the substrate temperature, T_s, and Z and P represent non-radiation recombination heating and Joule heating, respectively. The gain coefficient, g, is a Lorentzian in the frequency space, $g(\omega, T) = g_0(T)/\{1 + [\delta(T) - \omega]^2 / \Delta\omega_g^2(T)\}$, where $\delta(T) = \omega_g(T) - \omega_c(T)$ is the gain-cavity offset, $\omega = \text{Im}(\dot{E}/E)$ is the slowly-varying optical frequency, $g_0 = T_0/T$ is the gain peak and $\Delta\omega_g^2 = \Delta\omega_{g,0}^2(T/T_0)$ is the gain bandwidth, with T_0 being the reference room temperature [3,4].

The relevant simulation using this model described in chapter 8 were performed by Masoller and Torre [2]

References

[1] **M. Tang** and S. Wang, "Simulation studies of bifurcation and chaos in semiconductor lasers," Appl. Phys. Lett. Vol. 48, pp 900-902, Apr. **1986.**

[2] **Y. Hong,** Cristina Masoller, Maria S. Torre, Sanjay Priyadarshi, Abdulqader A. Qader, Paul S. Spencer, and K. Alan Shore, "Thermal effects and dynamical hysteresis in the turn-on and turn-off of vertical-cavity surface-emitting lasers", Optic. Lett. ,vol. 35, no. 21, pp3688 – 3690, Nov. **2010.**

[3] **M. S. Torre** and C. Masoller, "Dynamical hysteresis and thermal effects in vertical-cavity surface-emitting lasers," IEEE J. Quantum Elect., vol. 46, pp. 1788-1794, Dec. **2010.**

[4] **C. Masoller** and M. S. Torre, "Modeling thermal effects and polarization competition in vertical-cavity surface-emitting lasers," Optic. Expres., vol. 16, pp. 21282-21296, Dec. **2008.**